FOULING MITIGATION OF REVERSE OSMOSIS MEMBRANES USING LAYER BY LAYER DEPOSITION OF POLYELECTROLYTES

BY

SAQIB JAVED

A Thesis Presented to the
DEANSHIP OF GRADUATE STUDIES

KING FAHD UNIVERSITY OF PETROLEUM & MINERALS

DHAHRAN, SAUDI ARABIA

In Partial Fulfillment of the
Requirements for the Degree of

MASTER OF SCIENCE

In

CHEMICAL ENGINEERING

November, 2015

KING FAHD UNIVERSITY OF PETROLEUM & MINERALS

DHAHRAN- 31261, SAUDI ARABIA

DEANSHIP OF GRADUATE STUDIES

This thesis, written by **Saqib Javed** under the direction his thesis advisor and approved by his thesis committee, has been presented and accepted by the Dean of Graduate Studies, in partial fulfillment of the requirements for the degree of **MASTER OF SCIENCE IN CHEMICAL ENGINEERING.**

Dr. Mohammed Ba-Shammakh
Department Chairman

Dr. Salam A. Zummo
Dean of Graduate Studies

30/12/15
Date

Dr. Isam H. Al-Jundi
(Advisor)

Dr. Mazen Mohammad Khaled
(Member)

Dr. Basim Ahmed Ali Abussaud
(Member)

© Saqib Javed

2015

DEDICATED TO

MY PARENTS,

BIG B (ASIF JAVED),

BROTHER –IN-LAW (NASIR ALI NADEEM)

AND

MY AFFECTIONATE FRIEND (ADNAN HAIDER)

ACKNOWLEDGMENTS

All praises to Almighty Allah Who blessed me with strength, health and patience to pursue my MS degree at KFUPM. I would like to thank to my parents and family for their continuous support and prayers.

I pay my sincere and humble gratitude to my thesis advisor, Dr. Isam Aljundi for his constant support, mentoring, persistence, and exceptional guidance throughout my research. I would like to thank to Dr. Mazen Khaled for providing guidance and research facilities in his lab for fabrication of polyelectrolyte multilayer thin films. I am very grateful to Dr. Basim Abussaud for his contribution and input during thesis write-up.

I would like to thank Dr. Zafarullah Khan for providing his lab for performing permeation experiments. I would like to acknowledge Centre of Research Excellence in Renewable Energy for providing me membrane casting facilities and Centre of Excellence in Nanotechnology (CENT), KFUPM for providing membrane characterization services. I would like to gratefully acknowledge the financial support from Deanship of Scientific Research (DSR), KFUPM with grant number SB131003.

I would like to pay my heartiest acknowledgements to Chemical Engineering Department of King Fahd University of Petroleum and Minerals (KFUPM) for awarding me scholarship for the master degree in their esteem institution.

Last but not the least I pay my whole-hearted gratitude to my friends of Hetero Group (Rana Adeem, Lala Farrukh, Naeem, Waqar, Fahad and Aamir), affectionate brothers Dr. Munem, Dr. Zaheer and all Pakistani community for their support and love during my stay at KFUPM.

TABLE OF CONTENTS

LIST OF TABLES

LIST OF FIGURES

LIST OF ABBREVIATIONS

PDADMAC	Poly (diallyldimethylammonium chloride)
SPEEK	Sulfonated Poly (Ether Ether Ketone)
PAH	Poly (Allylamine Hydrochloride)
PET	Poly (Ethylene Terephthalate)
PEBAX	Polyether-polyamide block co-polymer
BSA	Bovine Serum Albumin
PSS	Poly (Styrene Sulfonate)
PEI	Poly (Ethylene Imine)
PVA	Poly (Vinyl Amine)
PVS	Poly (Vinyl Sulfate)
PAN	Poly (Acrylo Nitrile)
PAA	Poly (Acrylic Acid)
PEG	Poly (Ethylene Glycol)
PEO	Poly (Ethylene Oxide)
PAA	Poly (Acrylic acid)
SA	Sodium Alginate
CHI	Chitosan

ABSTRACT

Full Name : [Saqib Javed]

Thesis Title : [FOULING MITIGATION OF REVERSE OSMOSIS MEMBRANES USING LAYER BY LAYER DEPOSITION OF POLYELECTROLYTES]

Major Field : [Chemical Engineering]

Date of Degree : [November 2015]

Membrane technology has been recognized as one of the most important technologies in water desalination. However, this technology is challenged by the fouling phenomenon which causes higher operating pressure, flux decline, frequent replacement of membranes and eventually higher operating costs. Therefore, good antifouling membrane is needed for smooth operation. In this project, reverse osmosis membranes were synthesized and modified to enhance the fouling resistance with acceptable salt rejection and water flux. Interfacial polymerization of MPD and TMC was used for preparation of thin film composite membranes. Polysulfone ultrafiltration membranes were used as a support. The polyamide membranes were functionalized by Poly (ethylene imine) (PEI)/ poly (allylamine hydrochloride) (PAH) using spin assisted layer by layer technique. Box-Behnken design of experiment was used to study the effect of several parameters such as the number of layers, concentration of polyelectrolyte solution, and pH. Membrane characterization was performed using Atomic Force Microscope (AFM), Scanning Electron Microscopy (SEM), Fourier Transform Infra-Red (FTIR), Thermo Gravimetric Analysis (TGA) and contact angle. 50 bilayer modified membrane possess 15.8 L/m^2.hr pure water flux with 98 % salt rejection; these values are close to pristine polyamide. However, after three hours of bovine serum albumin (BSA) filtration, it was observed

that functionalized membranes managed to retain more than 88 % water flux as compared to pristine polyamide membrane which suffered from more than 42% flux drop. AFM and contact angle measurement showed that functionalized membranes have lower roughness and higher hydrophilicity that has enhanced the fouling resistance. Effect of number of layers, polyelectrolyte concentration, and pH was correlated with permeation performance and contact angle via statistical models derived from the design of experiment. An optimum preparation conditions were found and the predicted water flux is comparable with that of the pristine membrane while retaining higher salt rejection. In addition it was found that the optimum membrane will resist fouling much more than the pristine membrane and the corresponding flux is 50% higher.

ملخص الرسالة

الاسم الكامل: ثاقب جاويد

عنوان الرسالة: طبقة ترسيب باستخدام العكسي التناضح أغشية قاذورات من التخفيف بولي ايلايكترولايتيس من بطبقة

التخصص: هندسة كيميائية

تاريخ الدرجة العلمية: نوفمبر 5102

.المياه تحلية في التقنيات أهم من كواحدة الأغشية تكنولوجيا اعترف وقد هذه ذلك، ومع انخفاض التشغيل، ضغط ارتفاع يسبب الذي قاذورات ظاهرة تحدي هو التكنولوجيا ولذلك، .المطاف نهاية في أعلى تشغيل وتكاليف الأغشية من متكررة واستبدال التدفق، المشروع، هذا في .العمل سير لحسن جيدة السفن على للحشف المضادة غشاء مطلوب الرفض تدفق مع قاذورات المقاومة لتعزيز لوتعدي العكسي التناضح أغشية وتوليفها أغشية لإعداد TMC و MPD البيني السطح البلمرة واستخدمت .مقبولة المالحة والمياه .بولي يسولفوني أولترافيلتريشن الأغشية لدعم كوسيلة واستخدمت .المركب رقيقة بولي/(بي) (ايمين الإيثيلين) بولي من أميد بولي الأغشية في وذكتيونال يزيد كانت بعد طبقة تقنية مساعدة تدور (الهيدروكربونات) استخدام (هيدروكلوريد الليلاميني) عدد مثل المعلمات من العديد آثار لدراسة التجربة تصميم مربع بيهنكين واستخدمت .طبقة الغشاء توصيف إجراء تم .الحموضة ودرجة بوليايلايكترولايتي، لحل وتركيز الطبقات، وتحويل ،(SEM) الإلكتروني المجهر الضوئي المسح ،(AFM) الذرية لقوةا مجهر باستخدام .الاتصال وزاوية (TGA) الحراري الجاذبية وتحليل ،(FTIR) الحمراء تحت الأشعة فوريه هذه ؛٪ 98 المالح رفض مع النقية المياه تدفق $15.8\ L/m^2.hr$ غشاء تعديل 50 بلير تمتلك المصل ألبومين ترشيح ساعات ثلاث بعد ذلك، ومع .البكر أميد بولي من قريبة القيم تدفق من بأكثر الاحتفاظ من تمكنت فوذكتيونال يزيد الأغشية أن لوحظ ،(BSA) البقري

فـي 42 الـ تدفـ ق انـ خـ فاض من أكـ ثر من عانـ ت الـ تي الـ بكر أمـ يد بـ ولـ ي بـ غـ شاء مـ قارنـ ة 88% الـ مـ ياه وأعـ لى خـ شونـ ة أقـ لـ تـ يونـ الـ يزيـ دفـ ونـ ك الأغـ شـ ية أن أظهرت والاتـ صال فـ ؤاد زاويـ ة قـ ياس .الـ مائـ ة وتـ ركـ يز الـ طـ بـ قات، من عدد تـ أثـ ير .قـ انـ ذورات الـ مـ قاومة عززت الـ تي هـ يدروفـ يـ لـ يـ سـ يـ تي عن والاتـ صال الأداء زاويـ ة بـ تخـ لل يـ رتـ بط وكـ ان الـ حموضة ودرجة بـ ولـ يـ يـ لـ يـ كـ ترولـ يـ تي، أمـ ثل إعداد شروط عـ لى الـ عـ ثور تـ م .الـ تجربـ ة تـ صمـ يم من الـ مـ سـ تمدة الإحـ صائـ ية الـ نماذج طريـ ق .أعـ لى الـ مـ لح بـ رفـ ض احـ تـ فاظها مع الـ بكر الـ غـ شاء أن مع لـ لمـ قارنـ ة قـ ابـ ل الـ مـ توقـ عة الـ مـ ياه وتـ دفـ ق الـ بكر الـ غـ شاء من بـ كـ ثـ ير أكـ ثر قـ انـ ذورات سـ تـ قاوم الأمـ ثل الـ غـ شاء أن وجد ذلـ ك إلـ ى وبـ الإ ضافـ ة بـ نـ سـ بة أعـ لى هو الـ مطابـ ق والـ تمويـ ه 50%.

CHAPTER 1

INTRODUCTION

1.1 Introduction

Improving the access to clean drinking water is a serious concern around the globe. The simplified and justified answer lies in the relation between pure water and public health. But the scarcity of clean drinking water is an alarming situation throughout the world [1]. Water scarcity [2] and lack of pure water is leading to diarrheal diseases which cause death as indicated in Figure 1-1. According to WHO/UNICEF report, more than 1.1 billion people did not have access to better drinking water facilities and two third of this belongs to Asia [3]. Although due to joint international efforts this value has dropped to less than one billion but the situation is not yet satisfactory [1].

The water stress index (WSI), the ratio of fresh water that is drawn yearly to its availability with respect to hydrology of region, gives an indication about the unavailability of fresh water [4]. The severe value of WSI above the threshold of 40 % indicates serious water limitation. Many countries in North Africa, South Asia, Middle East, part of Europe and western America is under high WSI and this dispute is supposed to advance worse in the upcoming years [5].

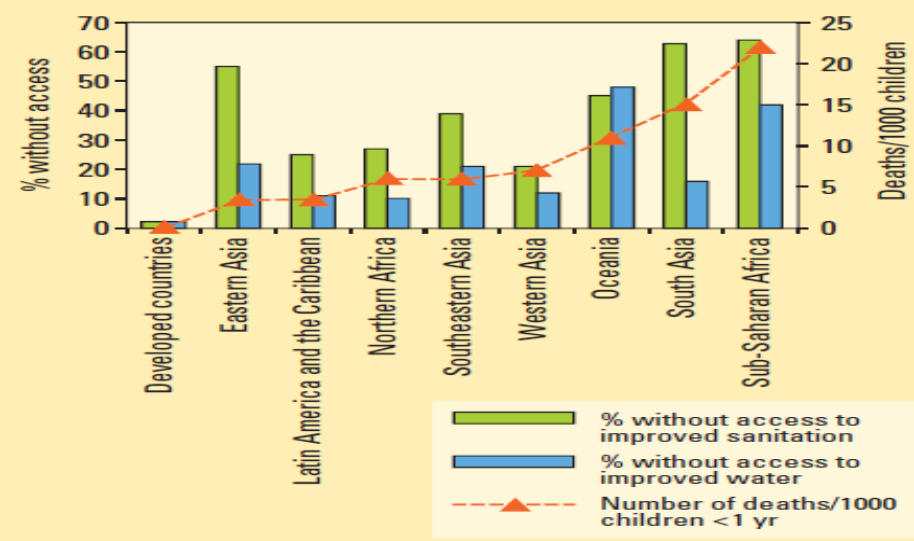

Figure 1-1: Assessment of lack of access to better-quality water & sanitation and deaths caused by diarrheal disease [3]

Desalination is the technology that converts saline water into clean drinkable-water. Therefore, it is the best solution to overcome water scarcity [6]. More than 70% of the surface of Earth contains water, of which 97.5 % can be found in the oceans and sea. Even if a small portion of this huge source is treated, it can have a substantial effect on water shortage around the globe [7]. Percentage of salts in seawater is enormous and it varies with respect to locations as it is indicated in Table 1-1[8]. Fresh water is the one that has salts less than 1000 mg/L and in some countries this standard has lower value of 500 mg/L [9]. If the concentration of salts or TDS is higher than 1000 mg/L, the physical properties like taste, color, and odor can be affected unpleasantly. The World Health Organization has announced a value of 1000 mg/L TDS [10] for drinking water and the Gulf region has also endorsed the same level for pure water.

Table 1-1: Concentration of salts in worldwide sources of water [8]

Water Source	Concentration (ppm)
Brackish water	500 - 3000
North Sea	21000
Gulf of Mexico and coastal waters	23000 - 33000
Atlantic Ocean	35000
Pacific Ocean	38000
Arabian Gulf	45000
Mediterranean Sea	38600
Red Sea	41000
Dead Sea	~ 300000

The first major desalination plant based on distillation was built in Netherlands in 1928 with an operating capacity 60 m^3/day. Then, Saudi Arabia built a desalination plant in 1938 [11]. Currently, more than 120 countries have desalination plants, of which 48 % of global production is associated to Middle East. In the Middle East, 61 % of the desalination capacity belongs to six Gulf States. Saudi Arabia is producing around one quarter of the total desalination capacity around the globe where the installed desalination capacity is more than 5.25 million m^3/day [12]. Figure 1-2 represents the capacity of desalinated water of each region along with the type of source water [13].

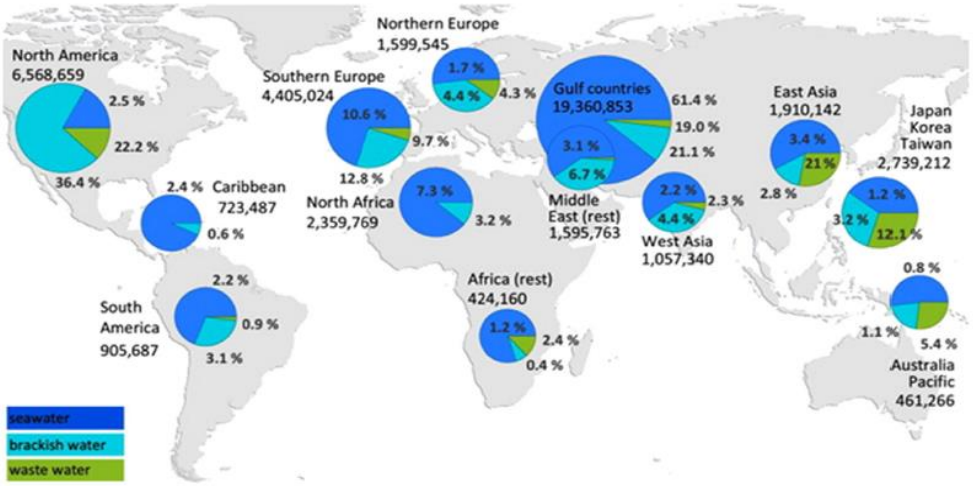

Figure 1-2: Worldwide desalination capacities along with water source [13]

The overall global capacity of desalinated water is estimated as 61 million cubic meters per day [14]. The main technologies to accomplish desalination are split into two sets, one is the thermal distillation and other is membrane separation.

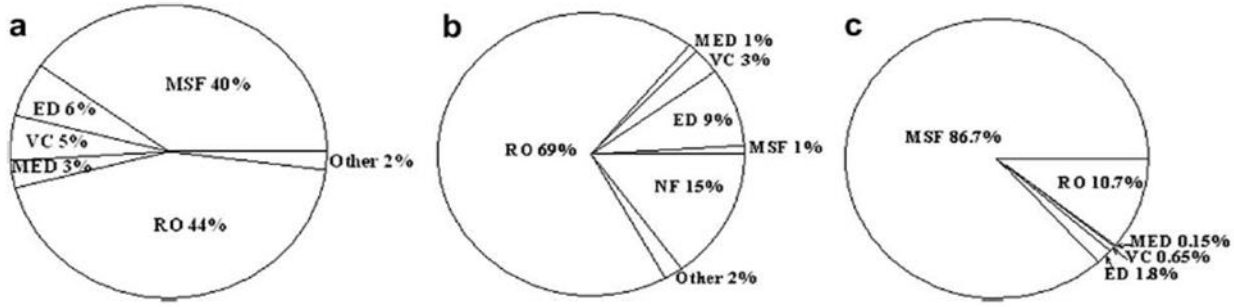

Figure 1-3: Capacity of desalination technologies in (a) World (b) USA (c) Middle East [10]

Thermal distillation includes Multi Effect Distillation (MED) and Multi Stage Flash (MSF) whereas membrane separation includes reverse osmosis (RO). Thermal technologies are largely depending on energy as they consume heat and distillate the fresh water at low temperature and pressure [15]–[17]. RO is rapidly developing

approach to attain pure water by eliminating salts from seawater or any other origin of saline water. Currently, the largest percentage of desalination plants is based on RO as shown in Figure 1-3 [10]. The reason behind greater contribution of RO is its lower energy requirements 4-7 kW.h/m^3 for seawater [18] as compared to high demand of 15.5 kW.h/m^3 for MSF.

The marketplace for RO equipment and membranes by the end of 2014 was around $5.4 billion and it is expected to stretch to $8.8 billion by 2019 with a compound annual growth rate of 10.5% [19]. The reason behind this development is that the utilization of energy has reduced considerably during the last decade for the RO processes along with the development of new and efficient membranes [20].

Membranes effectively remove contaminants from drinking water but fouling increase expense and decrease the applicability of membrane process. Apart from flux loss, bio-growth render membrane element inadequate by limiting feed channel flow [21]. Fouling can't be eliminated but it can be minimized using suitable pretreatment [22], for example coagulation, precipitation and filtration.

Surface modification of membrane can decrease extent of fouling. The surface roughness imparts significant contribution in membrane fouling. Smooth surface is inclined less to fouling as compared to membranes having rough surface [23]. Surface modification can be done by surface coating [24]–[27], surface grafting [28]–[30], plasma treatment [31]–[33], UV irradiation [34], [35] or by incorporation of nanomaterial [36]–[39].

Decent results have been attained with poly electrolyte multilayer (PEM) coatings using layer by layer (LbL) deposition technique due to the control of thickness at the nanometer

scale that yields better membrane performance. Due to its simplicity and robustness, layer by layer (LbL) technique has been adopted in this study.

So far, there is no statistical model present that can describe the performance of membrane with structure and its preparation conditions. There is no clear understanding of relationship between preparation conditions and performance. There is no optimized procedure to prepare polyelectrolyte membranes. Moreover, there is little study on the modification of polyamide reverse osmosis membrane, if present, either it involves the commercial polyamide membrane or it lacks the optimization.

1.2 Research Objectives

The main objective of this study is to prepare an antifouling reverse osmosis membrane with acceptable salt rejection and water flux using layer by layer assembly.

The specific objectives are:

1. To prepare Polyamide membrane using trimesoyl chloride and m-phenylene diamine as monomers through interfacial polymerization.
2. To successfully deposit polyelectrolytes on the polyamide membranes.
3. To optimize the operating conditions of the LbL process to get the best performance of the membrane in terms of permeability.

1.3 Thesis outline

The main outline of the thesis includes:

- **Chapter 2** : Literature Review

  It covers the membranes types and thin film composite membranes for desalination. The undesirable feature of fouling, its types and ways for its minimization are discussed. Layer by layer technique for polyelectrolyte deposition has been reviewed in detail. The main focus is given on the effect of various parameters on the performance of polyelectrolyte modified membranes.

- **Chapter 3** : Research Methodology

  It includes the basic approach to achieve the desired objectives. The detailed procedure to prepare polysulfone support and polyamide membrane has been explained. Layer by layer deposition of polyelectrolytes on the polyamide membrane using spin coating, characterizations and membrane evaluation procedure through filtration experiments are also included.

- **Chapter 4**: Design of experiment

  It includes the method to design the experiments using design expert software. The analysis of different responses after filtration study using ANOVA scheme has been discussed followed by the optimization.

- **Chapter 5**: Results and Discussions

It includes the results of characterization and comparison of the surface properties of polyelectrolytes modified and pristine membrane. Effect of input parameters on the membrane performance has been discussed after performing permeation and fouling study.

- **Chapter 6**: Conclusions and Recommendations

In the end, conclusions and recommendations were made in light of filtration, fouling and optimization study.

CHAPTER 2

LITERATURE REVIEW

2.1 RO Membranes, Fouling, and Modification

In RO membranes, the separation of the dissolved salts is accomplished because of the hydraulic gradient that is created across the semi permeable membrane. A pressure higher than the osmotic pressure (due to dissolved species) is applied to create gradient in operation [40]. RO membranes are currently being used in desalination of sea and brackish water resources [41]. The first commercialized RO membrane was developed by Loeb and Sourirajan in 1958 from Cellulose Acetate (CA) by using phase inversion method [42]. It was called asymmetric membrane and holds dense structure. It showed better performance at that time but CA membrane is easily compacted and hydrolyzed in the presence of water which leads to flux decline and eventually results in low efficiency of the system. The real boost in design of composite membrane was brought by Cadotte [43] who introduced thin film composite membrane (TFC). He used interfacial polymerization in which very thin membrane of aromatic polyamide material is synthesized straight on the surface of polysulfone material which serves as a porous support [44]. The composite membrane consists of bilayers formed in two steps that are totally different from each other as compared to asymmetric CA membrane which is homogenous in chemical composition and formed in one step. The structure of typical TFC membrane is shown in Figure 2-1 [45].

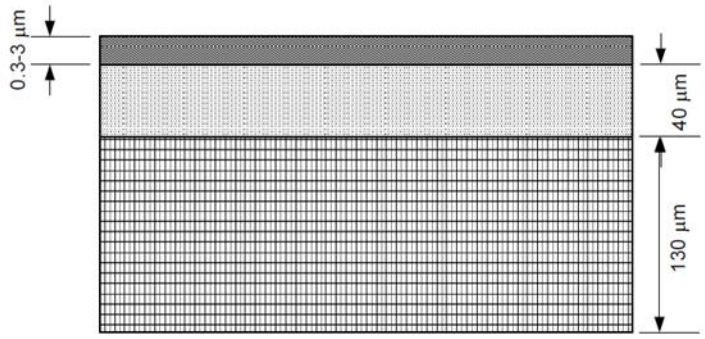

Figure 2-1: RO TFC membrane [29]

A typical TFC RO membrane comprises of three layers that are polyester (130 nm thick), polysulfone (40 nm thick) and polyamide (0.3 – 3 nm thick). The non-porous polyamide layer is the active layer that is responsible for the salt rejection. The advantage of TFC membrane over the asymmetric membrane is that each particular layer in a TFC membrane can be adjusted for its certain function. The thin barrier layer is adjusted to get a required consolidation of solvent flux and rejection of solute. The porous layer which act as a support enhance the maximum strength and provide compression resistance along with minimum resistance for flow of permeate [45]. The detailed mechanism for synthesis of polyamide membrane (PA) via interfacial polymerization by using m-phenylene diamine (MPD) and trimesoyl chloride (TMC) is discussed in detail by Krantz et al [46].

2.2 Membrane Fouling

Membrane fouling is a complex phenomenon for which there is no single exact definition, however it can be defined as “A condition when membrane experiences

blocking or coating by some component present in the processed stream, which eventually results in declining of flux" [47].

To some extent, fouling occurs in all RO systems. It is a leading restrictive feature in RO applications. Generally speaking, there are two fouling mechanisms that are commonly observed in membrane developments. These two mechanisms include fouling at the surface and in the pores. As far as RO membranes are concerned, they don't have distinct pores and are considered to be principally dense. Therefore, surface fouling is prominent in RO membranes [48].

Fouling of membranes can happen under various conditions which eventually lead to its cleaning. The severity of the fouling decides the cleaning frequency, which depends on several variables such as recovery rate of the system, characteristics of feed water and pretreatment methods. Because all membrane systems are attacked by fouling, it is better to understand the basic types and their origin which will allow enhancing the valuable life of RO membrane element along with improved efficiency and economy of RO plant [49].

2.2.1 Types of Fouling

During operation, reverse osmosis membranes are disclosed to every type of foulant. So, the understanding of each type is suitable to study and control specific foulant. Moreover, it is vital to recognize the interactive effects among numerous foulant on mechanism of fouling. For example, it has been reported that an increase in concentration polarization of salt ions can increase the osmotic pressure which eventually results in flux decline. Likewise, substantial rise in synergistic effects has been found during interactions

between colloidal and organic foulant. Furthermore, these interactions are responsible for flux decline [50].

RO membrane elements are attacked by different types of foulants that can be broadly categorized into four types: suspended particulate matter, dissolved organic substance, dissolved objects, and biological material [10], [51]–[53]

Because of the repulsive potential by electrical double layer of charges, suspended solids preserve their suspended position and when the attraction forces (van der Waals forces) reduces the electrical repulsion, these stable suspended solids become unstable and form agglomerate. Eventually, they settle on the surface of membrane. Metal oxides in colloidal forms, for instance iron or silica are typical suspended solids [54]. Dissolved solids are soluble in feed water and can form scales upon precipitation. These salts precipitate when the concentrations of these components in rejected brine stream increase. Examples of such precipitated compounds are calcium carbonate and sulphate of barium, calcium and magnesium.

Non-biological organic foulant are materials which are not living organisms but they possess carbon-based chemical structures. These carbon based structures have usual attraction for membrane. The major examples of non-biological organic foulant include oil, cationic surfactants, plant materials and hydrocarbons [53].

Biological activity can impact membrane process by two means. It can be through membrane decomposition with the help of biological material or formation of a flux-preventing layer [55]. Biological fouling arises while microbial cells gather and stick to surface of the membrane. Their continuous growth results in formation of biofilms.

Foulants are present in low quantity; however they grow into enormous numbers that successfully blocks permeate flow from the membrane.

It is evident that suspended and dissolved solids have significant contribution in fouling. As membrane fouling occurs, membrane efficiency deteriorates in the form of decreased salt rejection and permeate flux and increased pressure drop across the membrane. The flux drop of permeate is also caused by concentration polarization. But, fouling resistance play major role when flux decline is complemented with considerable rise in permeate purity [56].

2.3 Reduction of Membrane Fouling

Minimization and remediation are the two approaches to reduce the fouling effect. Remediation involves the frequent chemical cleaning at fixed intervals which is essential for all membrane processes. However, the cleaning frequency depends on concentration of existing foulant and it varies from weekly to yearly cleaning. Cleaning agents are commercially available and their selection is determined by feed characteristics. To remove precipitated salts, for instance $CaCO_3$, acid cleaning is appropriate. However, alkaline cleaning is suitable to remove adsorbed organic matter. To clean microfiltration and ultrafiltration membrane, a small water or air pulse is applied from permeate to feed side which removes foulants from pores. However, this technique is not useful for NF or RO processes [57], as thin-film composite membranes are involved in them. Higher pressures cannot be used to clean thin film composite membranes because they possess limited mechanical stability. Therefore, backwashing of RO membrane is performed by

reversing the flow of permeate to clean up the membrane surface from accumulated foulants.

Osmotic backwashing takes place when osmotic pressure at feed side beats the applied pressure through the membrane. This may be attained in different means [58];

1. By decreasing the applied pressure on feed-side.
2. By equalizing the trans-membrane pressure (TMP) while increasing the permeate side pressure.
3. By injecting a pulse at feed side that contains high concentration solution.

The detailed mechanism of osmotic backwashing is described by various authors elsewhere in [59]–[62]. Membrane cleaning is done to remove the fouling layer on the membrane surface which ensures stable operation of the system and to repair its performance when it drops lower than the estimated output. The reversible fouling is recovered by backwashing, however chemical cleaning is necessary to overcome irreversible fouling. Membrane cleaning is greatly affected by temperature because it can change the chemical reaction equilibrium. It can change the reaction kinetics and can change the solubility of fouling materials throughout the cleaning. In general, cleaning is more effective at higher temperatures. Membrane compatibility should also be checked along with other filter components concerning temperature [63]. The recovery of fouling layer is achieved in two steps [64];

1. First step involves the chemical reaction between foulants and the cleaning agent.
2. In the second step, foulants are discharged from membrane surface to the bulk solution by means of shear forces.

Selection of cleaning agents and accurate approach is of great importance in order to recover stable membrane operation through removal of fouling layer. Cleaning through aggressive agents will cause irreversible membrane damage that will eventually need membrane replacement. A less effective cleaning agent will increase time of cleaning and consequently energy consumption will be escalated [65].

Lee and Elimelech [66] showed that inert salts such as sodium nitrate, sodium chloride, potassium chloride and sodium sulfate can be effectively used for the cleaning of reverse osmosis membranes that are fouled by organic foulants like sodium alginate. Based on experimental results and AFM measurements, the most important mechanisms of salt cleaning are the swelling of gel layer and ion-exchange reaction as shown in Figure 2-2 [66].

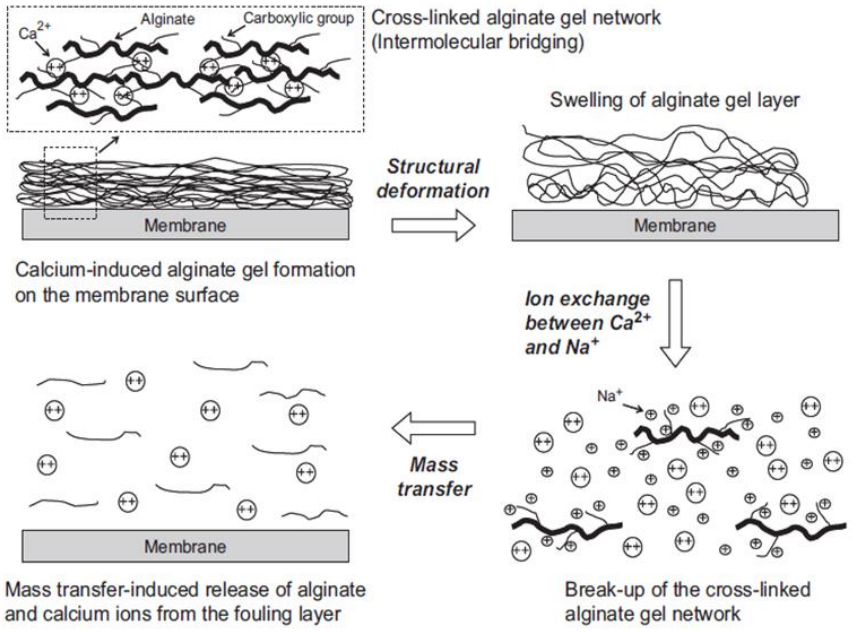

Figure 2-2: Membrane cleaning mechanism [66]

2.4 Polyelectrolyte Multilayer Films

Polyelectrolytes are the polymers whose repeating units comprise an electrolyte group. These electrolyte containing polymers have been exploited in the development of innovative entities recognized as polyelectrolyte multilayers (PEM). These thin films are prepared through a layer-by-layer (LbL) deposition method. In this technique, the membrane is dipped in dilute solution of positively charged polyelectrolyte solutions and then the same membrane is dipped in negatively charged polyelectrolyte solutions. Each time, a small quantity of polyelectrolyte solution is adsorbed on the membrane surface and consequently surface charge is reversed. This allows steady and precise assembly of electrostatically cross-linked films of opposite charged layers.

The fascinating feature of polyelectrolyte layers is the formation of polyelectrolyte complex when it is united with another oppositely charged polyelectrolyte. The main compelling force for organizing polyelectrolyte complex is rise in entropy [67] through discharge of oppositely charged ions, hydrogen bonding [68], hydrophobic interaction [69] or other Van der Waals attractive forces that might play their role in the development of the complex. When an oppositely charged polyelectrolyte complex is formed and the process is repeated several times, it leads to the formation of Polyelectrolyte Multilayer.

2.4.1 Layer by Layer

In 1966, Iler [70] presented a procedure in which contradictory charged colloidal particles could be constructed into layer by layer (LbL) films. In 1997, Decker explained

a systematic way for polyelectrolyte assembly and it became the most cited article in nature till 2008 [71]. The alternating adsorption of molecular layers is principally established on electrostatic interactions between the adjoining layers. Therefore, it is also attributed as electrostatic self-assembly.

LbL assembly is an eye-catching procedure for formation of thin film composite TFC reverse osmosis membranes. Through LbL, film thickness can be accurately organized at nanometer scale [72]. Furthermore, film properties can be enhanced by changing the polyelectrolyte type [73] and specifications of depositing poly-ionic solutions [74]. After deposition of polyelectrolyte solutions, surface of membrane becomes more hydrophilic, as polyelectrolytes are water-soluble polymers. The surface charge density rises by growing the number of deposited films; polyelectrolytes form loops and tails on surface of the substrate which additionally increase the hydrophilicity [75].

The LbL procedure involves the alternating consecutive immersion (dipping) of a solid substrate into oppositely charged solutions. Rinsing is necessary after depositing every layer to remove the weakly attached molecules. The schematic diagram of LbL scheme is presented in Figure 2-3 and the detailed procedure is discussed by Feng et al [76] and Decker [77]. Steps 1 and 3 are for the coating of polyelectrolytes whereas step 2 and 4 are for rinsing.

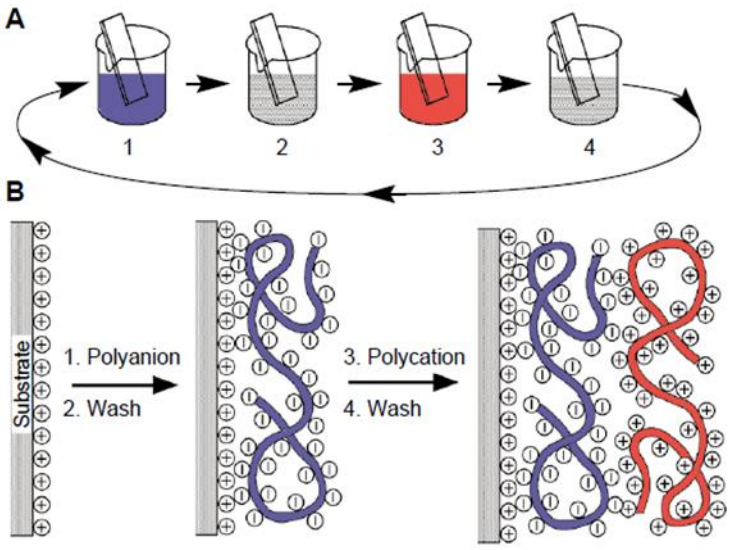

Figure 2-3: (A) Schematic diagram of LBL process (B) Representation of Molecular deposition [77]

Each layer of the LbL films has thickness at molecular scale where a few tens of films can be attained in a simple way. The LbL assembly is the simplest method to organize nano-layered films. Neither specific equipment nor particular polyelectrolytes are needed for this method. If condition of electrostatic interaction is fulfilled, it can be applied to a wide variety of materials and applications as discussed in [78]–[81].

The conventional dipping process is quite time consuming and usually takes 30 minutes for one dipping cycle [82], so automated dipping was developed. Hammond and Clark [83] used automatic dipping process to form defect-free uniform films. They deposited PSS/PDADMAC films through commercial slide stainer and found that the mechanization of LbL dip assembly resulted in micro fabricated films. Moreover, automated dipping provides films with improved selective deposition and multilayers with thicker pattern.

Similar automated dipping procedure was applied by Shiratori and Yamada [84] for synthesizing PAH/PAA films. They concluded that better film control is achieved up to nanometer level by the modified dipping procedure. Moreover, smooth surface morphology with excellent properties are gained compared to conventional dipping process [85] and are greatly illustrated in [86]–[93].

2.4.2 Spray Layer-by-Layer Self-Assembly

A change in dip coating is the spray method that was introduced by Schelnoff et al [94] in which oppositely charged polyelectrolytes are consecutively sprayed onto the substrate with a gap of just few seconds in each deposition step. After each cycle, the surface is washed by spraying deionized water. The results depicted that spraying technique produces a highly uniform multilayer within a small duration, however, morphology, homogeneity and chemical configuration of the sprayed multilayers are almost the same as the conventional ones [95]. The schematic diagram of spray LbL assembly is displayed in Figure 2-4 [96].

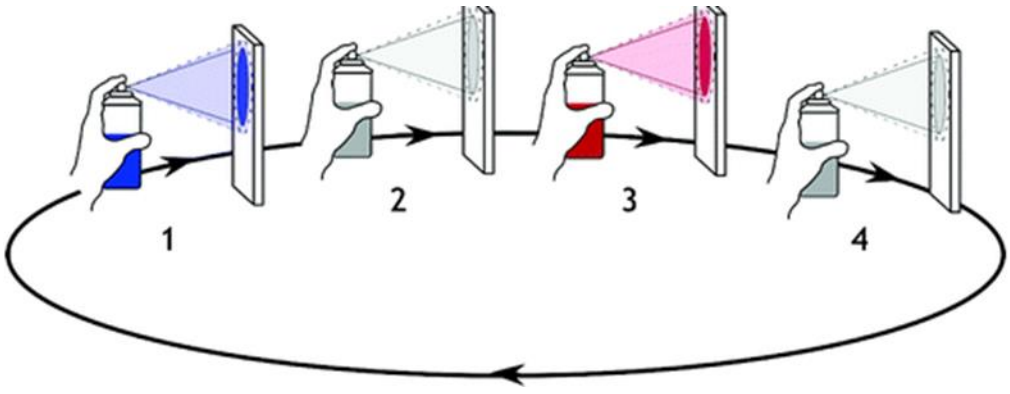

Figure 2-4: Spray LbL self-assembly cycle [96]

Films deposition by spray method allows uniform multilayer growth even under those conditions in which dip coating fails. Schelnoff et al [94]utilized PSS/PDADMAC pair of polyelectrolytes and found that drainage continually removes a definite amount of the additional solution that arrived at the surface. In fact, 99% polyelectrolyte solution is washed off. Therefore, this depletion of polyelectrolyte solution is a drawback of spray method but it can be overcome through recycling the solution.

The membranes prepared by spray technique offer high selectivity for the separation of species [97], [98] and they also provide very high flux. Spray method is beneficial for manufacturing large area membranes and to prepare films for protection from corrosion. Rinsing is vital for good quality multilayered structures.

Fery et al [82] used the LbL spray method to build nano-composite multilayered films that consist of Au nanoparticle and polycation nitro-diazo-resin. The multilayer films were of good quality with controlled structures. These films were helpful to prepare composite films with excellent mechanical properties and higher chemical stability.

Decher et al [96] fabricate polyelectrolyte films by consecutive spraying of PSS/PAH solutions and compared with dipping conditions. The deposition process in spraying is controlled by diffusion. It takes just few minutes to homogenize the surface by adsorption. However, film quality is far better than conventional dipping procedure. PSS/PAH dipping required 15-20 minutes per layer but sprayed films require only 6 seconds for deposition of each layer. Moreover, polyelectrolyte films synthesized by spraying are always thinner as prepared by dipping. These outcomes are in accordance with those that are reported by Schelnoff et al [94]

2.5 Spin Layer-by-Layer Technique

In spin assembly, the oppositely charged polyelectrolytes solutions are spun cast on the substrate by a spin-coater with in between rinsing by de-ionized water on the substrate. The adsorption is greatly enriched because the water molecules are removed by spinning from the surface of multilayer films. The detailed procedure was successfully reported by Char et al [99]. They also demonstrated the structural difference in dip and spin self-assembly methods by preparing the PAH/CdS multilayer films as shown in Figure 2-5.

It is clearly understood that the spin assembly can easily deliver the well-organized internal structure, which cannot be attained through conventional dip coating. The substantial difference in adsorption is the result of different mechanisms of adsorption. In usual dip coating, polyelectrolyte solution is diffused towards the substrate due to electrostatic interaction between oppositely charged chains. After adsorption, these chains reposition on the surface of substrate. Spin coating utilizes the various mechanisms simultaneously, for example, centrifugal and viscous force, air shear, and electrostatic interactions that effect enhanced adsorption, the readjustment of polymer chains on the substrate and removal of loosely bound solution at high rotation rate but in short time. This high speed spinning process is able to control the bilayer thickness as well as the surface roughness and also provides a well-organized inner assembly. During spinning, quick removal of water builds thick layers due to increase in molar concentration of polyelectrolytes. The shearing effect contributes in the alignment of chains in multilayers and therefore it provides a smoother surface. Various mechanisms that take place during spinning process are shown in Figure 2-6 [100]

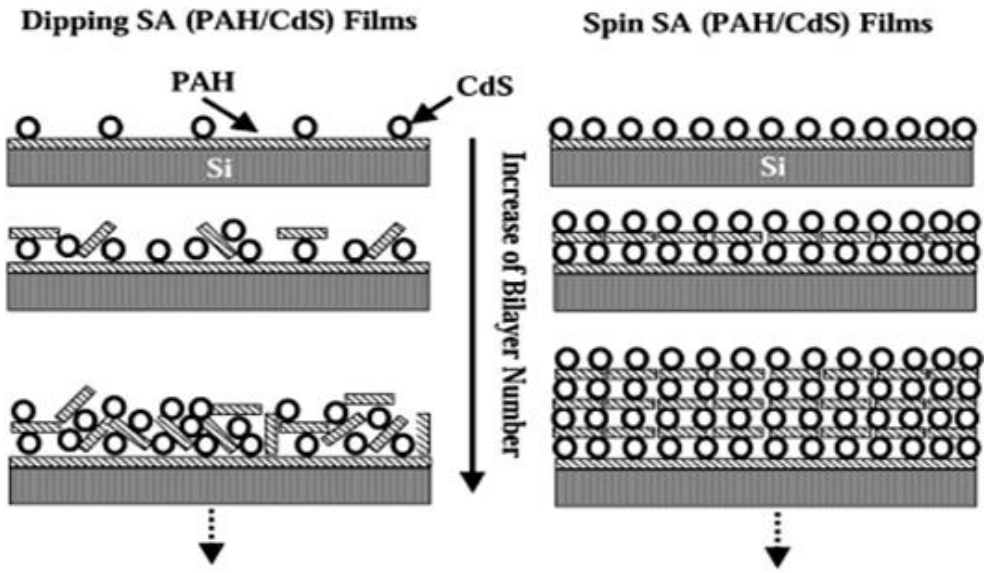

Figure 2-5: Interior structure of PAH/CdS multilayer films by dip and spin coating [99]

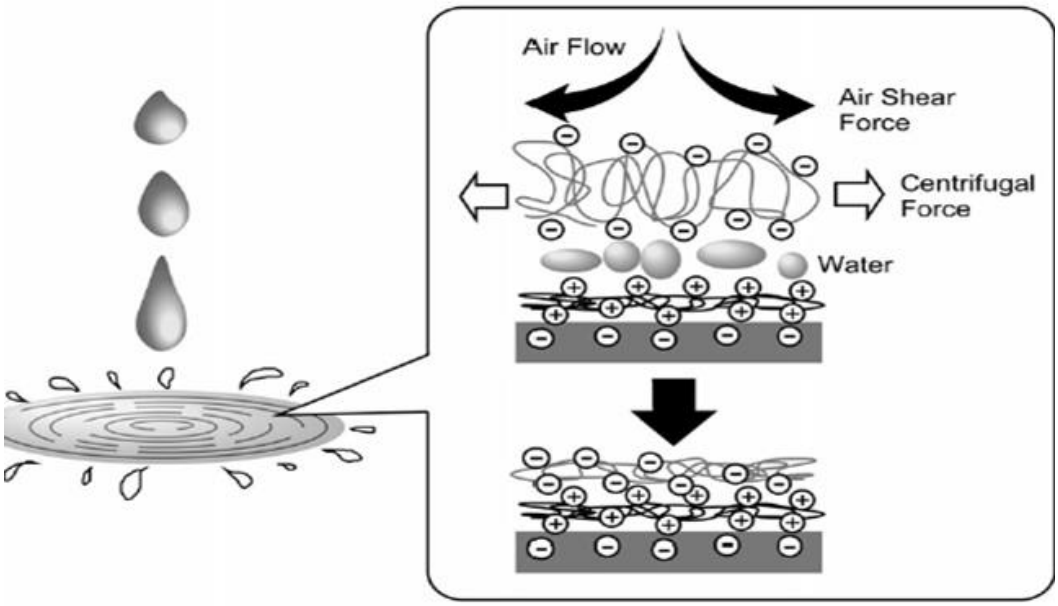

Figure 2-6: Mechanisms involved in spin coating [100]

Therefore, spin coating results in formation of highly ordered structure owing to mechanical effect upon air shear force. Due to this superiority of spin coating over conventional dip coating and spray technique, it is being widely used in these days.

In 2002, Wang et al applied this spinning process to PEI, PDADMAC and dendrimer and demonstrated that it is a useful method for assembling a variety of combinations for polyelectrolyte multilayers. From their experience, they revealed that use of opposite charged polyelectrolytes is not always required while building multilayered films through spin assembly. Therefore, new prospects opened for constructing thin films with similar charge polyelectrolytes [101].

After discussion on significance and difference of dip and spin layer by layer assembly, the effect of several parameters of polyelectrolytes multilayer thin films on membrane modifications and performance will be discussed in the upcoming section.

2.6 Factors Affecting Polyelectrolyte Multilayers Membrane

The deposited number of layers on the substrate has a great influence on the permeation performance. The substrate needs specific amount of layers to cover its surface. However, increase in layer number results in higher resistance. Therefore, by increasing the layer numbers, flux decline occurs. At the same time, salt rejection increases appreciably because of the dense polyelectrolyte multilayer film membrane. So, there should be an optimum number of layers that gives a reasonable flux with compromised salt rejection. Therefore, selection of number of layers demands a tradeoff between flux and salt rejection.

2.6.1 Effect of Layer Number on Permeation Performance

In 2001, Bruening et al [97] deposited PSS/PAH polyelectrolyte pair on porous alumina substrate to synthesize ultra-thin layers. Mixed feed solution was used to investigate flux of mono-, di-, and tri-valent anion. Five bilayers were enough to cover the substrate. SEM analysis showed a defect free film with only 5 bilayers. Flux was affected by varying the bilayers because pore coverage of the substrate depends on coating of layers. From 5 bilayers of PSS/PAH films, chloride flux was $6.5*10^{-8}$ mol/(cm^2.s), sulphate flux was $6.5*10^{-8}$mol/(cm^2.s) and $2.1*10^{-10}$ mol/(cm^2.s) flux of trivalent ions Fe $(CN)_6^{3-}$ was achieved. By increasing layer number to 10, additional resistance was transmitted to PSS/PAH films which decreased the flux. For 10 bilayers, Chloride flux shows slight change whereas SO_4^{2-} and Fe $(CN)_6^{3-}$ transport decreases 5 and 330 times respectively. Selectivity approaches to 7 with just 5 bilayers and is affected a little by varying the layer number. The decrease in flux is attributed to increase in Donnan exclusion effect, as surface coverage increases with deposition of additional layers along with thickness [97].

Bruening and Miller [102] prepared PEM thin films of PSS/PDADMAC on porous alumina substrate. Nano filtration performance was measured through homemade cross flow apparatus at 4.8 bars with feed solution of 0.01 M NaCl and 0.001 M sucrose. It was found that 4 bilayers of PSS/PDADMAC provides pure water flux of 2.5 m^3/ (m^2.day) with only 14 % salt rejection. But with 5 bilayers, flux increased to 3.3 m^3/ (m^2.day) and NaCl rejection enhanced to 21%. Pure water flux decreased to 2.3 m^3/ (m^2.day) with almost 22% salt rejection when the number of coating films were raised to 6.5. By decreasing the salt concentration in depositing solutions, surface charge will reduce, which ultimately results in reduced NaCl rejections or increased sucrose rejection [102].

In 2005, Tieke et al [103] prepared polyelectrolyte membrane by LbL adsorption of poly (vinyl amine) and poly (vinyl sulphate) on PAN/PET support to investigate the performance for RO conditions by changing the numbers of coating layers. It was found that NaCl rejection was increased by increasing layer numbers as indicated in Figure 2-7.

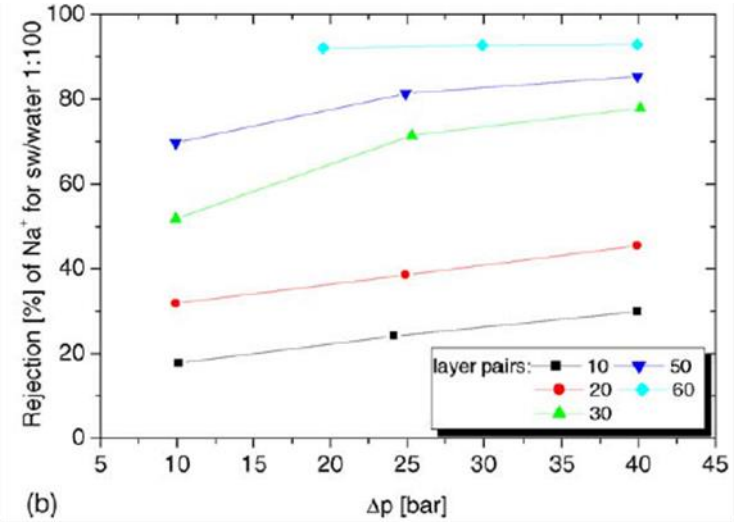

Figure 2-7: Effect of layer number on sodium salt rejection with increasing pressure [103]

It was noteworthy that with 10 or 20 layer numbers the highest possible rejection of sodium ions at 40 bar was not more than 30 and 45 %; respectively. Thus, to get a consistent and realistic statistics, as a minimum, thirty polyelectrolyte layer pairs were needed to be deposited on the porous substrate. When layer number increased to 30, salt rejection jumped to 78 % at 40 bars which indicates that 20 pairs of layers are not sufficient for proper coating, so at 60 layer pairs this rejection was further increased to 93% while operating at the same pressure. The permeation flux also increases by increasing the number of layers on the substrate. Initially the flux was low but for membranes that are modified using 30 or more bilayers, flux of nearly 4 L/m^2h was found at 40 bars which is still quite low. The most important reason of this low flux is the

relatively low hydraulic permeability of the supporting membrane so it was concluded that there is a need to alter the supporting membrane for comprehensive seawater analysis [103].

In 2005, Bruening and Malaisamy [104] prepared PSS/PDADMAC films on polyether sulfone ultrafiltration membrane and investigated the performance at 4.8 bar. Feed solution contains 1000 ppm of each Na_2SO_4 and NaCl. Low solution flux of 1.7 m^3/ (m^2.day) was achieved along with just 59% sulfate rejection from 2 bilayers. With 3 bilayers, flux increased to 1.8 m^3/ (m^2.day) and rejection enhanced to 95%. When number of layers was further increased to 4, solution flux dropped to 1.6 m^3/ (m^2.day) but salt rejection was further increase by 1 %.

Pavasant et al [105] prepared PEM membranes by utilizing CHI/PSS and CHI/SA on electro spun cellulose acetate fiber mat. The modified membranes turned out to be hydrophilic as they hold numerous functional groups that contribute in the hydrophilicity. The salt rejection was determined for the coated membrane samples using a 2000 ppm saline solution. For CHI/SA pair, water flux remains almost constant to 60 L/m^2.h for 15 and 20 bilayers but decreased to 40 L/m^2.h by increasing the layers to 25 as shown in Figure 2-8. In case of CHI/PSS modified films, high flux value of 130 L/m^2.h was initially achieved with 15 bilayers which decreased to 45 L/m^2.h when the number of layers approached 25. This high permeability is due to the porous nature of the substrate. However, with increased layer number, resistance increased and flux decreased through these thicker membranes.

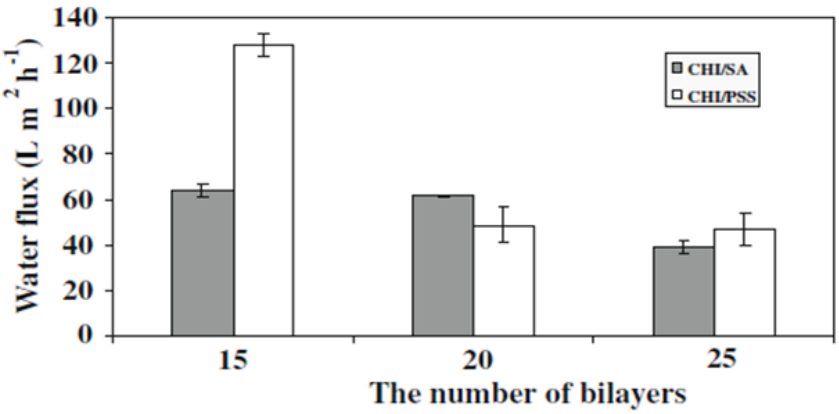

Figure 2-8: Effect of CHI/PSS and CHI/SA layer number on flux [105]

NaCl rejection remain low for both polyelectrolyte pair from 6 % for 15 bilayers and reaches to just 9 % when 20 bilayers are used for coating. On the other hand, for 25 bilayers, a substantial change in value was observed that is shown in Figure 2-9. CHI/SA films provide 14 % rejection as compare to 10 % in case of CHI/PSS multilayer films. This difference is due to dense structure of CHI/SA films. So, desalination performance of CHI/SA pair is far better than CHI/PSS coated films [105].

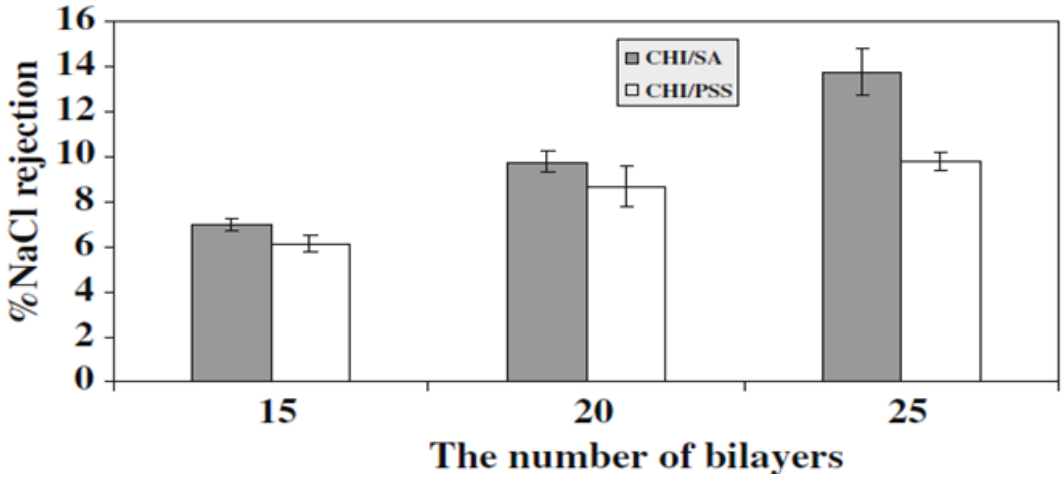

Figure 2-9: Effect of CHI/PSS and CHI/SA layer number layer number on salt rejection [105]

In 2009, Wang et al [106] prepared composite membrane for nanofiltration by depositing SPEEK and branched PEI on hydrolyzed PAN UF membrane. Performance was measured using a 2000 mg/L NaCl solution at 13.79 bars and room temperature. As the layer number increased from 3 to 5, salt rejection increased from 79 % to 89 % but flux declined from 0.60 $m^3/(m^2.day)$ to 0.27 $m^3/(m^2.day)$. After 8 bilayers, no improvement in salt rejection was observed while flux decreased to 0.16 $m^3/(m^2.day)$, as shown in Table 2-1. The performance of these modified SPEEK/PEI films was comparable to commercial RO membrane SWC-4 which provides 96 % salt rejection along with flux of 0.28 $m^3/(m^2.day)$.

Table 2-1: Effect of SPEEK/PEI layer number on Flux and Rejection [106]

Parameters	**Bilayer Number**			
	1	3	5	8
Salt rejection (%)	45	79	89	87
Flux ($m^3/m^2.day$)	1.12	0.60	0.27	0.16

In 2010, Bang et al [107] used the layer by layer assembly for coating of negatively charge polysulfone substrate with the help of weak polyelectrolytes including cationic PAH and anionic PAA. Desalination performance was investigated at 20 bar with NaCl feed solution of 2000 ppm. It was found that with 5 bilayers only 21 % salt rejection and 20 $L/m^2.h$ water flux was achieved. For 10 bilayers, salt rejection rose to 78 % due to dense structure. However, due to increase in hydrodynamic resistance, water flux declined to 8 $L/m^2.h$. As the layers increased to 20, salt rejection reached to 81 % as dense structure is further enhanced. However, the water flux was only 7 $L/m^2.h$. The modified membranes provided salt rejection as good as the commercial RO membrane but there is a need to upgrade water flux.

Malaisamy et al [108] modified the polyamide membrane by using PDADMAC/PSS pair of polyelectrolytes. 1000 mg/L feed solution was used to explore the effect of layer numbers on salt rejection and flux of monovalent ions in ternary mixtures. The permeate flux decreased from around 42 $L/m^2.h$ to 21 $L/m^2.h$ when the layer number increases from 4 to 8. Although water flux decreased by 50 %, the flux of modified membrane is still 30 % higher than that of the commercial BW30 reverse osmosis membrane. Flux Loss was solely due to increase in thickness of the membrane. Sulphate ions were completely rejected but rejection of fluoride ions through the unmodified membrane was 50 % which increased considerably to 70 % by coating 8 bilayers. In case of chloride ions, rejection first increased to 30 % with 4 bilayers which dropped to 20 % when bilayers increased to 8. This difference in salt rejection between these ions is due to their difference in hydration energies which is highest for sulphate and lowest for chloride ions.

Ishigami et al [109] deposited PSS/PAH on commercial RO membrane. The concentration of 500 mg/L of NaCl solution was used as feed to measure salt rejection after 120 minute of filtration experiment. With 6 layers, the obtained flux is around 3.1 L/m^2.h.atm which decreased to 2.5 L/m^2.h.atm by coating 12 bilayers. This is due to increase in hydrodynamic resistance in the polyelectrolyte multi-layered RO membrane. The salt rejection improved from 98 % to 99.4 % as layer number increased from 6 to 12. Results in Figure 2-10 are consistent with the literature because the hydrodynamic resistance increases due to increase in thickness of multilayer films while the effective mass diffusivity in the polyelectrolyte multilayered RO membrane decreases. Thus, the performance of PEM reverse osmosis membrane can also be tuned by varying the deposition cycle on the substrate.

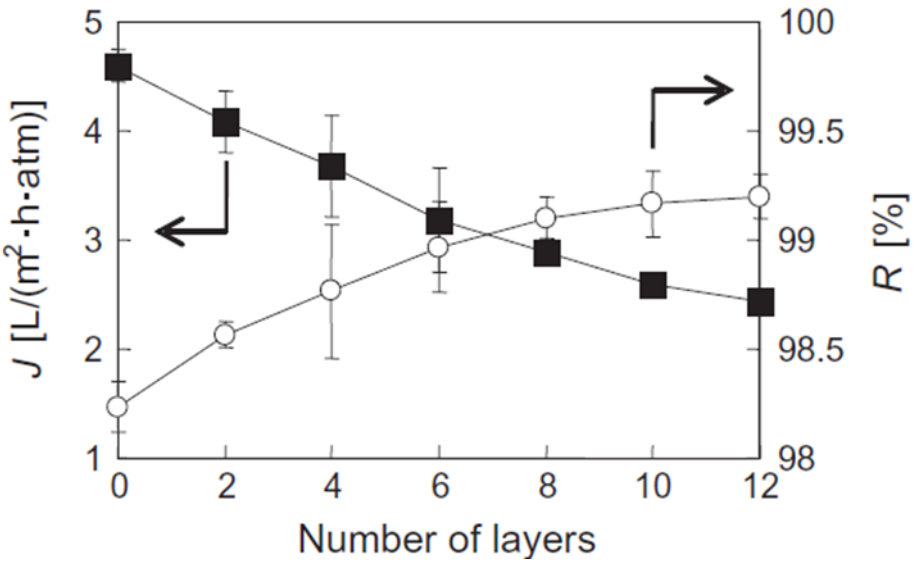

Figure 2-10: Effect of layer number on performance of PSS/PAH modified RO membrane [109]

Kentish et al [110] studied the behavior of polyamide reverse osmosis membrane by depositing PEG acrylate multilayers. Permeation tests were performed in artificial seawater with 30.83 g/L NaCl and 1.11 g/L $CaCl_2$ under 800 Psi (55 bar) for 3 h. They showed that membrane modified with one pair of layer have somewhat lower flux compared to two layer pairs. This is due to the variation in performance of the each individual polyamide layer. The virgin membrane has 122 $L/m^2.h$ water flux which decreased to almost 100 $L/m^2.h$ and 112 $L/m^2.h$ by coating one and two bilayers, respectively. Flux decreased but salt rejection increased as compared to the base membrane which had 92 % salt rejection. The rejection rises to 94% by depositing one and two bilayers. The increased salt rejection is relatively small which indicates that coating is thinner. The hurdle in achieving 99% rejection as expected in commercial RO membranes is due to higher concentration polarization in the arrangement of dead end cell apparatus.

Farid et al [111] modified the membrane using spin assisted layer by layer assembly by depositing 60 and 120 bilayers of PAH and PAA. To inspect the stability of membrane, cross flow permeation test was conducted for 40 hour under conditions of 40 bars, salt concentration of 2000 ppm and pH of 6. Under same conditions it was revealed that 60 bilayers gave 58 % salt rejection which was increased to 65 % when bilayers were doubled. Flux provided by the 60 bilayers is around 30 $L/m^2.h$ but when bilayers are increased to 120, flux declined 50 % and reached a value of $L/m^2.h$. These values are in accordance with solution diffusion theory which states that flux and membrane thickness are inversely proportional to each other. Therefore, flux drop occurred by the growth of thickness as the number of bilayers increased over the substrate. A very interesting

finding was noticed where slight increase in salt rejection showed that Donnan Exclusion is not playing its role; otherwise significant rise in rejection must be noted.

In a separate study, performance of PAH/PAA modified films with a higher feed saline water concentration of 15000 ppm at 700 psig (48 bars) was discussed [112]. With 15 bilayers almost 75 % salt rejection was achieved which increased to 88 % with 35 bilayers as shown in Figure 2-11.

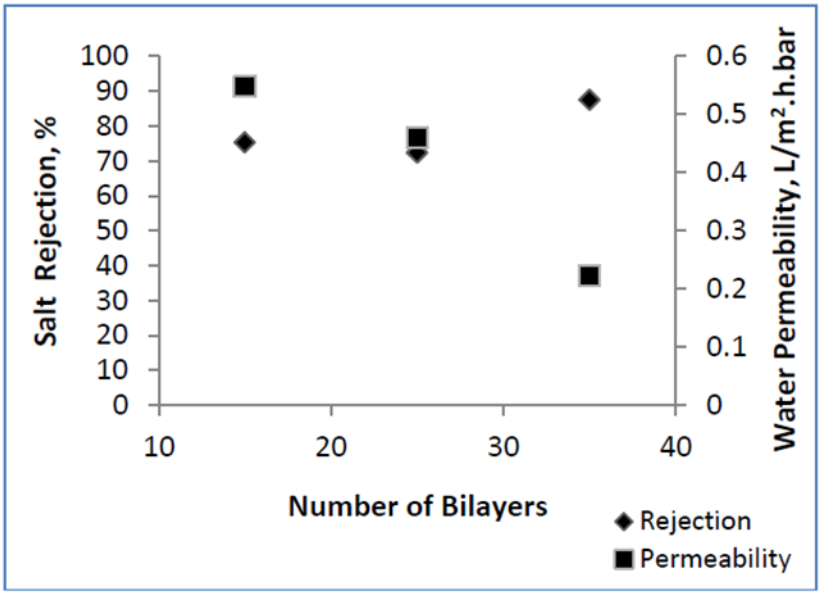

Figure 2-11: Effect of layer number on Salt Rejection and Water permeability [112]

It was found that 15 and 25 bilayer membranes produced nearly identical salt rejection but with a different flux. This consequence suggested that coating might not completely cover the substrate. Moreover, this result also point out that flux was considerably influenced by thickness of films. Fifteen bilayers provided almost 0.55 L/m^2.h.bar of water flux but 25 bilayers reduced this value to 0.46 L/m^2.h.bar which further reduced to almost 0.22 L/m^2.h.bar by coating 35 layers on the substrate. Higher Donnan potential

offers greater electrostatic repulsive force to the ions which in turn yields higher rejection.

In 2013, Lee et al [113] synthesized polyamide membrane from MPD and TMC on PAN UF support via LbL assembly. Before synthesis, they blocked the pores of the support using single layer of PEI/PAA. Performance was evaluated at 15.5 bar using cross flow apparatus with 2000 mg/L aqueous solution of NaCl. They found that flux and rejection is greatly dependent on number of bilayers. As the layer number increased from 10 to 15, flux decreased from 21.5 to 20.7 $L/m^2.h$ but rejection increased from 95.7 to 98.7 %. This is in accordance with solution diffusion model which states that flux is inversely related to thickness of multilayer films. They also compared their result with membrane performance that was prepared through interfacial polymerization (IP). Membranes prepared with conventional IP exhibited a flux of 11.8 $L/m^2.h$ with 96.8 % salt rejection. The flux was far less than that attained by membranes prepared with LbL (21.5 $L/m^2.h$ and 95.7%) showing the superiority of the LbL method and its suitability for RO applications [113].

2.6.2 Effect of Layer Number on Film Thickness

As layer number has its effect on permeation performance, it also has a pronounced effect on film thickness. Increasing the number of layers, convey more quantity of polyelectrolyte on the substrate which results in greater thickness and consequently will have an effect on performance of prepared membranes.

In 2001, Bruening and his coworkers [114] described the building of PAA/PAH films on alumina support. The deposition results in ultrathin composite membranes. Thickness was measured by ellipsometry. Thickness is affected by increasing layer numbers which eventually change the anionic flux. Four bilayers provided 316 Å thick-films which increased 23% to 390 Å by only increasing layers to 4.5. Excessive thickness of layers will offer large mass transfer resistance that will reduce flux and will drop the overall membrane performance.

Bruening and Miller [102] prepared PEM thin films of PSS/PDADMAC on porous alumina substrate for Nano filtration application. The thickness of 3.5 layers film was 17.3 nm which increased to 21 nm for 4 bilayers and to 34 nm for 5 bilayers. It is consistent with earlier results which indicate that the increase in layer number will increase the film thickness.

Deratani et al [115] prepared polyelectrolyte multilayer thin films consisting of CHI/ALG pair of polyelectrolytes. The chosen substrate was cellulose acetate membrane. The coating thickness of films was measured by ellipsometry. It was found that an increase of 0.6 nm thickness took place with each pair of ALG/CHI. 19 nm thick membrane was achieved with 30 layer pairs, which provide excellent performance.

In 2007, Bruening et al [116] prepared PSS/PAH and PSS/PDADMAC film through dip-LbL assembly. For 3 layers of PSS/PDADMAC, 16.4 nm films were obtained which increased to 26.7 nm for 4 bilayers. In addition, the film thickness increased to 32.9 nm when 5 bilayers were deposited. Deposition by PSS/PAH generated relatively thinner films as compared to PSS/PDADMAC. With 4 bilayers, 13.7 nm thick films were obtained which increased to 19.4 nm for 5 bilayers. It is clear that PSS/PAH films are thinner than PSS/PDADMAC which provides comparatively better performance.

Seo et al [117] studied the surface morphology of multilayer films by depositing hydrophobically modified PEO/PAA on silicon wafers by using dip and spin LbL methods. Initially, the film development of dip coated films displays exponential growth and become linear after 15 layers as indicated in Figure 2-12. For 20 bilayers, 2000 nm thickness was obtained which increased to 4000 nm for 30 bilayers and 11000 nm for 50 layer pairs. Therefore, an average of 210 nm increment per bilayer takes place by dip coating. Spin coating provides linear growth in thickness by increasing layer numbers. In the range of 10 to 50 bilayers of coating, an average increment of 21 nm per bilayer was recorded. It was also concluded that spin layer by layer method provides distinct surface morphology with thin multilayer films which is an indication of better performance.

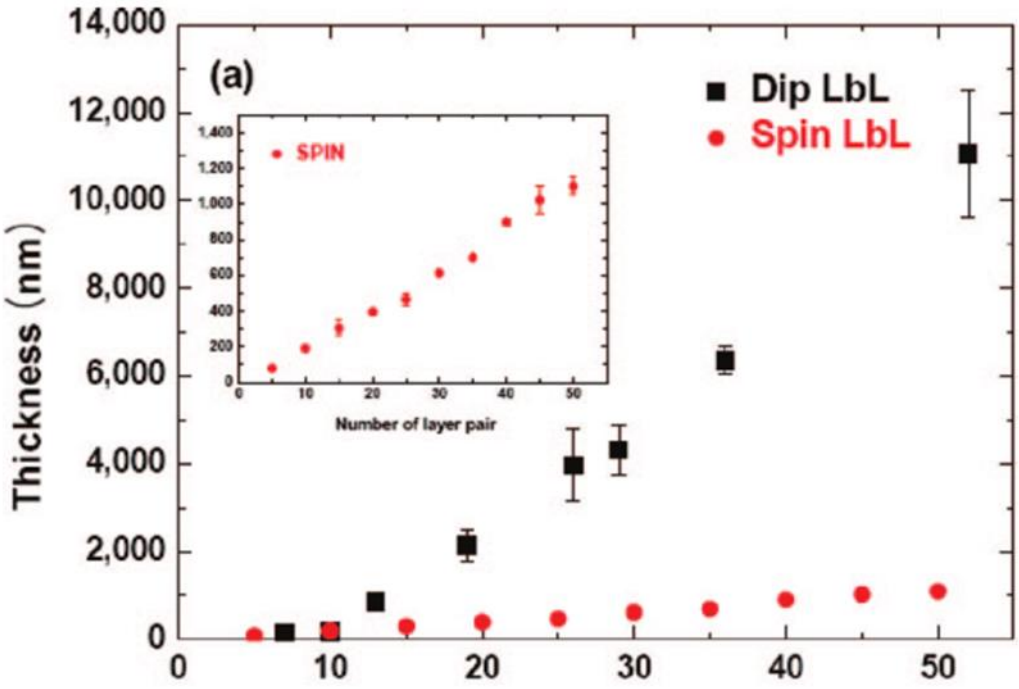

Figure 2-12: Effect of layer numbers on PEO/PAA multilayers using dip and spin coating [117]

Bang et al [107] used LbL assembly for coating a negatively charged polysulfone substrate with the help of a weak polyelectrolytes including cationic PAH and anionic PAA. Various pH combinations were applied but LbL assembly produced the thickest layers under a pH of 7.5 for PAH and pH of 3.5 for PAA. They found that as the layer number increase from 1 to 10, the thickness of the modified multilayer films increase from 3 nm to 250 nm, as shown in Figure 2-13. The coating of these multilayers pursues a unique exponential growth design. Because PAH diffuses into the film during deposition, it diffuses out during rinsing and further diffuses out during PAA deposition. This is known as in-out diffusion mechanism which is the foundation for exponential thickness growth.

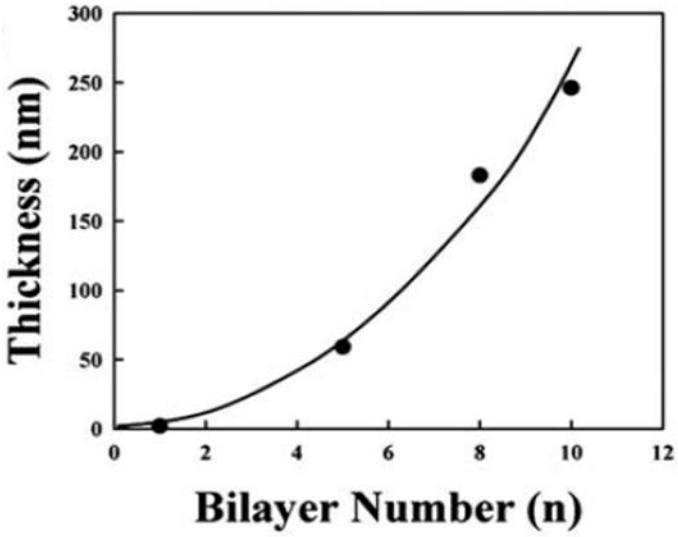

Figure 2-13: Effect of layer number on PAH/PAA film thickness [107]

The cross-section SEM image for 10 layer substrate with thickness of 250 nm is shown in Figure 2-14 [107]

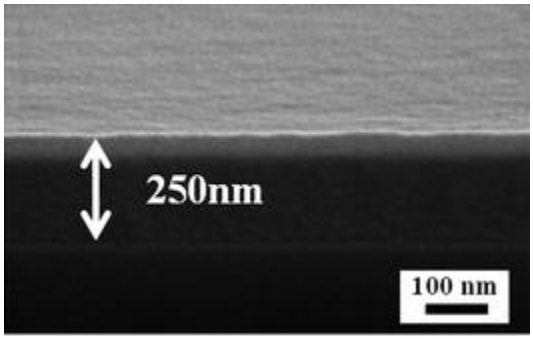

Figure 2-14: Cross-section SEM image of 10 layers PAH/PAA film [107]

Effect of thickness of PAH/PAA pair was also demonstrated by Farid et al [112]. Spin assembly was applied at 3000 rpm to study effect of layer numbers on film thickness. With 10 bilayers, 27 nm thick films were achieved, while for 12 bilayers around 34 nm film thickness was achieved which reached to 44 nm for 16 bilayers. 3-4 nm thickness

was amplified by increasing each bilayer which depicts the promising feature of spin coating.

2.6.3 Effect of Layer Number on Zeta Potential

Measurement of Zeta potential is performed through a streaming potential analyzer. This analyzer investigates the surface charges on the membrane. The quantity of surface charge will improve the interaction between the substrate surface and the depositing polyelectrolytes [118].

Bruening et al [116] investigated the effect of layer numbers on zeta potential by depositing PSS/PDADMAC films through dip coating. It was found that on going from 4 to 5 bilayers on negatively charged polyethersulfone (PES) membrane, zeta potential was reduced from -6.86 mV to -1.2 mV. The detailed description behind this, along with its effect on performance was not discussed.

Ouyang et al [73] compared the zeta potential of PSS/PAH and PSS/PDADMAC films by depositing them on polyethersulfone membrane. Measurement was done by streaming potential analyzer to show that the charge of PEMs surface plays an important role in ion separation. KCl solution served as an electrolyte. The bare PES membrane has a potential of -18mV. For PSS/PAH layer, zeta potential increased to 25 mV after the first bilayer, to 30 mV for 2 bilayers, remained constant after 3 bilayers, and decreased to approximately 22 mV after depositing the fourth bilayer. In case of PSS/PDADMAC films, zeta potential increased to 32 mV just after the first bilayer and reached to 35 mV after the third and continuously increased to about 37 mV after fourth bilayer. For PSS/PDADMAC films, zeta potential always increases by increasing layer number.

Moreover, positive zeta potential induced by PDADMAC is always higher than that which is induced by PAH. The combined results are shown in Figure 2-15.

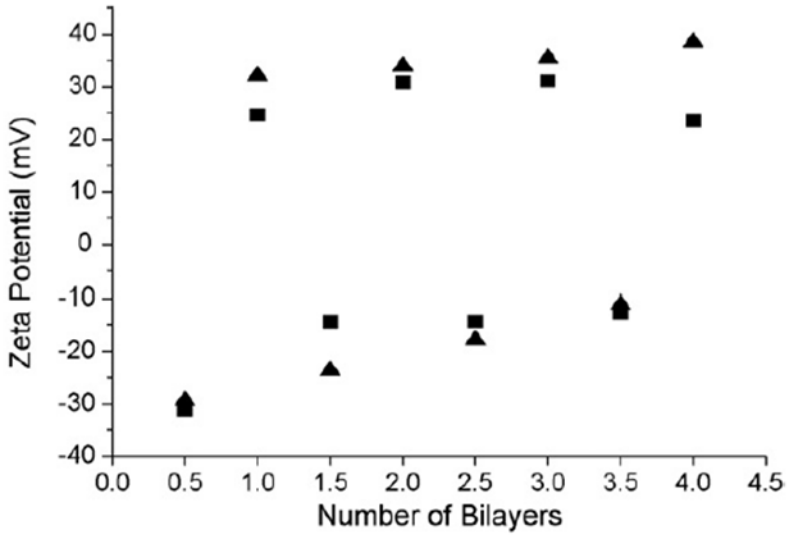

Figure 2-15: Comparison of Zeta potential of PSS/PAH (squares) and PSS/PDADMAC (triangles) multilayer films along with increasing layer numbers [73]

Malaisamy et al [119] modified the polyamide membrane by using PDADMAC/PSS. The negative zeta potential of −25 mV is a clear sign that unmodified NF270 membrane is negatively charged. The number of coating layers has substantial impact on zeta potential. The zeta potential turned into +20 mV when one layer of PDADMAC was deposited on the substrate, and inverted again to -20 mV by depositing another layer of PSS as indicated in Figure 2-16. The zeta potential has repeatedly increased by growing number of layers. Greater quantity of negative surface charge is desirable for the studied system because when dealing with a mixture of ions, greater magnitude of zeta potential will significantly affect the selectivity of ions.

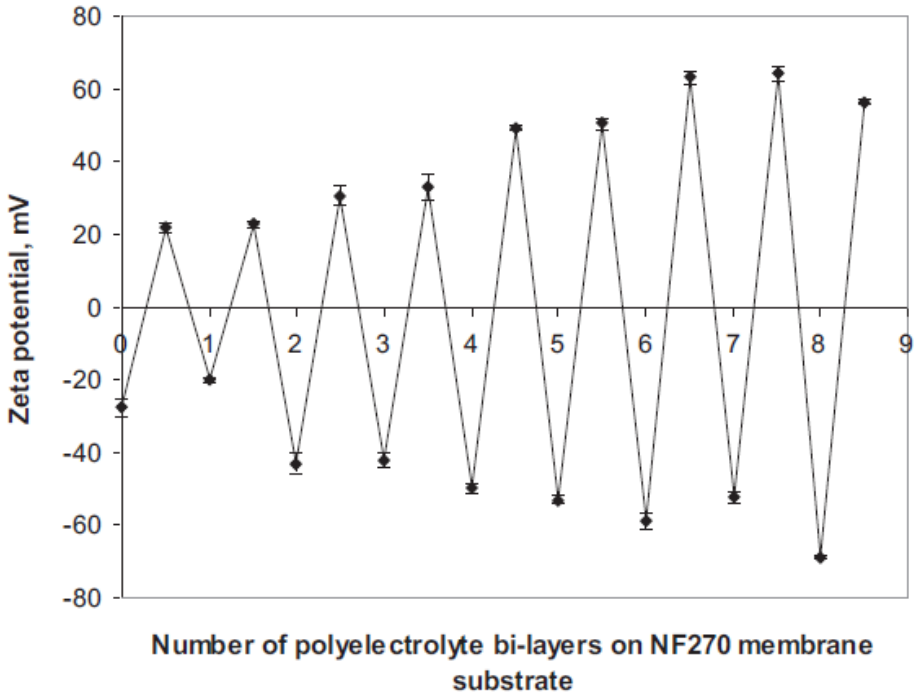

Figure 2-16: Effect of PDADMAC/PSS layer number on zeta potential [119]

Ishigami et al [109] deposited PSS/PAH via LbL method on commercial RO membrane to improve its performance. Zeta potential was measured by electrophoretic apparatus by adjusting pH of depositing solution at 5.5. A value of –18 mV of original RO membrane indicates that it is negatively charged. The zeta potential of the membrane after 2 layers was shifted to -30 mV and it moved to +18mV after depositing a third layer. So, the surface charge becomes positive each time after depositing PAH and returns to negative after adsorption of PSS. For 6 and 8 bilayers, zeta potential remain almost same (-16 mV) which is higher than the base membrane as shown in Figure 2-17.

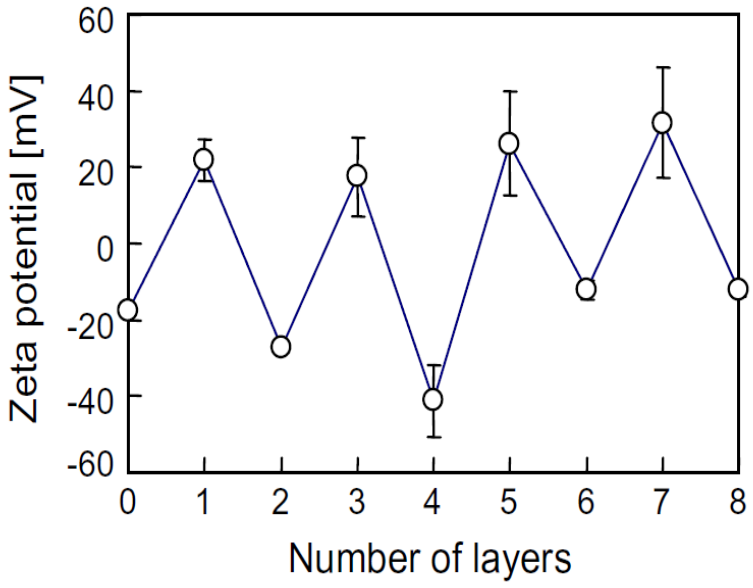

Figure 2-17: Effect of PSS/PAH multilayer films on zeta potential [109]

2.6.4 Effect of Layer Number on Contact Angle

In order to attain hydrophilic surface, low value of contact angle is required. By increasing the number of layers, contact angle decreases which in turn enhance the hydrophilicity of membranes.

Char et al [120] studied the wetting behavior of multilayer films by measuring contact angle. They deposited hydrophobically modified PEO/PAA on silicon wafers by using dip and spin LbL methods. For dip assembly, contact angle increased to a maximum level of 90^{o} for 26 layers and then fell down to 35^{o} after 40 layers. It eventually dropped to less than 10^{o} for 52 layer pairs. However, for spin-assisted films, advancing contact angle remains comparatively constant and vary between 70-80^{o} when layer number increased from 20 to 52. It was concluded that there is a limit of layers -in case of dip coating- above which the surface became rough. However, uniform layers with smooth surface are generated from spin assisted LbL coating.

Kochen et al [121] modified the polyether sulfone ultrafiltration membranes by alternately depositing PEI and PSS. Contact angle of modified membrane was determined after PEI coating by using dynamic Wilhelmy method. The unmodified PES substrate has advancing angle of 65^{o} which decreased to 52^{o} by deposition of PEI. The decrease in contact angle shows that the surface has become more hydrophilic after coating.

Malaisamy et al [108] modified the polyamide membrane by using PDADMAC/PSS pair of polyelectrolytes. A goniometer was used to check the hydrophilicity of the modified surfaces by measuring the contact angle. The unmodified membrane possesses a contact angle of 32° indicating that surface is already hydrophilic. After depositing the first layer of PDADMAC, contact angle increased to a value of 65° indicating that surface has become less hydrophilic. A drop in contact angle to 25^{o} was observed after 5 bilayers, as indicated in Figure 2-18. Then, an increase in hydrophilicity was detected with 6 and 8 bilayers. This increased hydrophilicity is attractive while dealing with aqueous separations. Therefore, it was concluded that PDADMAC terminated films make the surface hydrophobic but hydrophilicity is achieved by PSS terminated films.

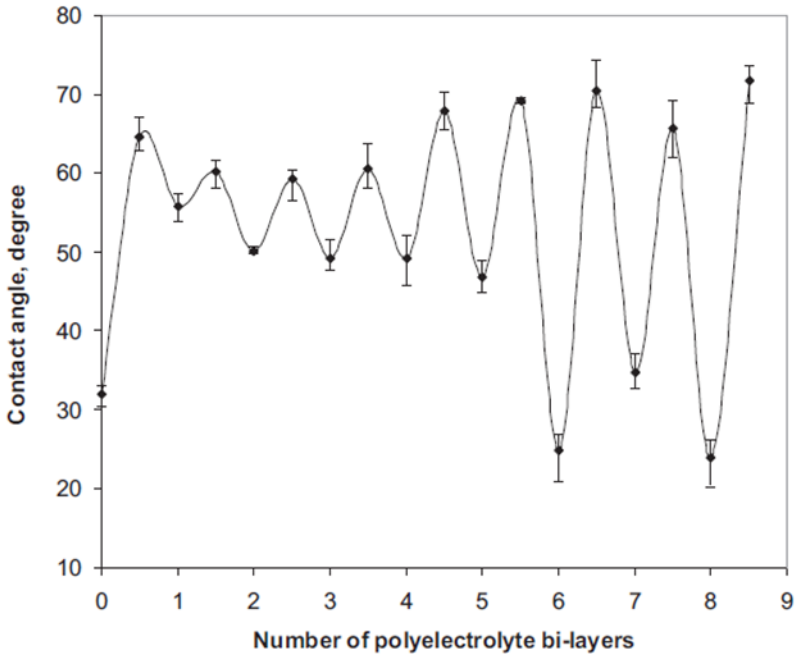

Figure 2-18: Effect of PDADMAC/PSS layer number on contact angle [109]

PSS/PAH pair of polyelectrolytes were used to modify a commercial RO membrane via LbL method [109]. To evaluate membrane surface hydrophilicity, air bubble contact angle was measured. It is shown in Figure 2-19 that as the layer number increased, contact angle also increased. Air bubble contact angle of unmodified RO membrane was 80^{o} and increased to 85^{o} after 2 bilayers. Thus, the modified surface becomes more hydrophilic by growing the layer number. More hydrophilicity was achieved when contact angle approached to 100^{o} by coating 10 bilayers. The reason of increased hydrophilicity is that polyelectrolytes are water soluble substances and they form loops and tails which also increase surface charge density. This rise in surface charge density contributes in the hydrophilicity of the membrane.

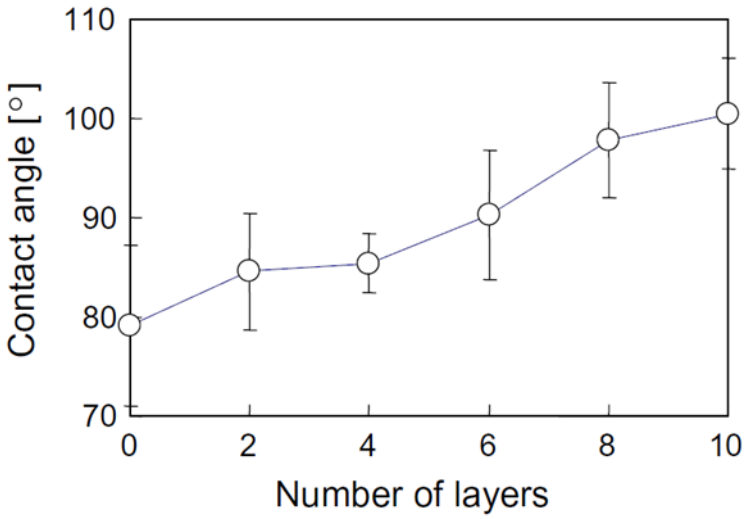

Figure 2-19: Effect of PSS/PAH multilayer films on contact angle [109]

Wang et al [122] studied the behavior of seawater (SW30) and brackish water (BW30 LE) polyamide RO membrane by depositing just two PEG acrylate multilayers. Seawater of unmodified membrane has a contact angle of 63^{o} which decreased to 52^{o} and 41^{o} after coating one and two bilayers respectively. Brackish water unmodified membrane has contact angle of 42^{o} which decreased to 25^{o} and 24^{o} after deposition of first and second bilayer accordingly. Higher contact angle designates higher hydrophobicity of membrane surface. However, in both cases, contact angles of the modified membranes are lower as compare to virgin membrane. Though, the improvement is less observed in case of brackish water membrane. Overall, the surface showed better hydrophilicity as the number of deposited bilayers increased.

The hydrophilicity of PSF membrane was investigated when modified by 60 and 120 bilayers of PAH/PAA [111]. A goniometer was used to measure contact angle through sessile drop method. The measured contact angle of the membrane after 60 bilayers was 35.48^{o}, while it was 34.53^{o} after 120 bilayers. The decrease in value was markedly

observed after 60 bilayers as compare to bare PSF substrate that has a contact angle of 79.8^{o}. However, no substantial variation was observed when number of layers increased from 60 to 120 bilayers. Overall, the surface became smoother and more hydrophilic after polyelectrolyte deposition. Modified multilayers contact angle was also compared with commercial seawater membranes as shown in Table 2-2.

Table 2-2: Effect of PAH/PAA layers on contact angle and roughness [111]

Membrane type	**Contact angle (degree)**	**RMS roughness (nm)**
$[PAH/ PAA]_{60}$	35.48 ± 6.38	11.26 ± 1.80
$[PAH/PAA]_{120}$	34.53 ± 3.48	10.33 ± 1.58
PSF	79.81 ± 8.51	28.18 ± 4.73
Hydronautics SWC	96.05 ± 4.35	136.56 ± 15.95
Hydronautics ESPA	46.23 ± 4.07	103.67 9.98

2.6.5 Effect of Layer Number on Roughness

Decreasing the membrane surface-roughness is an effective method to control the membrane fouling. Using LbL polyelectrolyte deposition, the rough ridge and valley surface of the membrane will be covered and the surface roughness will be decreased.

Seo et al [117] studied the surface roughness of multilayer films by depositing hydrophobically modified PEO/PAA on silicon wafers by using dip and spin LbL methods. It was found that with dip coating, roughness increased from nanometers to micrometers with increasing layer numbers. Interestingly, roughness increased too much after 26 pairs of layers as shown in Figure 2-20. However, with spin assembly roughness remains almost constant with increasing number of layers. This small surface roughness shows that the temporary aggregation of polyelectrolytes chains is suppressed for spin coating. However, this micelle formation was prominently observed in the dip method. Therefore, spin assisted assembly of polyelectrolytes provided smoother films.

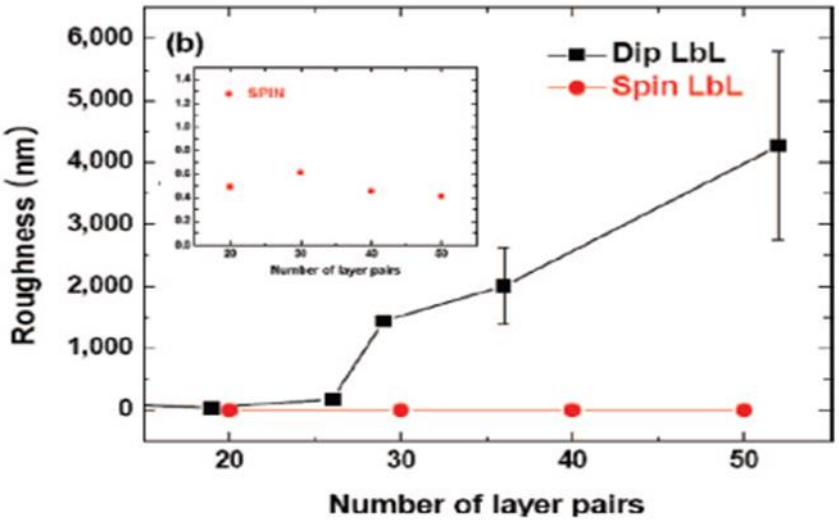

Figure 2-20: Effect of PEO/PAA layer number on roughness [117]

Xu et al [123] prepared multilayered film on PAN ultrafiltration membrane through dynamic LbL assembly. The surface roughness was studied after depositing the copolymer PSS co-maleic acid along with PAH and PSS. The average roughness for one bilayer was approximately 7.2 nm but increased to 21.95 nm with 2 bilayers. Maximum roughness observed was 41.66 nm with 4 bilayers. Since hydrophilic surface is advantageous for improving the fouling resistance, the membrane with lower bilayer number showed better performance in terms of salt rejection and flux.

Kentish et al [110] studied the roughness behavior of polyamide reverse osmosis membrane after deposition of PEG acrylate multilayers. After the AFM analysis, it was revealed that with one bilayer coating roughness increased to 52 nm and remains constant even after 2 bilayers. However, the virgin membrane roughness was 42 nm. Therefore, polyethylene glycol multilayers didn't improve roughness in this case. This might be due to low number of deposited layers or due to formation of thin films.

Ishigami et al [109] deposited PSS/PAH on commercial RO membrane through layer by layer method. They found that the number of layers has significant effect on the roughness. The roughness of original RO membrane was 54.9 nm. After 6 bilayers, it decreased to 44 nm and continued to decrease to 34.8 nm with 12 bilayers. These results indicate that roughness is inversely proportional to the number of layers. Therefore, morphology of this smooth surface is projected to enhance the antifouling potential of modified membranes.

The SEM images of base and modified membranes are presented in Figure 2-21 [109]. It is obvious that the surface becomes smoother by increasing the layers number.

Membrane surface is covered with thin layer when it is deposited with 6 layers (B1), but with 12 layers the membrane surface is more covered with polyelectrolytes which makes the membrane surface smoother (C1).

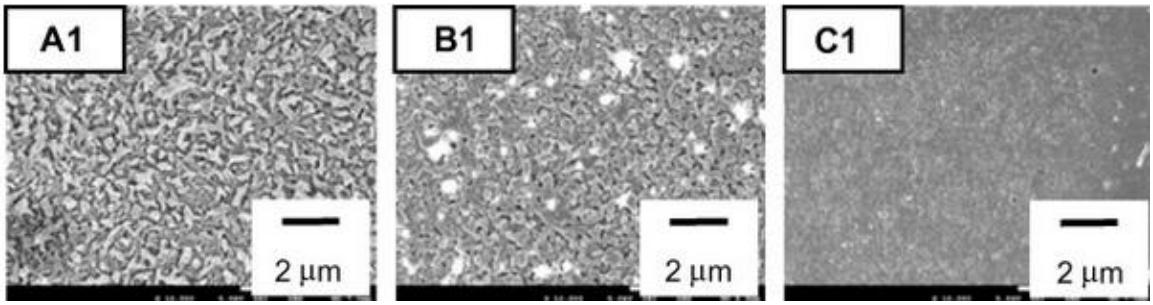

Figure 2-21: SEM image of base membrane (A1), 6 layered (B1) and 12 layered (C1) membrane [109]

The rough valley parts of the membrane are filled with the polyelectrolyte deposition and it is confirmed with AFM images as shown in Figure 2-22 [109].

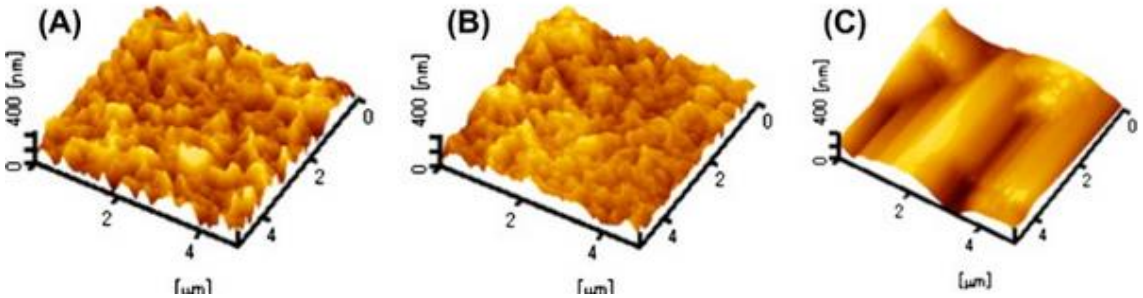

Figure 2-22: AFM images of base membrane (A), 6 layered (B) and 12 layered (C) membrane [109]

Effect of layer number on surface roughness was investigated by depositing 60 and 120 bilayers of PAH/PAA on membrane with spin assisted layer by layer assembly [111]. AFM images showed that bare substrate has roughness of 28.18 nm which decreased to 11.26 nm after 60 bilayers. When the number of layers was increased to 120, roughness decreased further to 10.33 nm. The surface roughness decreased significantly due to large number of layers on the substrate which also enlarged its thickness.

2.6.6 Effect of Polyelectrolyte pH on Film Thickness

pH of depositing polyelectrolyte solution has pronounced effect on multilayer film thickness. Depending upon the type of polyelectrolyte, increase in pH either produces thick or thin films since each polyelectrolyte has its specific charge density and distinct dependence of pH on ionization state.

Bruening et al [124] studied effect of pH on film thickness by depositing polyelectrolyte multilayers on porous alumina including PAA/PAH and PAA/PDADMAC. Dip coating was used to construct these layers. Film thickness was measured by ellipsometry. When the pH of each depositing solution was adjusted to 4.5, the film thickness was 51.7 nm after 4 bilayers of PAA/PAH. However, upon changing the pH to 7.0, the film thickness decreased 77% and dropped down to 11.9 nm. By increasing the pH of solution, surface charge density increased and degree of ionization of both PAA and PAH increased from 65% to 80%. In case of 5 bilayers of PAA/PDADMAC, the film thickness was 37.2 nm at a pH of 4.5. In addition, the flux was greater than PAA/PAH films, however the sulfate rejection declined. Thickness decreased significantly to 4.3 nm when the pH increased to 7.0. Although, flux was high but rejection was too low as film was very thin. It was concluded that separation is greatly affected by of multilayer film thickness and the pH of the polyelectrolyte solutions.

Tieke et al [125] alternately deposited the polyvinyl amine and Hexacyclen trisulfate on porous polymer support and investigated effect of pH on film thickness. Measurement was recorded for 12 bilayers. Film thickness of 5 to 6 nm was achieved at pH 2 and 4. Thickness continued to increase with the pH of dipping solutions. When the pH changed

to 6.0, the thickness of film increased to 10 nm and further increased to 20 nm at pH of 8.0. The reason of increased thickness is that PVA is partly protonated at higher pH and to counterbalance the previously adsorbed carboxylate groups of Hexacyclen trisulfate, additional PVA has to be deposited.

The performance of PAH/PAA modified films can by controlled through the thickness of films via tuning the pH of polyelectrolyte solutions [112]. Ellipsometry was used to measure film thickness. At low pH of PAH and high pH of PAA comparatively thin films are generated as shown in Figure 2-23.

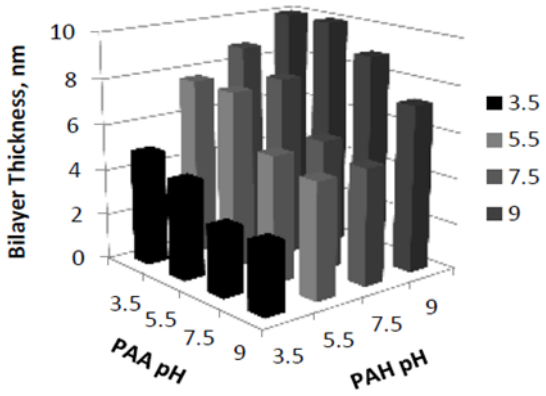

Figure 2-23: Effect of PAA/PAH pH on film thickness [112]

For example, 3.5 pH of PAH and 9.0 pH of PAA yield almost 2 nm thick films. Thickness increased to approximately 10 nm when pH of 9.0 for PAH was used along with pH of 3.5 for PAA. This decrease in thickness was due to the strong effect of pH on the degree of ionization of both polyelectrolytes. In addition, earlier adsorbed layer has to neutralize the new adsorbed layer to attain optimum thickness.

Hong et al [126] deposited PSS/PDADMAC on porous alumina support for selective removal of phosphate ions. Results revealed that flux and rejection are strong functions of

pH. By increasing the pH from 5.6 to 7.0, flux remained constant at 2.2 m^3/m^2.day but rejection increased from 85.6 to 90.8 %. Further increase in the pH to 8.4, flux slightly increased to 2.4 m^3/m^2.day but rejection increased to 98.3 %. A little rise in flux is due to the fact that both are strong polyelectrolytes and charge density doesn't vary largely with pH.

2.6.7 Effect of Polyelectrolyte Coating on Membrane Fouling

In 2007, Aravind et.al [120] fabricated a novel ultrafiltration membrane by modifying the surface of micro filtration membrane using CHI/PSS polyelectrolyte pair. They performed the fouling study using BSA with modified membranes at a pressure of 10 Psi by varying the number of bilayers. It was found that protein rejection increased with increase in layer number but flux decreased. With 5 bilayers, 11 % rejection of BSA was found with flux of 16 $m^3/ (m^2$.day) which increased to 72% for 7 bilayers. Maximum rejection of 94.7 % was resulted for 9 bilayers with flux of 0.49 $m^3/ (m^2$.day). This study points out that proteins can be filtered by depositing few bilayers of polyelectrolyte on micro filtration membrane.

In 2009, Wang et al [106] investigated antifouling ability of composite membrane by depositing SPEEK/ PEI (branched) on hydrolyzed membrane. Performance of prepared membrane with 3 bilayers was analyzed by dead end filtration system using model foulant such as humic acid (HA), bovine serum albumin (BSA), and sodium alginate (SA). Foulants were tested individually using 2000 mg/L NaCl solution with 1000 mg/L foulant solution at 13.79 bars and room temperature. Figure 2-24 shows that polyelectrolyte multilayered membrane demonstrated nearly constant performance in

terms of normalized flux (flux/initial flux) with time, whereas commercial NTR 7450 membrane showed a slight flux drop during filtration. It was anticipated that improved fouling resistance is the result of hydrophilic ionic crosslinks that were present in PEMs. Similar observation was recorded in case of humic acid and sodium alginate. Contact angle and surface roughness were not studied to further explore the antifouling characteristics.

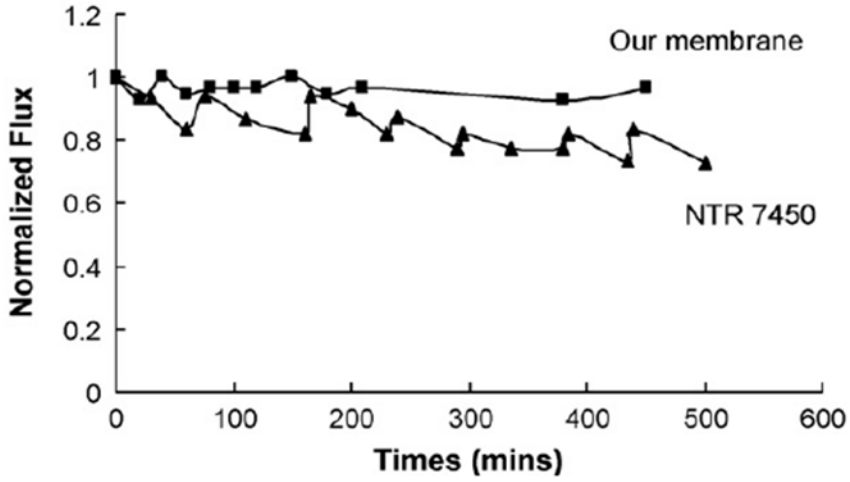

Figure 2-24: Fouling performance using BSA as foulant [106]

Kentish et al [110] studied the fouling behavior of modified polyamide reverse osmosis membrane by depositing Polyethylene glycol acrylate multilayers. Fouling tests were executed with artificial feed composition of 30.83 g/L NaCl and 1.11 g/L $CaCl_2$.

100 mg/L of sodium alginate was added as a model foulant. Three experiments with dead end filtration were performed at 800 psi for 3 hours. Before fouling, the flux of a two-bilayers-modified membrane was 112 L/m^2.h which somehow remained constant after the first run. However, for second and third run a slight drop in flux (110 L/m^2.h) was observed. AFM analysis revealed that there was no improvement in the surface roughness

after 2 bilayers deposition but the contact angle decreased to 41^{o} as compared to un-coated membrane with contact angle of 63^{o}. Therefore, increased hydrophilicity was the major justification for improved fouling resistance. It can be seen in Figure 2-25 that coated membranes are capable of maintaining water flux even after three runs, which is an indicator of their enhanced fouling resistance. Moreover, two bilayers modified membrane is better in terms of flux as compare to one bilayer membrane.

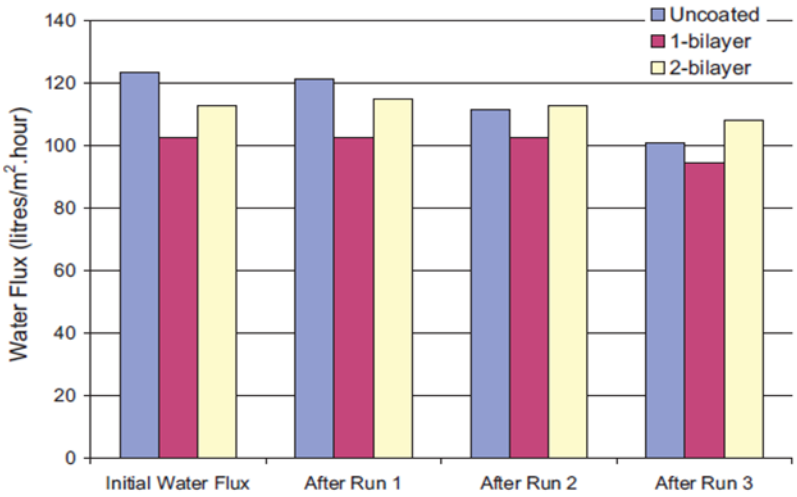

Figure 2-25: Water Flux at 800 Psi before and after fouling

Ishigami et al [109] deposited PSS/PAH on commercial RO membrane to investigate antifouling resistance. It was anticipated that increased hydrophilicity and decrease in roughness will improve the fouling resistance. For this purpose, filtration experiment was performed for 120 min with BSA solution. From the relative permeability as shown in Figure 2-26, it is clear that antifouling ability is upgraded with increase in layer number. Since BSA is negatively charged with isoelectric point of 4.8 [127] and from the zeta potential of -40 mV, it was confirmed that modified membrane with 4 bilayer is highly negatively charged. Therefore, the electrostatic repulsion also contributes in improving

fouling resistance. Moreover, it is clear that 4 bilayers are optimum in this case as it gave the highest flux in fouling conditions.

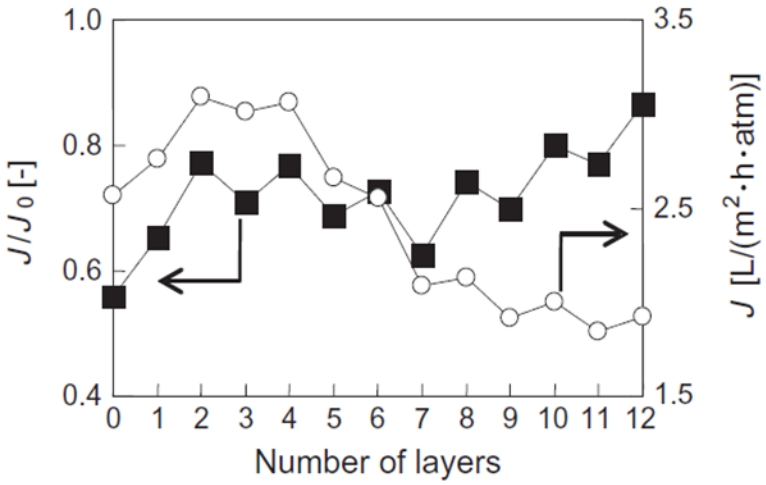

Figure 2-26: Effect of layer number on Permeability under 120 minutes BSA filtration experiment [109]

2.6.8 Effect of Operating Pressure on Permeability

During cross flow experiments, operating pressure has significant effect on permeation performance. By increasing the operating pressure, water molecules diffuse faster and flux increase linearly. This increase in flux with pressure is in accordance with Darcy's law. However, salt rejection follows solution diffusion mechanism and it also increase with pressure [128].

Tieke et al [129] studied the effect of operating pressure for PVA/PVS films. Investigations were carried out for reverse osmosis conditions up to 40 bars with different salt concentrations. Increasing the operating pressure from 5 to 20 bar, the monovalent (Na^{+}) rejection improved from 84 to 92% however at 40 bar, rejection turned up to 93.5%. In case of divalent ions (Na^{+2}), analogous linear increasing trend of flux and

rejection observed with operating pressure [130]. Tieke et al [125] confirmed this observation in a separate study where they used different polyelectrolyte pair of Hexacyclen trisulfate/PVA.

Deng et al [123] prepared multilayered film on PAN membrane through dynamic LbL assembly. They used copolymer PSS co-maleic acid along with PAH and PSS. Experiments were performed at 1000 mg/L Na_2SO_4 in cross-flow permeation cell with pressure from 2 to 8 bars. Figure 2-27 shows that increasing the pressure from 2 to 4 bars; permeate flux increased from 30 to 59 L/m^2.h but rejection approximately remained constant to 90 %.

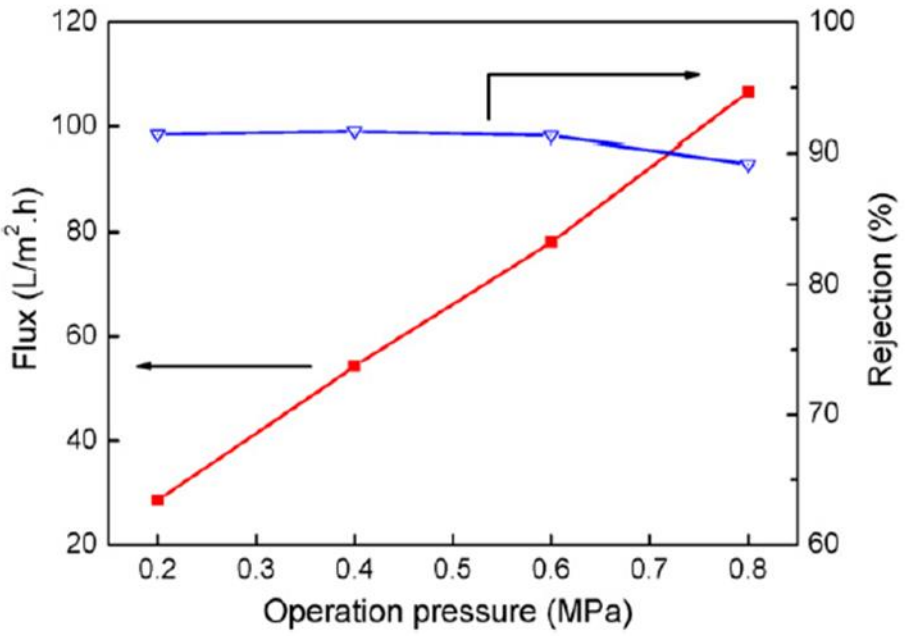

Figure 2-27: Effect of operating pressure on permeation performance [123]

Similar increasing trend was observed at 8 bar when flux increased to 108 L/m^2.h accompanied by constant Na_2SO_4 rejection. This observation is in accordance with earlier study of Deratani et al [115] who prepared CHI/ALG on cellulose acetate membrane.

Permeation experiments were performed at pressures up to 14 bars. It was demonstrated that increasing the pressure from 2 to 14 bar, pure water flux amplified linearly from 5 to 41 L/m^{2}h. Therefore, irrespective the nature of substrate and type of polyelectrolyte used, flux increased linearly with the operating pressure.

Farid et al [111] performed the permeation test in cross flow apparatus to investigate the RO performance of PAH/PAA modified ultrafiltration membrane. Performance was examined with a solution of 2000 ppm salt concentration and a pH of 6.0. The pressure study confirmed that water flux increases linearly with pressure. At 300 psi, the flux was 7 L/m^2.h with 56 % salt rejection. However, by increasing the pressure to 600 psi, flux approximately increased to 15.7 L/m^2.h with an increase in salt rejection to 65 % as displayed in Figure 2-28.

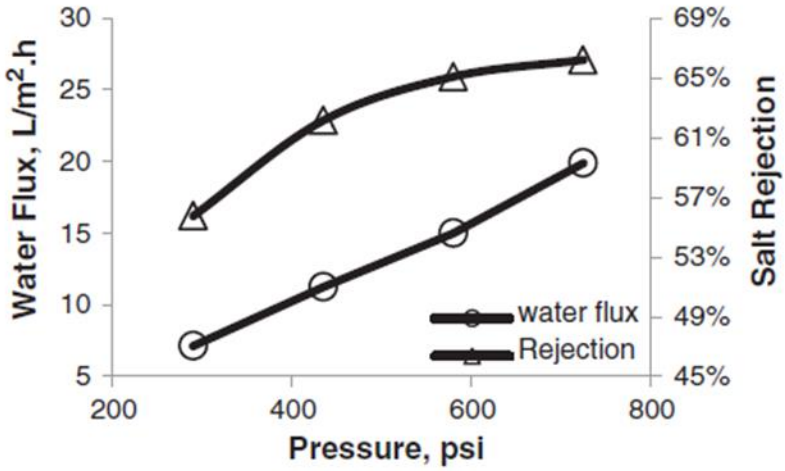

Figure 2-28: Effect of operating pressure on permeation performance of PAH/PAA multilayer films [111]

CHAPTER 3

RESEARCH METHODOLGY

3.1 Approach

Layer by layer assembly has been used to deposit polyelectrolytes on the reverse osmosis polyamide membrane. This method is selected due to its simplicity and controllability of film thickness. Design expert software with Box-Behnken Model was used to get the required number of experiments. The selected input range for number of layers is 5-50, pH is from 4-8 and the polyelectrolyte concentration is in the range of 20-200 mg/L.

After successful deposition, several characterizations were performed to analyze the prepared membranes. After experiments, analysis has been done to investigate the effect of input parameters on performance of membranes. Design of experiments has been applied to optimize the operating conditions such as number of layers, pH and polyelectrolytes concentrations.

3.2 Materials and Reagents

3.2.1 Polysulfone

Polysulfone pellets with molecular weight of 35 kDa were purchased from Sigma-Aldrich and used for membrane casting as a base polymer. It is a thermoplastic polymer with formula of $(C_6H_4C(CH_3)_2C_6H_4OC_6H_4SO_2C_6H_4O)n$ and known for its toughness. It

remains stable even at high temperatures and pH. It can be used as a filtration media [131].

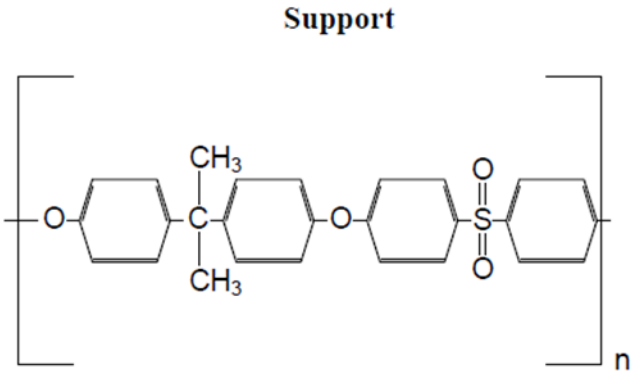

PSF

3.2.2 Di (methylacetamide)

Di (methylacetamide) which is the organic compound with the formula C_4H_9NO was purchased from Sigma-Aldrich. This colorless and high boiling liquid is miscible in water and commonly used as a polar solvent in organic synthesis. It was used to dissolve polysulfone pellets for preparation of polysulfone base membrane. It is an ideal solvent for preparing polysulfone membrane [132] .It has a boiling point of 166 ^{o}C with a density of 840 kg/m^3.

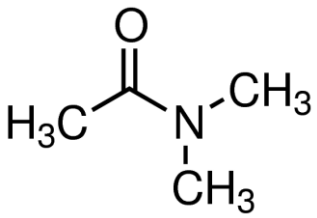

Dimethylacetamide

3.2.3 Polyester fabric

Polyester non-woven fabric support [Novatexx – 2413] was purchased from [Freudenberg Filtration Technologies (Germany)]. It is comprise of 100 % polyester fiber. The fabric was in the form of sheets and was used as support during casting of polysulfone membrane.

3.2.4 Deionized water

Millipore deionized water (18MΩ.cm resistivity) was used throughout the research. It served as non-solvent in coagulation bath during preparation of polysulfone base membrane. DI water was used as a solvent for M-phenylene diamine. It was also used for cross flow filtration experiments. Moreover, all the membranes were stored in deionized water after preparation or modification.

3.2.5 Sodium Hydroxide

Sodium hydroxide (>97%) was purchased in the form of white pellets from Sigma-Aldrich. It has a formula of NaOH with molecular weight of 40 g/mol. It is easily soluble in water and was used as pre-treatment of polysulfone membrane before preparing thin layer of polyamide membrane. Its purpose was to remove any impurities from the polysulfone membrane and to enhance its hydrophilicity.

3.2.6 Meta Phenylene diamine

Meta Phenylene diamine, MPD, (>99%) has formula of $C_7H_{10}N_2$ was purchased from Sigma-Aldrich. It is also known as 1, 3-diamino-benzene from its IUPAC name. It was used in preparation of polyamide membrane by means of interfacial polymerization. It is

a water soluble monomer having molecular weight of 122.2 g/mol along with high boiling point of 123.5^{O}C [133].

3.2.7 Trimesoyl Chloride

Trimesoyl chloride, TMC, (>98%) has formula of $C_6H_3(COCl_3)$ was purchased from Sigma-Aldrich. TMC is also known as benzene-1,3,5-tri carbonyl chloride. It was used in preparation of polyamide membrane along with Meta phenylene-diamine (MPD) through interfacial polymerization. It is soluble in organic solvents like hexane and toluene. It has molecular weight of 265.48 g/mol with boiling point of 180^{O}C.

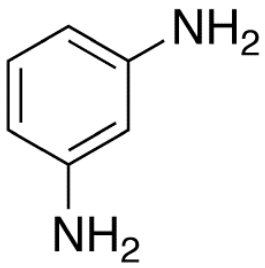

Meta Phenylene Diamine

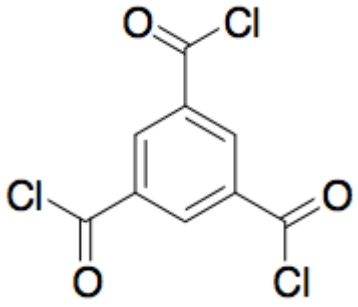

Trimesoyl chloride

3.2.8 Hexane

Hexane (>95%) was purchased from Sigma-Aldrich having molecular weight of 86 g/mol. It was used as solvent for tri-mesoyl chloride and also served as rinsing agent after preparation of polyamide membrane. It is has formula of C_6H_{14} with boiling point of 68^oC.

3.2.9 Poly (Ethylene Imine)

Poly (Ethylene Imine) has linear formula of $H(NHCH_2CH_2)nNH_2$ and it is also named aziridine. PEI with molecular weight of 25,000 g/mol (< 1 % water) was obtained from Sigma Aldrich.

PEI is branched polyamine with high charge density. It is a hydrophilic polymer and soluble in water. It was used as a polyelectrolyte to provide a compatible coating on polyamide membrane. It has density of 1.030 g/mL and viscosity of 13,000-18,000 [134].

3.2.10 Poly (allyl amine hydrochloride)

Poly (allyl amine hydrochloride), has formula of C_3H_8ClN and it is also named as prop-2-en-1-amine hydrochloride. PAH with molecular weight of 120,000-180,000 g/mol was obtained from Sigma Aldrich in the form of white solid. It is a cationic hydrophilic polymer and is soluble in water. It was used as a coating solution on existing polyamide membrane.

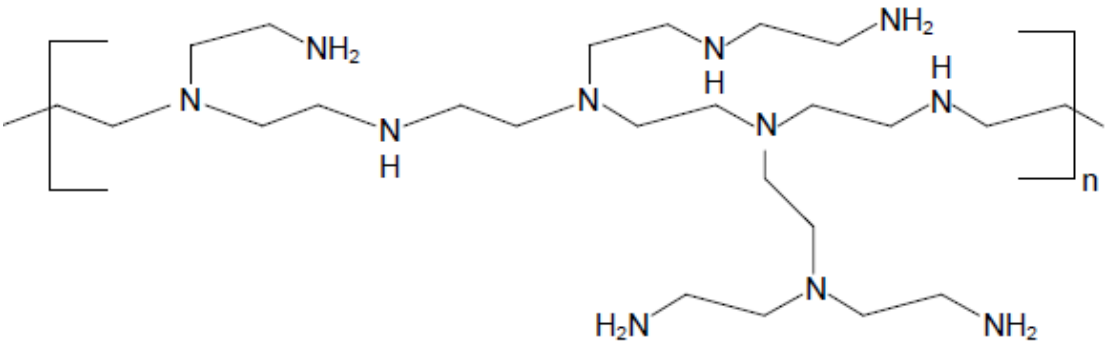

PEI

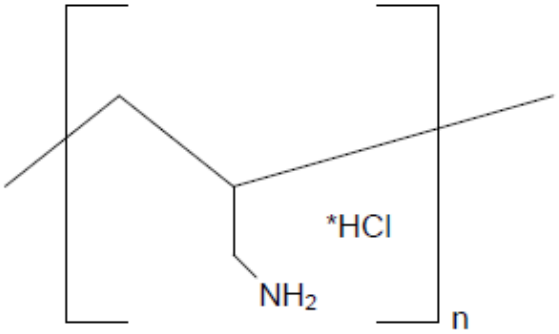

PAH

3.2.11 Sodium Chloride

Sodium Chloride (>99.5%) was purchased from Sigma Aldrich in the form of white powder. Its formula is NaCl with molecular weight of 58.5 g/mol. It was used in membrane testing to introduce artificial saline conditions at a certain concentration.

3.2.12 Bovine Serum Albumin

Bovine Serum Albumin, BSA, with molecular weight of 66 kDa and pH of 7 was also purchased from Sigma Aldrich. It is a globular protein with isoelectric point of 4.7 and is

soluble in water. It was used at certain concentration during investigation of fouling of the prepared membranes.

3.2.13 Sodium do-decyl sulphate

Sodium dodecyl sulfate, SDS, (>99%) is an organic compound with the formula CH3(CH2)11SO4Na was purchased from Sigma Aldrich. It has a molecular weight of 288.38 g/mol and it is soluble in water. It was used in Poly (Ethylene Imine) solution to produce a defect free substrate by enhancing binding with charged Poly (Ethylene Imine) [135].

3.3 Preparation of Polysulfone Support

Polysulfone pellets were dried in an oven overnight at 110^0C to remove any moisture or absorbed water vapor. The 20 wt. % solution of polysulfone was prepared in di-methylacetamide (DMA) in an Erlenmeyer flask. The flask was put onto magnetic stirrer for 6 hours after maintaining the temperature at 60^0C. After 6 hours, dissolution of polymer was completed and clear transparent liquid was left in an open atmosphere for 24 hours to remove any air bubble present in solution. The non-woven fabric was placed on the glass plate of dimensions (25.70 cm by 22.80 cm) and attached by using double sided tape. Before casting, fabric was made firmly straight, so that there is no gap or air bubble left on the surface. Solution casting was done at ambient temperature with constant shear rate of 15.6 mm/s and constant thickness of 150 µm. Polysulfone solution was poured and casted while using casting blade. Casting blade is shown in Figure 3-1 that is used in preparation of support. After casting, the prepared polysulfone membrane was immediately immersed into coagulation bath at ambient temperature for 1 day to

complete the phase inversion process. The de-ionized water served as a non-solvent in water bath that is required for phase inversion process. After that, polysulfone base membrane was stored in fresh de-ionized water till further use [136], [137].

Figure 3-1: Casting blade for preparation of polysulfone support

3.4 Preparation of Thin Film Composite Polyamide Membrane

Polysulfone support was kept in sodium hydroxide solution overnight. 2 wt. % solution of MPD was prepared by dissolving in de-ionized water. TMC solution of 0.15 wt. % was prepared in hexane and left on stirring for 3 hours. Interfacial polymerization was used in synthesis of active polyamide layer by means of dip coating. Polysulfone support, taped to glass plate was allowed to contact with MPD solution for 10 minutes and then excess solution was removed by using rubber roller. After rinsing, it was dipped in TMC solution for 30 seconds to complete the reaction for synthesis of polyamide layer. Hexane was used as rinsing agent to remove unreacted/excess TMC solution. This, polyamide membrane then, kept in an oven for 10 minutes at 70^{o}C, to increase the cross-linking.

Finally, the Polyamide membrane was stored in DI water till further use [46] [138]–[140].

3.5 Layer by Layer Modification of TFC Membrane by Polyelectrolytes

Layer by layer deposition technique involved in consecutive deposition of dilute polyelectrolyte solutions. Drying and rinsing is done after depositing each polyelectrolyte solutions. Polyamide membrane was dried under ambient conditions and cut in 8*8 cm^2 size. The pre-cut membrane was placed on a glass plate by using double sided tape. Spin grower of Absolute Nano Inc. was used to build multilayer film. Glass plate with membrane was placed on spinning support of spin coater. The plate was grasped by applying vacuum through vacuum pump. Spinning rate of 1000 rpm was fixed by using G3P software, installed in the same system. The deposition, drying and rinsing time along with number of layer to be deposited was adjusted through spin grower software. They were remained constant for all set of experiments. Now everything was established and spin coater was started. Once, it reached to the desired speed of 1000 rpm, coating was started by giving signal to spin grower control. PEI was deposited first, at a flow rate of 0.4 mL/s for 10 seconds, followed by drying for 15 seconds. This dried film was rinsed with deionized water, to remove weakly bound/attached polyelectrolyte at a flow rate of 0.4 mL/sec for 10 seconds and then drying for 15 sec. PAH was deposited in the same way and the cycles were repeated till the desired number of layers was coated.

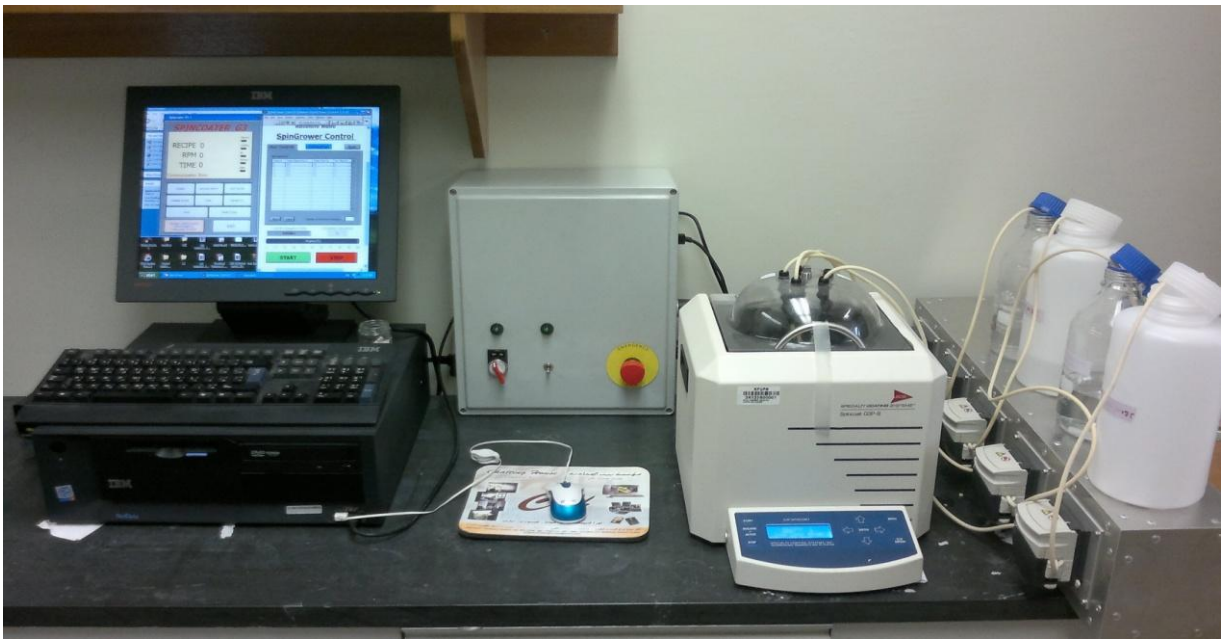

Figure 3-2: Spin coating set up for polyelectrolyte deposition

3.6 Design of Experiments

Design-Expert 8.0.10 trial software (Stat-Ease Inc., Minneapolis, USA) was used in this study to generate the set of experiments. Box-Behnken Model with four numeric factors and one center point was used to generate the design. The selected factors include the number of layers, pH and the concentration of both polyelectrolytes. After the experimentation, all the responses were inserted in the model and analysis was done. Analysis of variance (ANOVA) was performed to compare the magnitude of errors between the estimated and experimental data. Model was developed for each response with its significant influencing factors. In the end, optimization was performed on the basis of ANOVA analysis.

3.7 Characterization

3.7.1 Scanning Electron Microscopy

The surface morphology of membranes was studied by Field Emission Scanning Electron Microscopy (FE-SEM). TESCAN Scanning Electron Microscopy (Model JSM6400) as shown in Figure 3-3, operated with 20 kV was used to analyze the membrane samples. Before analysis, 1 mm membrane sample was coated with gold by using sputtering machine (Quorum Q150R S) to make the surface conductive. It was then studied under various resolutions ranging from 2 µm to 200 nm. To measure the cross section thickness, membrane was fractured by liquid nitrogen. Sample was dipped in liquid nitrogen for 1 minute and then cut by using sharp knife and hammer. It was then gold coated and analyzed in similar way using FE-SEM.

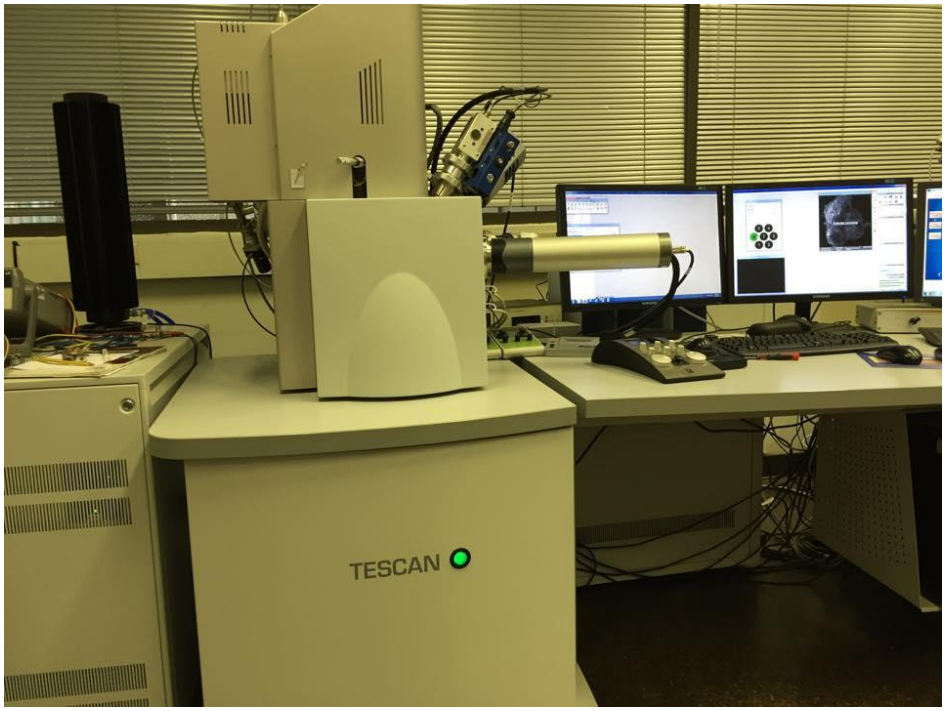

Figure 3-3: TESCAN FE-SEM used in this study

3.7.2 Contact Angle

The extent of wettability of membrane surface was studied by measuring contact angle. Sessile drop contact angles were measured by DM-501 device (Kyowa Interface Science Co.) as shown in Figure 3-5. Dry membrane sample of at least 2cm*2cm was taped to glass slide using double sided tape. It was made firmly straight to get the exact measurement. Then, 2 μL of deionized water droplet was fallen from syringe on the membrane. The angle formed from the tangent of water droplet at liquid-gas interface with the solid surface (liquid-solid interface) was then calculated as shown in Figure 3-4. Contact angle was measured at 5 different locations of membrane and then reported as an average contact angle.

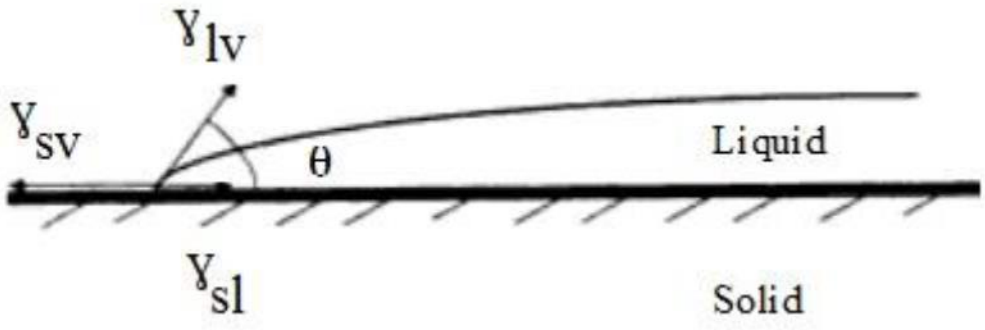

Figure 3-4: Schematic diagram of contact angle measurement

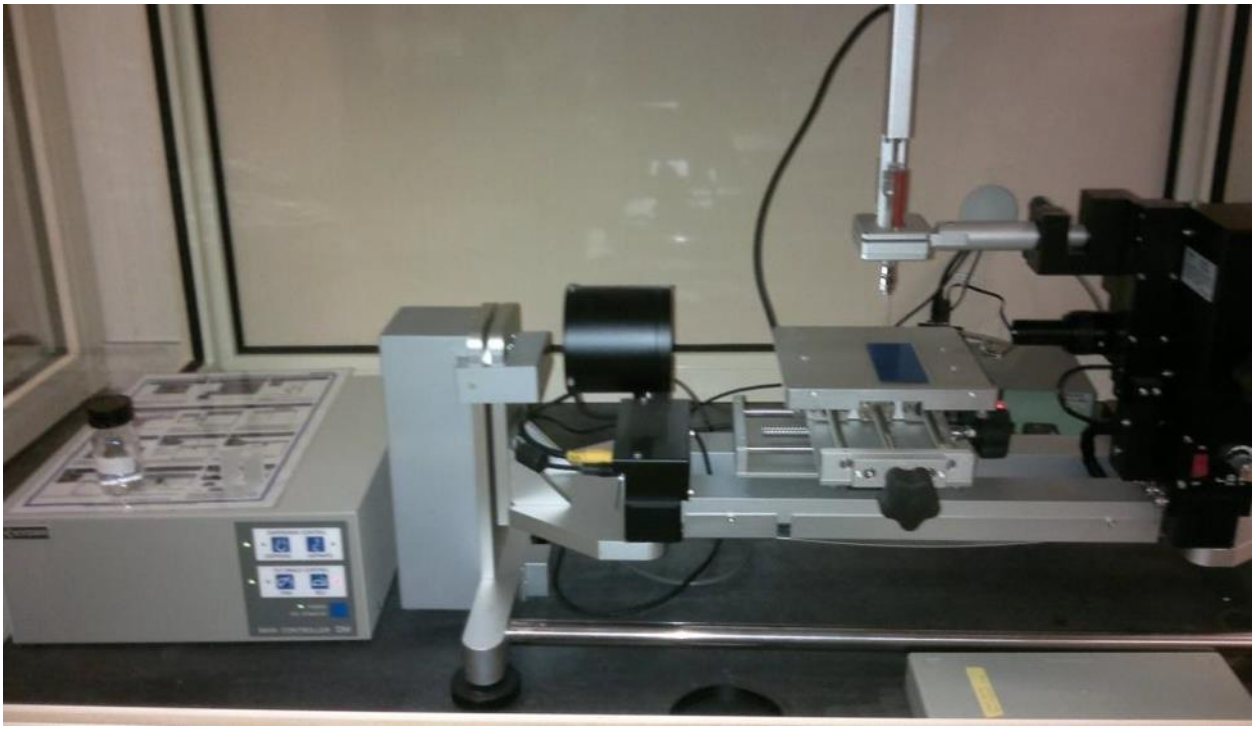

Figure 3-5: Contact angle DM-501

3.7.3 Atomic Force Microscopy

The membrane surface roughness was studied using atomic force microscope. Veeco Metrology Nano scope IV as shown in Figure 3-6, with Dimension of 3100 SPM was used to study the surface topography of layer by layer membrane samples. Dry membrane sample of at least 2cm*2cm was taped to glass slide using double sided tape. These dried samples were scanned in tapping mode at room temperature in air using RTESP tip (Veeco) with spring constant of 20-80 N/m. The roughness was measured over 5×5 μm scan size and assessed in terms of average roughness (Sa) at three different locations.

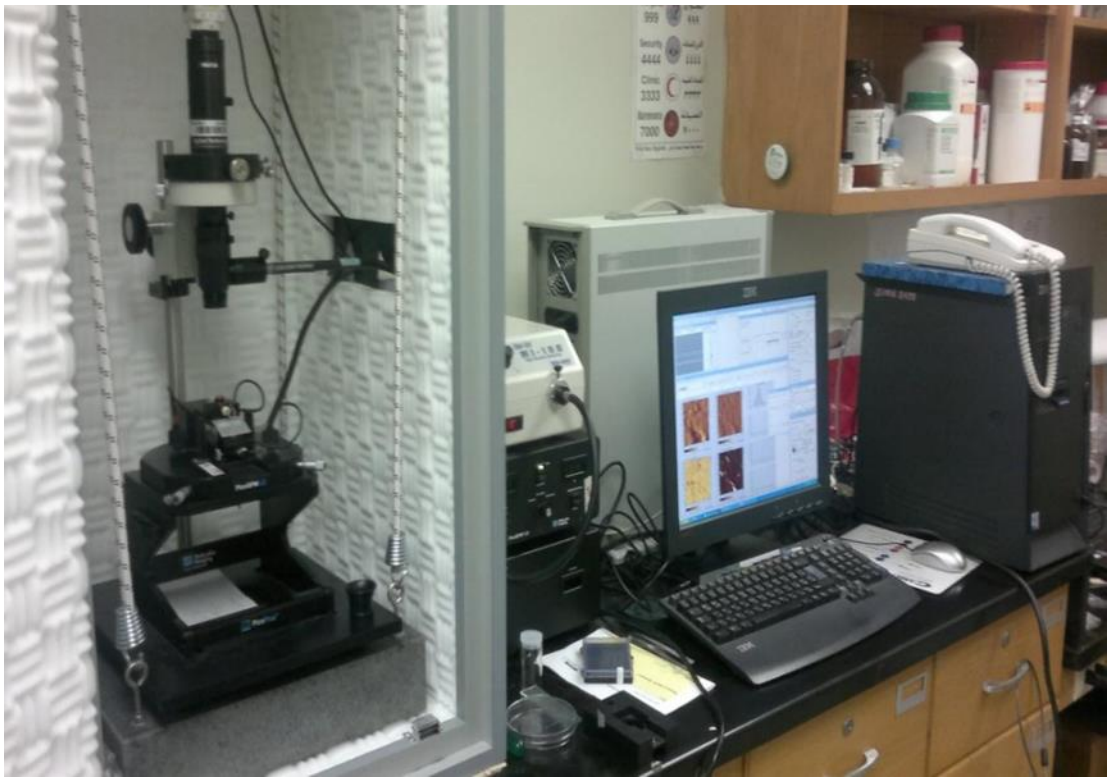

Figure 3-6: Nano scope IV AFM

3.7.4 Fourier Transform Infra-Red

FTIR was used to investigate the functional groups of layer by layer polyelectrolyte membrane surface. The iTR-FTIR Nicolet 6700 Model (Thermo scientific) as shown in Figure 3-7 was used for the analysis. It was operated in Attenuated Total Reflectance (ATR) mode without any special sample preparation. The penetration depth into membrane sample was between 0.5 and 2 micrometers. The phenomenon of total internal reflection is occurred in ATR mode in which a beam of infrared light is passed through the ATR crystal. This beam is reflected off from the internal surface in contact with the membrane sample and the wave is then recorded and analyzed for further study.

Figure 3-7: FTIR Nicolet 6700 Model (Thermo scientific)

3.7.5 Thermogravimetric Analysis

Thermo-gravimetrical analysis (TGA) was used to investigate the thermal stability of LbL membrane samples. TA instrument SDT Q600 as shown in Figure 3-8 was used for the analysis in nitrogen environment for temperature range of 25 ^{o}C to 900 ^{o}C. Heating rate of 10 ^{o}C per minute was maintained with nitrogen flow rate of 100 mL/min. Alumina pan was tarred and 5 mg membrane sample was used without any further preparation. The analysis was obtained in terms of thermo grams and reported.

Figure 3-8: TGA instrument SDT Q600

3.7.6 Membrane Testing

The filtration experiments were conducted in a cross flow apparatus using Sterlitech CF-042 membrane cell with an effective membrane area of 42 cm^2. The test unit was consisted of a feed tank, chiller, pump, bypass and control valves, membrane assembly and pressure gauges. Membrane assembly is shown in Figure 3-11. The filtration experiments were performed at temperature of 23±2 ^{0}C which was controlled using chiller (Proline RP 1845, Lauda). The polyelectrolyte modified membrane was cut in dimensions of 9.2 cm*4.57 cm and then installed in the membrane assembly. Pressure was increased gradually to reach the final value of 15 bars. Pure water flux was measured for 2 hours with 20 minutes interval. 2000 ppm NaCl concentration was used to test at brackish water conditions. The saline conditions were also studied for 2 hours of continuous operation. The schematic diagram is shown in Figure 3-9.

Water flux was calculated by using following relation;

$$J_0 = \frac{V}{A.t}$$

Where;

J_0 *is the volumetric flux* $(L/_{m^2.hr})$

A *is the active membrane area* (m^2)

t *is the permeation time* (hr)

V *is the permeate volume* (L)

NaCl rejection was calculated by the following relation:

$$R_{NaCl} = \left(1 - \frac{C_p}{C_f}\right) * 100$$

$R_{NaCl} is\ the\ Salt\ Rejection\ (\%)$

$C_p\ is\ the\ feed\ salt\ concentration\ \ (^{mg}/_{L})$

$C_f\ is\ the\ permeate\ salt\ concentration\ \ (^{mg}/_{L})$

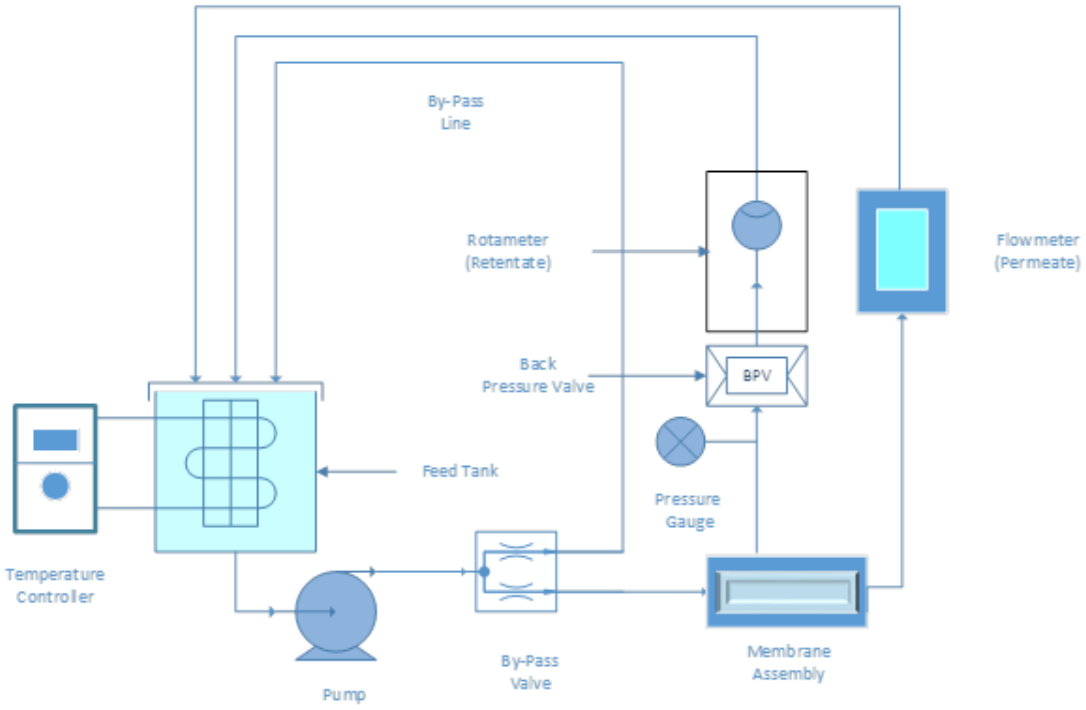

Figure 3-9: Schematic diagram of cross flow setup

To investigate the antifouling characteristics, BSA solution of 100 mg/L concentration was used at pH 7.0. Above iso-electric point of protein (pH=4.7), the interaction between protein and membrane surface is relative weak and rejection is higher as both protein and

membranes are negatively charged (repulsive). Brackish water conditions of 2000 ppm NaCl concentration along with 15 bar pressure was also maintained as was in the previous case. Experiment was run for 3 hours of continuous operation and flux was recorded after interval of 20 minutes. After that, membrane was rinsed with pure deionized water for 1 hour to examine the flux recovery of each membrane. Experimental cross flow set up is shown in Figure 3-10.

Flux loss was calculated as;

$$Flux\ Loss\ (\%) = \left(\frac{Jo - Jf}{Jo}\right) * 100$$

$J_0\ is\ the\ initial\ pure\ water\ flux\ (^{L}/_{m^2.hr})$

$J_f\ is\ the\ flux\ after\ fouling\ \ (^{L}/_{m^2.hr})$

Figure 3-10: Cross flow filteration set up

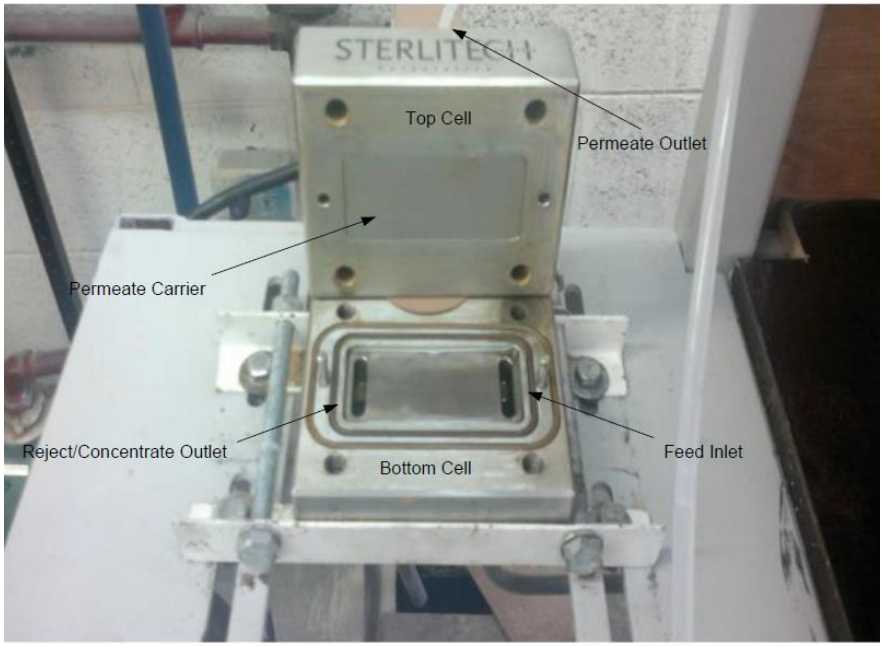

Figure 3-11: Membrane Assembly CF042

CHAPTER 4

Design of Experiment

4.1 Experiment Layout by Design Expert

Box-Behnken Model with four numeric factors and one center point was used to generate the design. The selected factors include the number of layers, pH and the concentration of both polyelectrolytes. The input values with their codes are given in table and design expert layout is also shown in figure below. The lowest input is given code of -1 and +1 indicates the maximum input value, whereas, zero is the midpoint for all the input.

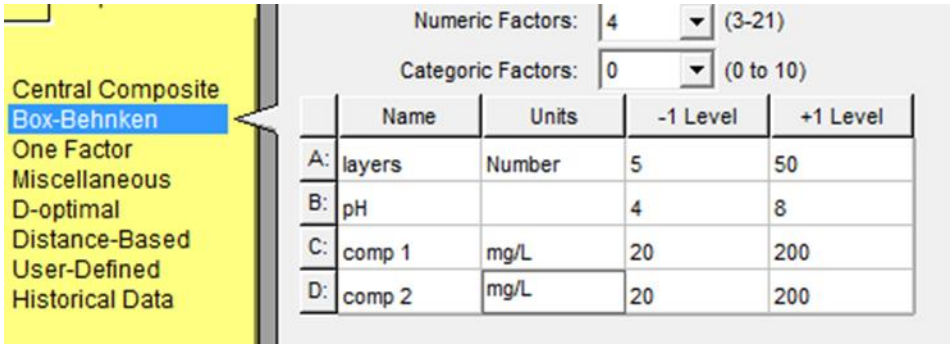

Figure 4-1: Box Behnken layout from Design Expert

The complete design layout of all the experiments along with their input values is given in Table 4-1. After performing all the experiments, the obtained responses were put against each run as shown in Table 4-2.

A second-order model was selected to describe the responses as a function of the coded factors:

$$Y_i = b_o + \sum_{i=1}^{n} b_i x_i + \sum_{i=1}^{n} b_{ii} x_i^2 + \sum_{i=1}^{n-1} \sum_{j=i+1}^{n} b_{ij}\, x_i x_j$$

In this equation, Y_i is the predicted response (pure water flux, saline water flux, rejection, and flux after fouling, recovery flux, and contact angle), b_o is the intercept term, linear and second order polynomial coefficients are represented by b_i and b_{ii} respectively. Interaction terms are given by b_{ij} whereas x_i and x_j are the coded independent variables. The relationship between the coded factors and the actual values are given by the following equations;

$$x_1 = \frac{A - 27.5}{22.5}$$

$$x_2 = \frac{B - 6}{2}$$

$$x_3 = \frac{C - 110}{90}$$

$$x_4 = \frac{D - 110}{90}$$

Table 4-1: Experiment Layout from Design Expert

Run	Block	Factor 1 A:layers No	Factor 2 B:pH	Factor 3 C:PEI mg/L	Factor 4 D:PAH mg/L
1	Block 1	27.50	8.00	20.00	110.00
2	Block 1	50.00	6.00	110.00	200.00
3	Block 1	27.50	6.00	110.00	110.00
4	Block 1	5.00	6.00	200.00	110.00
5	Block 1	5.00	6.00	20.00	110.00
6	Block 1	50.00	6.00	110.00	20.00
7	Block 1	27.50	6.00	110.00	110.00
8	Block 1	27.50	8.00	110.00	200.00
9	Block 1	5.00	8.00	110.00	110.00
10	Block 1	27.50	4.00	200.00	110.00
11	Block 1	27.50	4.00	110.00	20.00
12	Block 1	50.00	8.00	110.00	110.00
13	Block 1	27.50	4.00	110.00	200.00
14	Block 1	27.50	6.00	200.00	200.00
15	Block 1	27.50	8.00	200.00	110.00
16	Block 1	50.00	6.00	20.00	110.00
17	Block 1	5.00	6.00	110.00	20.00
18	Block 1	27.50	8.00	110.00	20.00
19	Block 1	50.00	4.00	110.00	110.00
20	Block 1	27.50	6.00	200.00	20.00
21	Block 1	27.50	6.00	110.00	110.00
22	Block 1	50.00	6.00	200.00	110.00
23	Block 1	27.50	6.00	110.00	110.00
24	Block 1	5.00	4.00	110.00	110.00
25	Block 1	5.00	6.00	110.00	200.00
26	Block 1	27.50	6.00	20.00	200.00

Table 4-2: Response against each experiment run

Run	Response 1 Pure Water Flux L/m2.hr	Response 2 Saline Flux L/m2.hr	Response 3 Salt Rejection %	Response 4 Fouling Flux L/m2.hr	Response 5 Recovery Flux L/m2.hr	Response 6 Contact Angle Degree
1	10.13	8.770	93.50	6.120	7.17	52.3
2	11.7064	10.200	95.00	8.844	9.67	53
3	12.64	12.100	90.50	10.740	11.69	54.6
4	15.105	14.150	90.50	12.193	13.11	51
5	10.418	9.060	90.50	6.926	8.26	52.8
6	10.726	9.620	94.00	8.770	9.18	48.8
7	13.272	12.705	91.00	11.277	12.27	54.7
8	12.422	10.490	94.00	9.517	10.10	57.6
9	13.352	12.490	88.00	11.134	11.89	63
10	11.899	10.140	93.00	8.987	9.56	50.4
11	11	10.000	91.50	9.237	9.50	52.5
12	11.2	10.280	95.00	9.309	10.18	55
13	12.8513	10.920	93.00	9.882	10.96	54.6
14	15.813	14.500	96.00	12.816	13.90	48
15	14.2108	13.400	92.00	11.814	11.96	49.1
16	7.842	6.460	94.00	4.400	4.67	46.9
17	14.268	12.740	90.50	11.777	12.48	57
18	9.889	8.960	92.00	8.129	8.60	52
19	11.39	9.750	94.50	7.899	8.62	53.3
20	15.2842	14.180	96.00	12.794	13.25	51
21	13.272	12.705	91.00	11.277	12.27	54.7
22	13.0588	12.490	94.50	10.633	10.90	46.5
23	12.008	11.495	90.00	10.203	11.11	54.5
24	15.11	13.140	93.50	11.700	13.05	61.3
25	13.696	11.850	91.50	10.705	11.53	62.8
26	9.488	9.240	90.50	8.414	9.12	47

Now, each response is discussed individually based on Quadratic polynomial model for ANOVA study.

4.2 Pure Water Flux

4.2.1 Analysis of Variance (ANOVA)

The coefficient of determination, R^2 for the model was 0.85, close to 1 which is acceptable [141]. This explains that only 14.77 % of the overall variablity is not explained by this model.

The Model F-value of 5.77 suggests that model is significant. The significance of model terms was indicated by Values of "Prob > F". p value less than 0.0500 indicates that model terms are significant. In the case of pure water flux, A and C are significant terms.

Values greater than 0.1000 indicate the model terms are not significant. The "Lack of Fit F-value" of 3.77 implies the Lack of Fit is not significant relative to the pure error. "Adeq Precision" measures the signal to noise ratio. A ratio greater than 4 is desirable and here ratio of 9.386 indicates an adequate signal. In short, this model can be used to study the design space. ANOVA summary for pure water flux is given in Table 4-3.

Model Equation in Terms of Actual Factors

$$\boldsymbol{Pure\ Water\ Flux}\ \left(\frac{L}{m^2.hr}\right) = +10.71306 - 0.14779 * layers + 0.76540 * pH + 0.21222 * PEI - 5.02665 * 10^{-3} * PAH + 8.71111 * 10^{-3} * layers * pH + 6.54074 * 10^{-5} * layers * PEI + 1.91654 * 10^{-4} * layers * PAH + 2.915 * 10^{-3} * pH * PEI + 9.46806 * 10^{-4} * pH * PAH + 1.40988 * 10^{-5} * PEI * PAH + 1.43547 * 10^{-4} * layers^2 - 0.12249 * pH^2 - 7.26703 * 10^{-5} * PEI^2 - 1.12798 * 10^{-5} * PAH^2$$

By ignoring insignificant terms, model is reduced to a better expression as follows;

$$\boldsymbol{Pure\ Water\ Flux}\ \left(\frac{L}{m^2.hr}\right) = PEI * 0.21222 - 0.14779 * layers + 10.71306$$

Table 4-3: ANOVA summary for pure water flux

Response 1	Pure Water Flux				
ANOVA for Response Surface Quadratic Model					
Analysis of variance table [Partial sum of squares - Type III]					
Source	Sum of Squares	df	Mean Square	F Value	p-value Prob > F
Model	96.18	14	6.87	5.77	0.0012
A-layers	*21.40*	*1*	*21.40*	*17.98*	*0.0008*
B-pH	*0.077*	*1*	*0.077*	*0.065*	*0.8025*
C-PEI	*66.08*	*1*	*66.08*	*55.52*	*< 0.0001*
D-PAH	*2.42*	*1*	*2.42*	*2.04*	*0.1755*
AB	*0.61*	*1*	*0.61*	*0.52*	*0.4842*
AC	*0.070*	*1*	*0.070*	*0.059*	*0.8117*
AD	*0.60*	*1*	*0.60*	*0.51*	*0.4885*
BC	*1.10*	*1*	*1.10*	*0.93*	*0.3524*
BD	*0.12*	*1*	*0.12*	*0.098*	*0.7593*
CD	*0.052*	*1*	*0.052*	*0.044*	*0.8372*
A^2	*0.034*	*1*	*0.034*	*0.029*	*0.8677*
B^2	*1.56*	*1*	*1.56*	*1.31*	*0.2719*
C^2	*2.25*	*1*	*2.25*	*1.89*	*0.1910*
D^2	*0.054*	*1*	*0.054*	*0.045*	*0.8342*
Residual	16.66	14	1.19		
Lack of Fit	*15.06*	*10*	*1.51*	*3.77*	*0.1063*
Pure Error	*1.60*	*4*	*0.40*		

4.2.2 Graphical Residual Analysis

Residual analysis is a significant and effective model validation test method. It was used to check the suitability of the constructed model. Figure 4-2 shows the predicted values versus actual values of pure water flux. It can be seen that predicted flux values were close to the actual experimental values with a little deviation of few points. This indicates

that developed model was fruitful in capturing the relationship between the input variables and the output of flux.

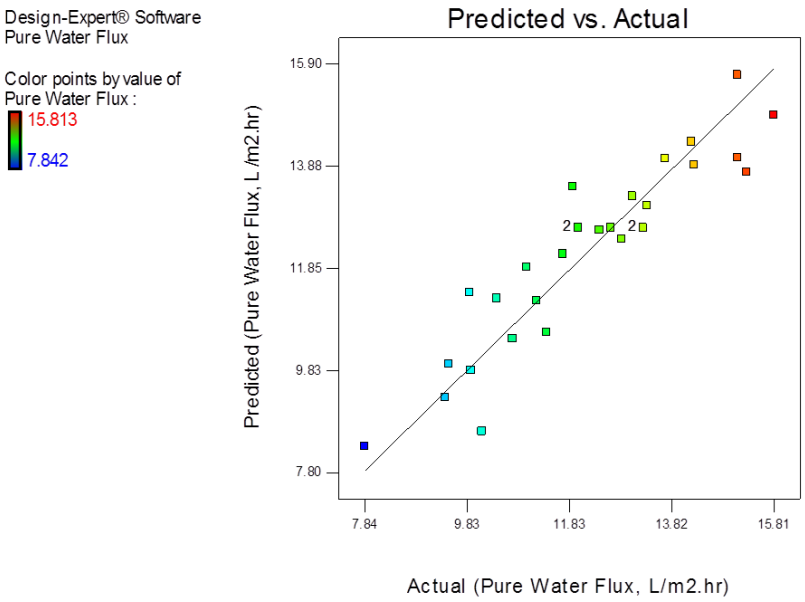

Figure 4-2: Predicted versus actual pure water flux

Validation of the Box Behnken design model was based on the residuals. The calculation of residual indicates the observed value of the response/flux less than the predicted flux value. Figure 4-3 shows the normal plot of residuals. Since all residuals lie on straight line that indicates residuals follow normal distribution. So, there is good correlation between the experiment values and the model.

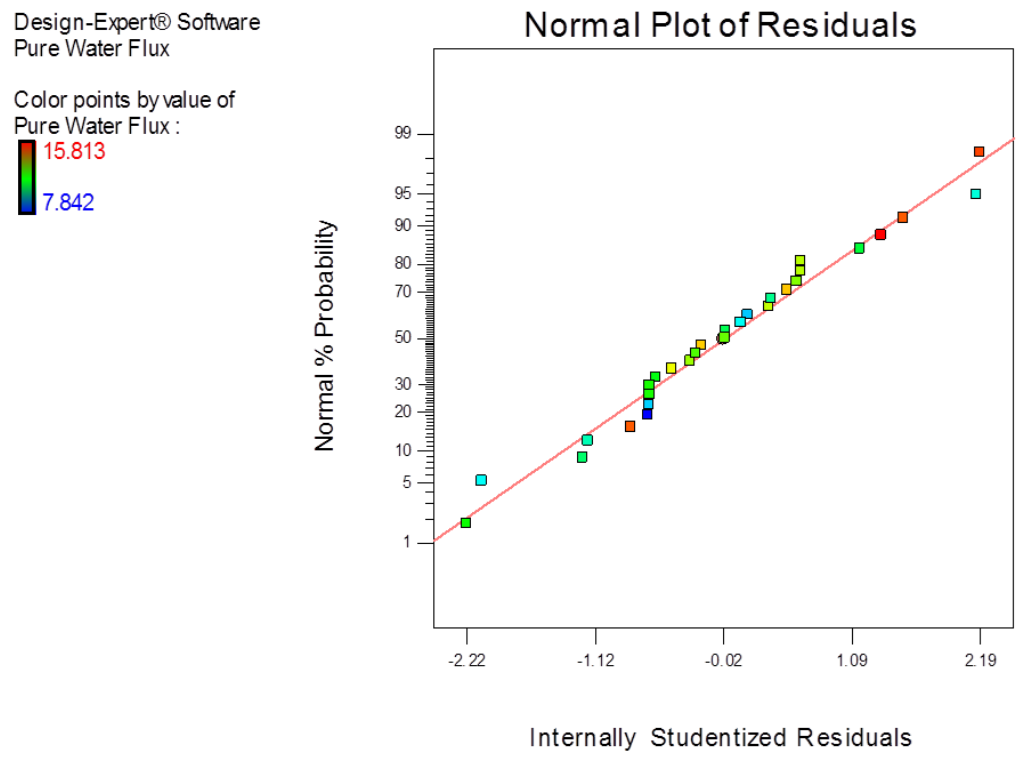

.

Figure 4-3: Normal plot of residuals

4.2.3 Three dimensional studies for pure water flux

Figure 4-4 shows the effect of number of layers and pH on pure water flux at fixed concentration of 110 mg/L for both polyelectrolytes. It can be seen that low pH and less number of layers are favorable for maximum pure water flux. As, less number of layers imparts less thickness to the surface that will offer slight resistance to flow. With 5 layers and pH of 4, flux has maximum value of 15.11 L/m^2.hr, keeping the concentration of both polyelectrolytes constant at 110 mg/L. When the layer number increased to 50 and pH raised to 8 the pure water flux decline to 25.87%.

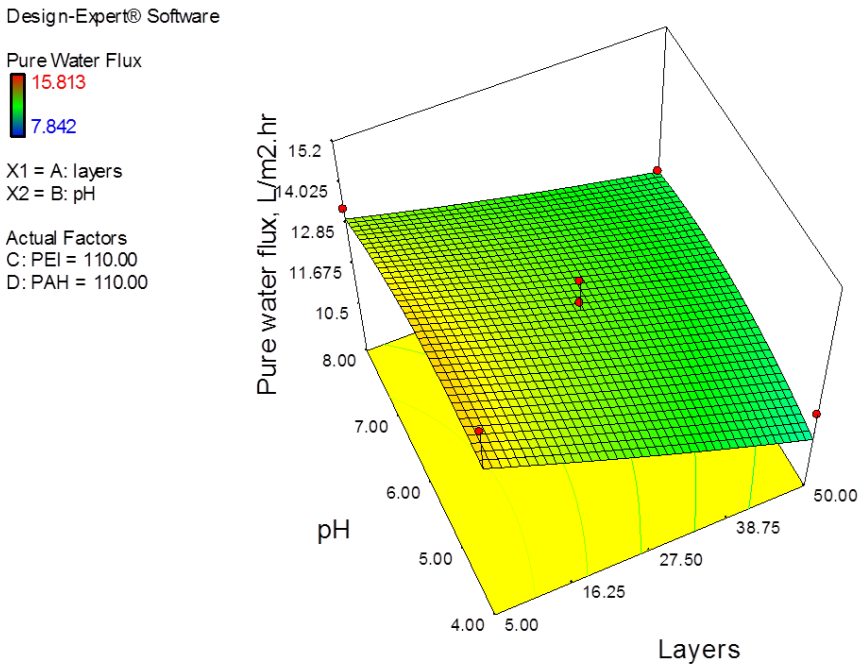

Figure 4-4: Response plot of pure water flux affected by number of layers and pH (PEI=PAH=110mg/L)

Figure 4-5 shows the effect of number of layers and Poly (ethylene) concentration on pure water flux at fixed concentration of PAH (110 mg/L) and fixed pH of 6.0. It is clear that higher PEI concentration and lower number of layers are resulted in higher pure water flux. Higher PEI concentration will add greater hydrophilicity to the surface that will definitely promote water flow. Greater concentration will enhance hydrophilic functional groups on membrane surface. However, PEI concentration has strong effect on pure water flux even at constant pH and layers. By increasing the PEI concentration from 20 mg/L to 200 mg/L, flux raised to 15.105 L/m^2.hr from 10.418 L/m^2.hr, which is an increase of more than 31 %.

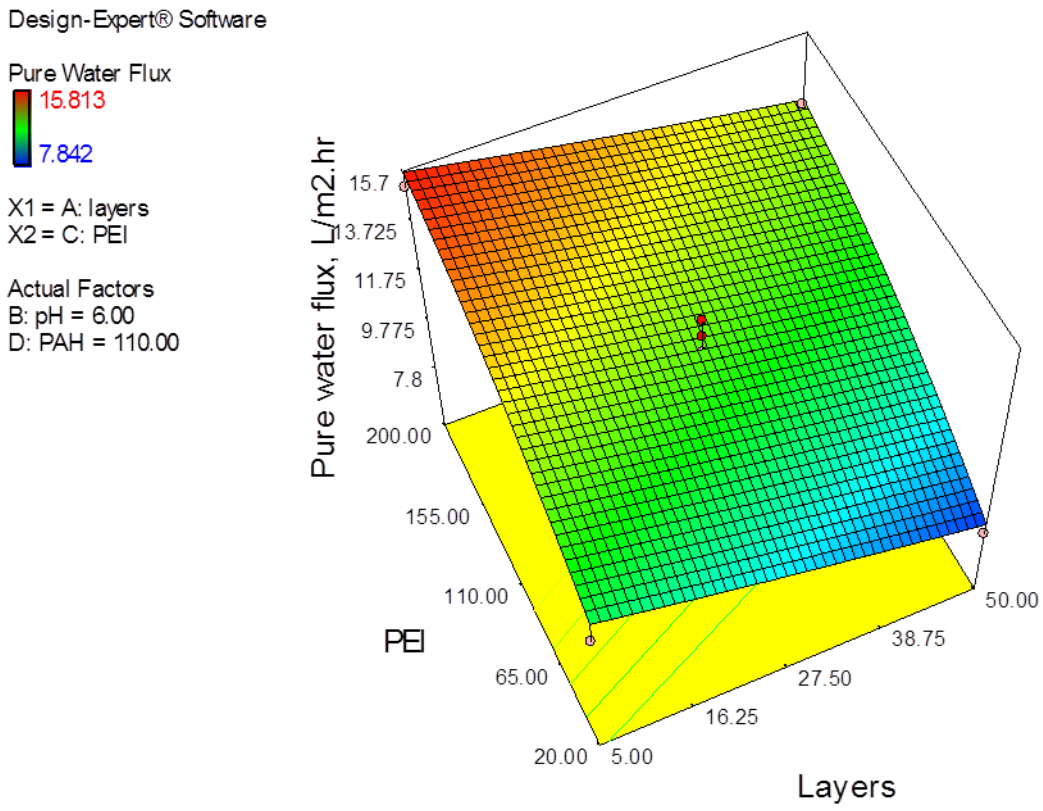

Figure 4-5: Response plot of pure water flux affected by number of layers and PEI concentration (pH =6; PAH=110mg/L)

4.3 Saline Flux

4.3.1 Analysis of Variance (ANOVA)

The coefficient of determination, R^2 for the model was 86.30%. This explains that only 13.7 % of the overall variablity is not expalined by this model. The Model F-value of 6.30 recommends that model is significant. The significance of model terms was indicated by Values of "Prob > F". p value values greater than 0.10 indicate the model terms are not significant whereas p value less than 0.0500 shows the significance of model. In the case of saline water flux, A, C and B^2 are significant terms.

The "F-value" of 3.88 implies the Lack of Fit is not significant relative to the pure error. "Adeq Precision" measures the signal to noise ratio. Here ratio of 9.417 indicates an adequate signal. So, this model can be used to study the design space. The ANOVA summary is given in Table 4-4.

Table 4-4: ANOVA summary to study response of saline water flux

Response 2 Saline Flux						
ANOVA for Response Surface Quadratic Model						
Analysis of variance table [Partial sum of squares - Type III]						
Source	Sum of Squares	df	Mean Square	F Value	p-value Prob > F	
Model	98.74	14	7.05	6.30	0.0007	significant
A-layers	*17.84*	*1*	*17.84*	*15.93*	*0.0013*	
B-pH	*0.21*	*1*	*0.21*	*0.19*	*0.6691*	
C-PEI	*67.02*	*1*	*67.02*	*59.88*	*< 0.0001*	
D-PAH	*1.06*	*1*	*1.06*	*0.95*	*0.3465*	
AB	*0.35*	*1*	*0.35*	*0.31*	*0.5859*	
AC	*0.22*	*1*	*0.22*	*0.20*	*0.6637*	
AD	*0.54*	*1*	*0.54*	*0.48*	*0.4986*	
BC	*2.77*	*1*	*2.77*	*2.48*	*0.1379*	
BD	*0.093*	*1*	*0.093*	*0.083*	*0.7774*	
CD	*0.16*	*1*	*0.16*	*0.14*	*0.7145*	
A^2	*0.78*	*1*	*0.78*	*0.69*	*0.4185*	
B^2	*6.20*	*1*	*6.20*	*5.54*	*0.0338*	
C^2	*3.22*	*1*	*3.22*	*2.88*	*0.1118*	
D^2	*1.76*	*1*	*1.76*	*1.57*	*0.2301*	
Residual	15.67	14	1.12			
Lack of Fit	*14.21*	*10*	*1.42*	*3.88*	*0.1016*	*not significant*
Pure Error	*1.46*	*4*	*0.37*			

Model Equation in Terms of Actual Factors:

$$Saline\ Flux = 4.08975 - 0.0\,8863 * layers + 2.21694 * pH + 0.017148 * PEI + 0.010071 * PAH + 6.5555556\,E^{-3} * layers * pH + 1.16049\,E^{-4} * layers * PEI + 1.81481\,E^{-4} * layers * PAH + 4.62\,500\,E^{-3} * pH * PEI + 8.47222\,E^{-4} * pH * PAH - 2.43827\,E^{-5} * PEI * PAH - 6.83951\,E^{-4} * layers^2 - 0.24437 * pH^2 - 8.70370\,E^{-5} * PEI^2 - 6.43519\,E^{-5} * PAH^2$$

By neglecting the insignificant terms, model equation reduced to the following expression;

$$Saline\ Flux\ \left(\frac{L}{m^2.hr}\right)$$

$$= -0.0\ 8863 * layers + 0.017148 * PEI - 0.24437 * pH^2 + 4.08975$$

4.3.2 Graphical Residual Analysis

Residual analysis is an effective model validation test method. It was used to check the suitability of the model. Figure 4-6 shows the predicted values versus actual values of flux during saline conditions. It can be seen that majority of actual values lie close to the straight line with a slight deviation of few points. This indicates that developed model was fruitful in developing the relationship between the input variables and the saline flux.

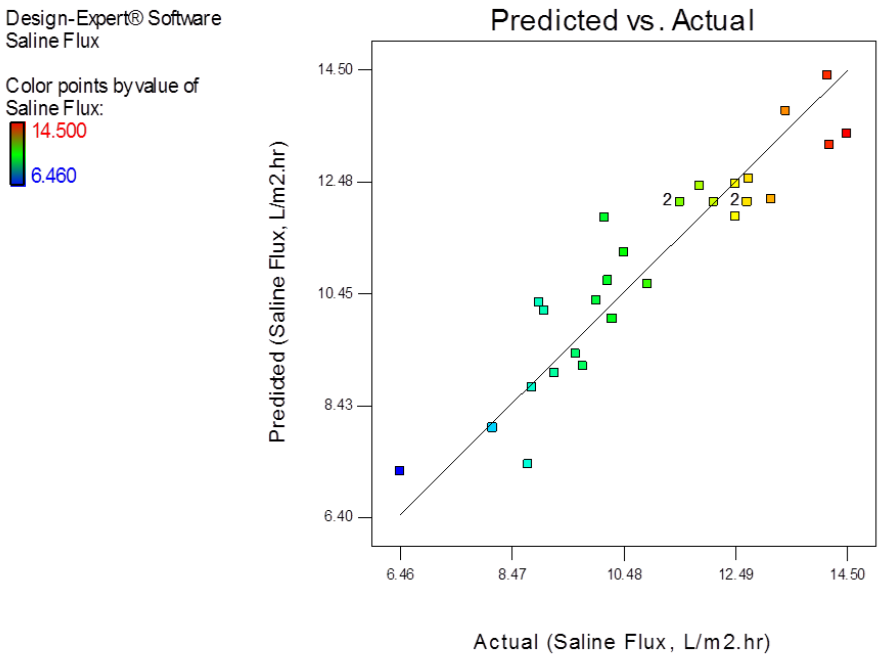

Figure 4-6: Predicted versus actual saline flux

Validation of the Box Behnken design model was based on the residuals. The calculation of residual indicates the observed value of the saline flux less than the predicted value. Figure 9 shows the normal plot of residuals for saline flux. Since all residuals lie on straight line with mean of zero. This shows that residuals follow normal distribution. So, there is decent correlation between the experiment values and the model.

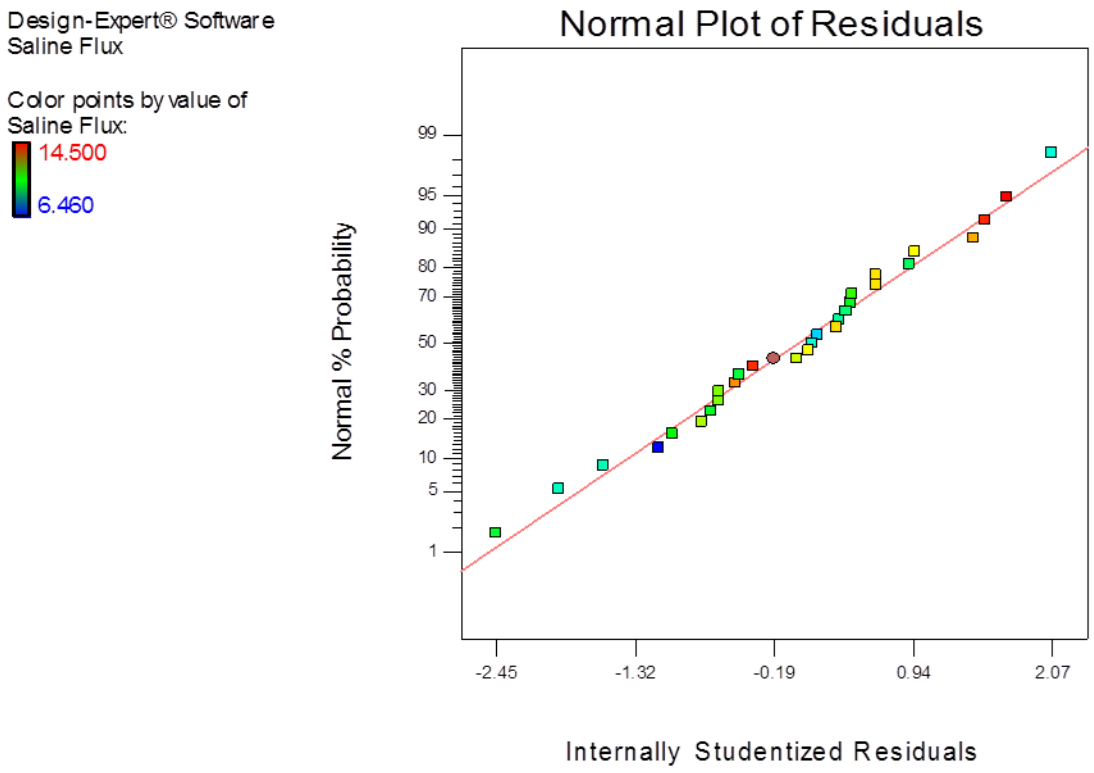

Figure 4-7: Normal probability of residuals

4.3.3 Three Dimensional study for saline flux

Figure 4-8 shows the effect of number of layers and pH on saline water flux at fixed concentration of 110 mg/L for both polyelectrolytes. It can be seen that low pH and less number of layers are favorable for saline flux. With 5 layers and 4.0 solution pH; flux has

maximum value of 13.14 L/m^2.hr, keeping the concentration of both polyelectrolytes constant at 110 mg/L. When the layer number increased to 50 and pH raised to 8 the saline flux declines; either by increasing the one factor, or the other or both. The decrease in flux can be explained as a result of additional thickness over the membrane after depositing greater number of layers. Greater thickness, will offer more resistance to flow; thereby reducing the flux in saline conditions.

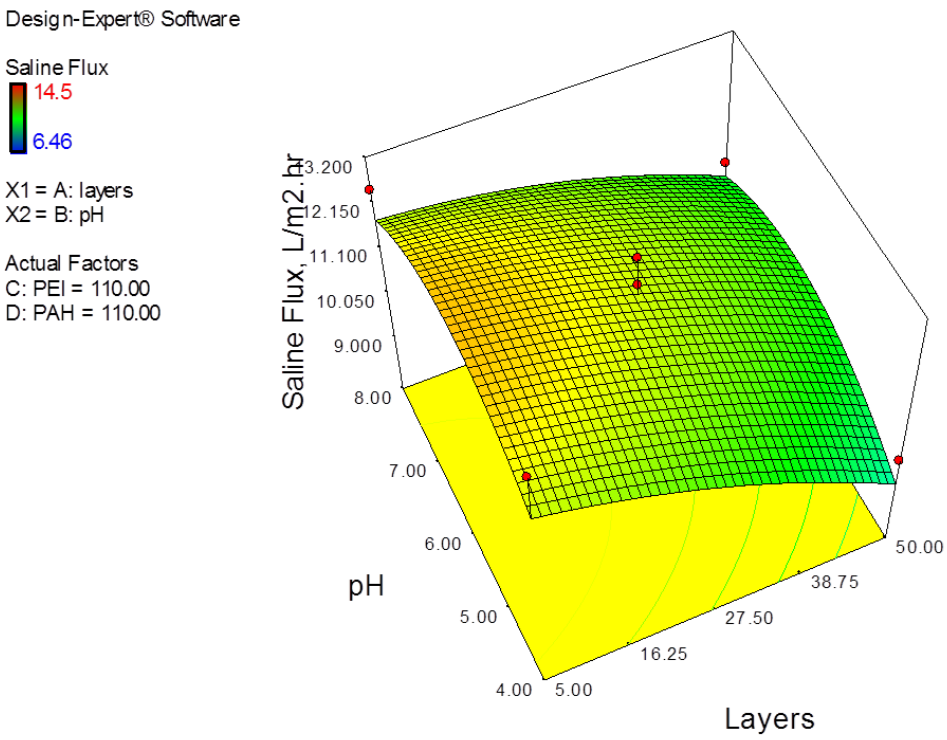

Figure 4-8: Response plot of saline flux affected by pH and number of layers (PEI= PAH=110mg/L)

Figure 4-9 shows the effect of number of layers and PEI concentration on saline water flux at fixed pH of 6 and concentration of 110 mg/L PAH. It can be seen that less number of layers and high PEI concentration are in favor of higher saline flux. With 5 layers and 20 mg/L PEI concentration, saline flux was 9.06 L/m^2.hr whereas at 200 mg/L concentration of PEI, flux raised to 14.15 L/m^2.hr keeping the layers constant. This

increase of 35.97 % in saline flux can be explained in terms of increasing smoothness and hydrophilicity by depositing higher PEI concentration. However, saline flux decreased by increasing the layers even at low and high PEI concentration.

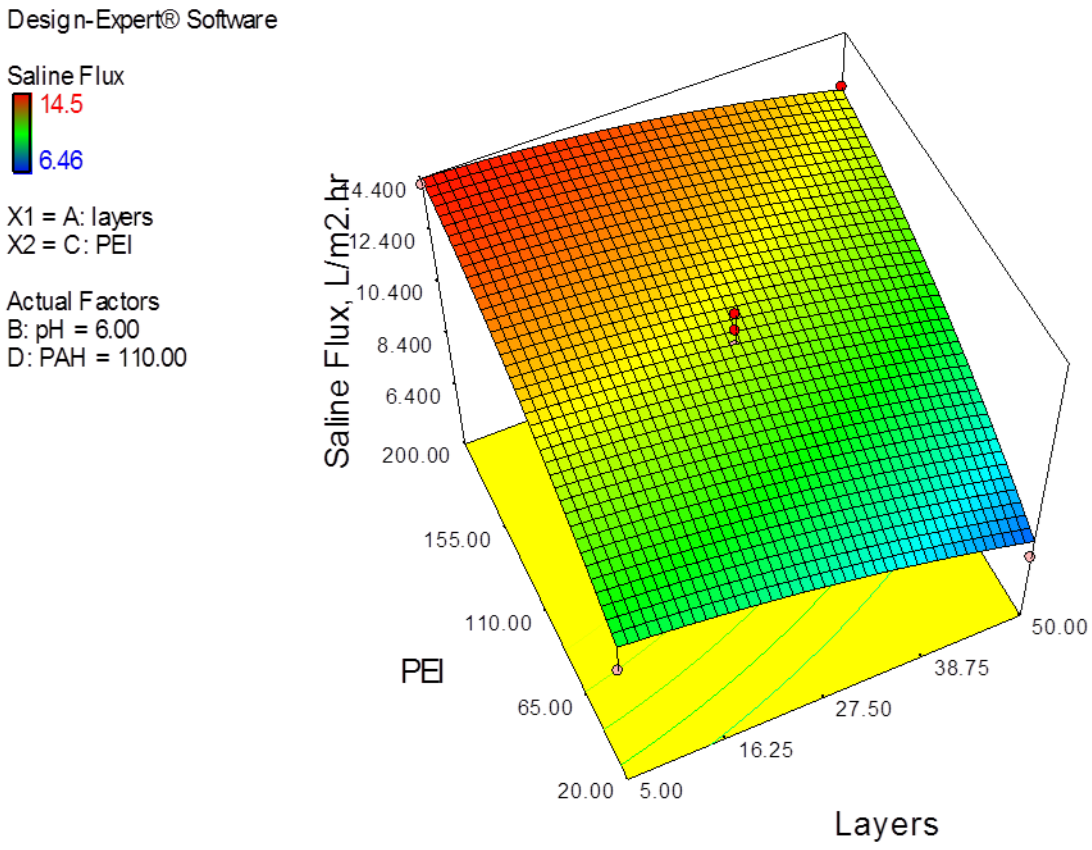

Figure 4-9: Response plot of saline flux affected by number of layers and PEI concentration (pH=6; PAH=110mg/L)

Figure 4-10 shows the effect of pH and PEI concentration on saline water flux at fixed number of layers and PAH concentration of 110 mg/L. It is noticeable that higher pH and higher PEI concentration are helpful in achieving greater saline flux. At 20 mg/L PEI concentration and 4.0 pH, 8.84 L/m^2.hr saline flux was observed, however (13.4 L/m^2.hr) 34 % flux rise was observed at 200 mg/L PEI and 8.0 pH; layer number was constant.

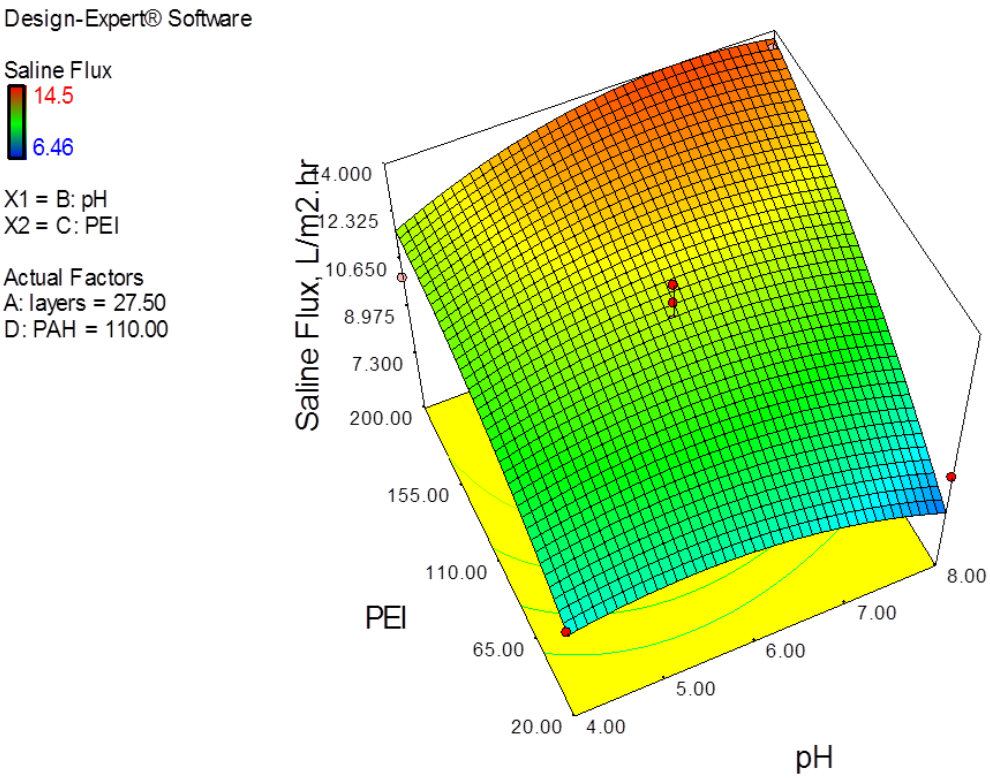

Figure 4-10: Response plot of saline flux affected by pH and PEI concentration (layers=27.5; PAH=110mg/L)

4.4 Salt Rejection

4.4.1 Analysis of Variance (ANOVA)

The coefficient of determination, R^2 for the model was 85.81%. The Model F-value of 3.13 recommends that model is significant. The significance of model terms was indicated by values of "Prob > F". p value values greater than 0.10 indicate the model terms are not significant whereas p value less than 0.0500 shows the significance of model. In the case of salt rejection, A, C^2 and D^2 are significant terms.

"Adeq Precision" measures the signal to noise ratio. Here ratio of 6.746 indicates an adequate signal. In short, this model can be used to study the design space. The ANOVA summary is given in Table 4-5.

Final Equation in Terms of Actual Factors:

$$Salt\ Rejection\ (\%) = 109.22222 - 0.20267 * layers - 3.68056 * pH - 0.042935 * PEI - 0.063786 * PAH + 0.033333 * layers * pH + 6.17284E^{-5} * layers * PEI + 0000000 * layers * PAH - 2.08333\ E^{-3} * pH * PEI + 6.94444\ E^{-4} * pH * PAH + 1.38889\ E^{-4} * PEI * PAH + 1.44033\ E^{-3} * layers^2 + 0.22917 * pH^2 + 1.98045\ E^{-4} * PEI^2 + 2.05761\ E^{-4} * PAH^2$$

By negelecting the insignificant model terms, the expression for salt rejection reduced as follows;

$$Salt\ Rejection\ (\%) = -0.20267 * layers + 1.98045\ 10^{-4} * PEI^2 + 2.05761\ 10^{-4} * PAH^2 + 109.22222$$

Table 4-5: ANOVA summary for salt rejection

Response 3	Salt Rejection				
ANOVA for Response Surface Quadratic Model					
Analysis of variance table [Partial sum of squares - Type III]					
Source	Sum of Squares	df	Mean Square	F Value	p-value Prob > F
Model	91.32	14	6.52	3.13	0.0203
A-layers	*42.19*	*1*	*42.19*	*20.26*	*0.0005*
B-pH	*1.33*	*1*	*1.33*	*0.64*	*0.4369*
C-PEI	*2.52*	*1*	*2.52*	*1.21*	*0.2897*
D-PAH	*0.083*	*1*	*0.083*	*0.040*	*0.8443*
AB	*9.00*	*1*	*9.00*	*4.32*	*0.0565*
AC	*0.063*	*1*	*0.063*	*0.030*	*0.8649*
AD	*0.000*	*1*	*0.000*	*0.000*	*1.0000*
BC	*0.56*	*1*	*0.56*	*0.27*	*0.6113*
BD	*0.063*	*1*	*0.063*	*0.030*	*0.8649*
CD	*5.06*	*1*	*5.06*	*2.43*	*0.1412*
A^2	*3.45*	*1*	*3.45*	*1.66*	*0.2189*
B^2	*5.45*	*1*	*5.45*	*2.62*	*0.1280*
C^2	*16.69*	*1*	*16.69*	*8.02*	*0.0133*
D^2	*18.02*	*1*	*18.02*	*8.65*	*0.0107*
Residual	29.15	14	2.08		
Lack of Fit	*28.15*	*10*	*2.81*	*11.26*	*0.0161*
Pure Error	*1.00*	*4*	*0.25*		

4.4.2 Graphical Residual Analysis

Residual analysis was used to check the suitability of the model with the experimental data. Figure 4-11 shows the predicted values versus actual values of salt rejection. It can be seen that predicted values were scattered around the actual experimental values. It shows that there was some variability in the data that was not being explained by this model. But, still the developed model was productive in developing the comprehensive relationship between the input variables and the salt rejection.

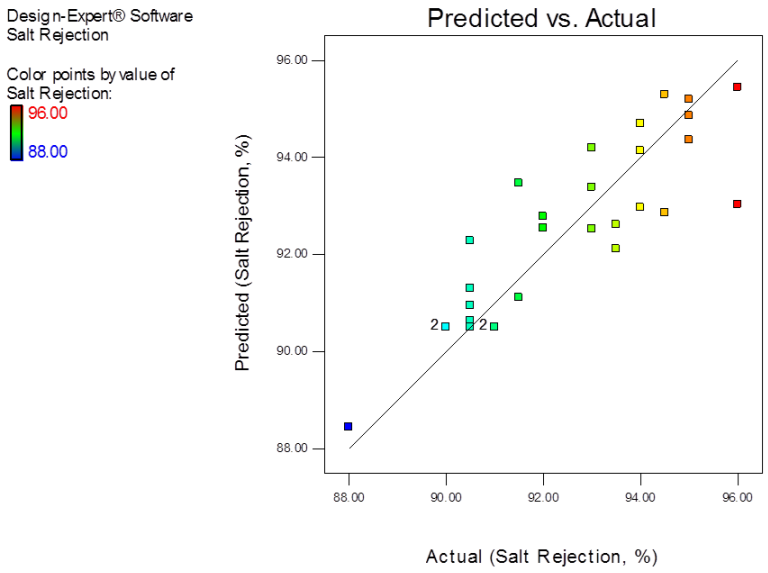

Figure 4-11: Predicted versus actual salt rejection

Figure 4-12 shows the normal plot of residuals for salt rejection. Since, all residuals lie on straight line except a couple of points. It indicates that residuals follow normal distribution.

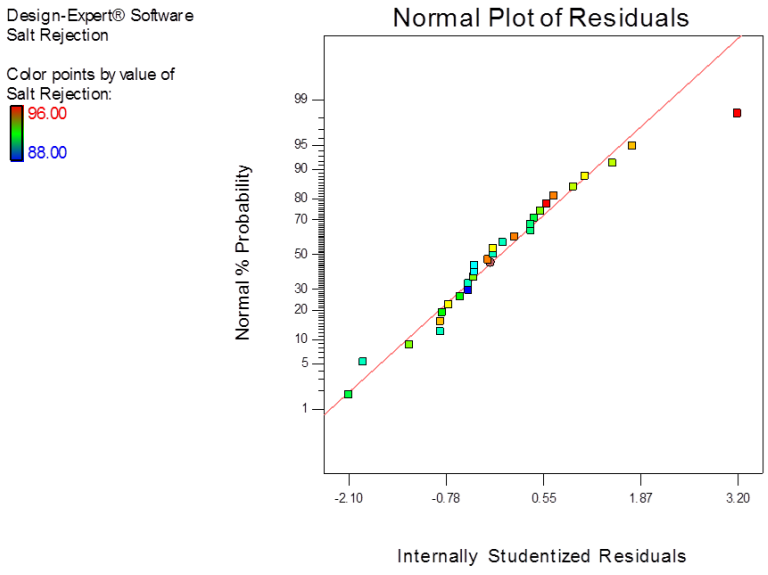

Figure 4-12: Normal probability of residuals

4.4.3 Three dimensional study for salt rejection

Figure 4-13 shows the effect of concentration of both the polyelectrolytes on salt rejection, keeping the pH and number of layers constant. Clearly, it shows some interesting behavior, different as compared to the previous discussion. Similar concentration of both polyelectrolytes favors the salt rejection. Moreover, when concentration of both polyelectrolytes increased, percentage rejection increases. It can be estimated that more compact and dense structure is obtained at these concentrations that has increased the salt rejection. For example, at 20 mg/L, salt rejection was 95 % but when concentration increase to 200 mg/L for both polyelectrolytes, salt rejection increased to 96 %. However, PEI has dominant impact on salt rejection. Salt rejection was 90.5% with 20 mg/L PEI but escalated to 96 % by increasing the PEI to 200 mg/L; keeping the second depositing polyelectrolyte at constant concentration of 200 mg/L in both conditions.

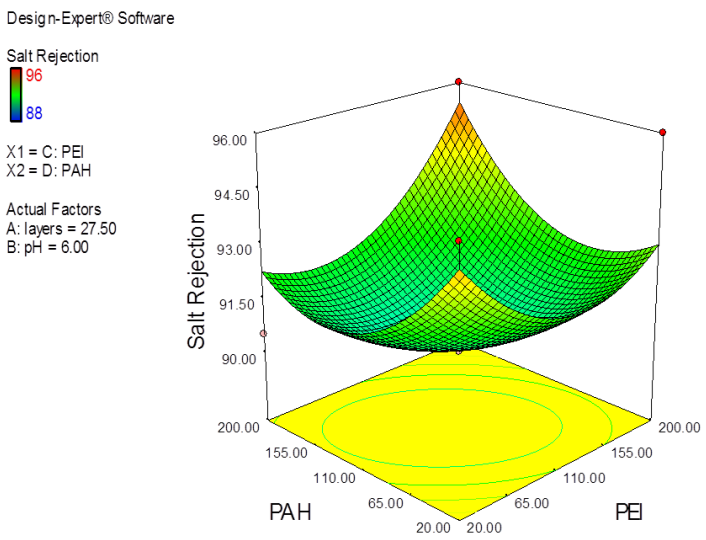

Figure 4-13: Response plot of salt rejection affected by PAH and PEI concentration (layers=27.5; pH=6)

Figure 4-14 shows the contour plot of salt rejection affected by number of layers and PAH concentration. It can be seen that increase in the layer number has profound effect on salt rejection as compared to increase of PAH concentration. 90 % salt rejection was achieved by depositing five bilayers of polyelectrolytes at 20 mg/L PAH; keeping the pH and PEI at constant levels. However, there was only 1% increase in salt rejection by increasing the PAH concentration up to 10 times. On the other hand, salt rejection increased to 95 % by depositing 50 bilayers of polyelectrolytes, due to increase in dense structure.

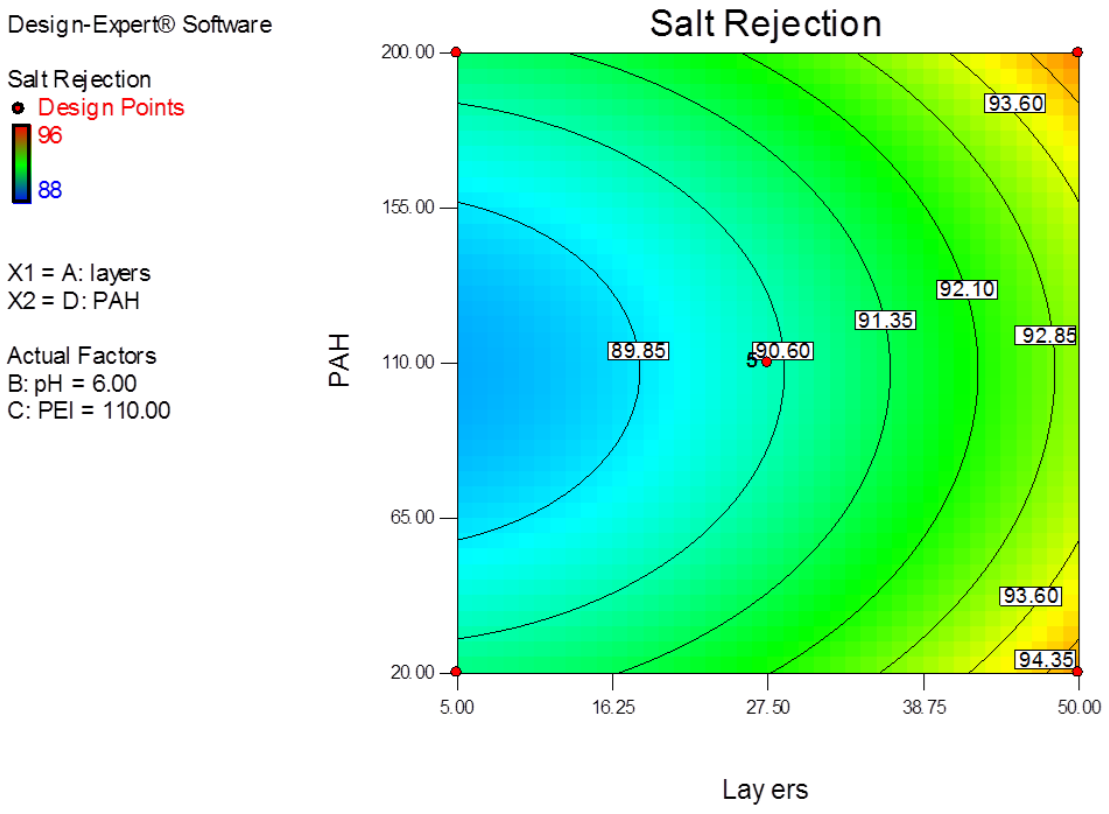

Figure 4-14: Contour plot of salt rejection affected by number of layers and PAH concentration (pH=6; PAH=110 mg/L)

4.5 Fouling Study

4.5.1 Analysis of Variance (ANOVA)

The coefficient of determination, R^2 for the model was 89.23%. The Model F-value of 8.28 recommends that model is significant. The larger F value and the smaller corresonding "Prob > F" (p value) shows the significant terms in the model. In the case of fouling flux, A, C, B^2 and C^2 are significant model terms. Signal to noise ratio of 10.508 indicates an adequate signal. In short, this model can be used to study the design space. The ANOVA summary is given in Table 4-6.

Final Equation in Terms of Actual Factors:

$$Fouling\ Flux\ \left(\frac{L}{m^2.hr}\right) = 2.57982 - 0.095924 * layers + 2.22202 * pH + 0.034629 * PEI - 4.02687E^{-3} * PAH + 0.010978 * layers * pH + 1.19259E^{-4} * layers * PEI + 1.41531\ E^{-4} * layers * PAH + 4.27083\ E^{-3} * pH * PEI + 1.03167\ E^{-3} * pH * PAH - 3.53241\ E^{-5} * PEI * PAH - 9.56881\ E^{-4} * layers^2 - 0.25216 * pH^2 - 1.45871\ E^{-4} * PEI^2 - 5.10288\ E^{-7} * PAH^2$$

By counting the significant model terms ,the expression was improved as follows;

$$Fouling\ Flux\ \left(\frac{L}{m^2.hr}\right) = -0.095924 * layers + 0.034629 * PEI - 0.25216 * pH^2 - 1.45871 * 10^{-4} * PEI^2 + 2.57982$$

Table 4-6: ANOVA summary for fouling flux

Response 4	Fouling Flux				
ANOVA for Response Surface Quadratic Model					
Analysis of variance table [Partial sum of squares - Type III]					
Source	Sum of Squares	df	Mean Square	F Value	p-value Prob > F
Model	110.87	14	7.92	8.28	0.0002
A-layers	*17.71*	*1*	*17.71*	*18.52*	*0.0007*
B-pH	*0.32*	*1*	*0.32*	*0.33*	*0.5740*
C-PEI	*73.81*	*1*	*73.81*	*77.19*	*< 0.0001*
D-PAH	*0.41*	*1*	*0.41*	*0.43*	*0.5225*
AB	*0.98*	*1*	*0.98*	*1.02*	*0.3295*
AC	*0.23*	*1*	*0.23*	*0.24*	*0.6290*
AD	*0.33*	*1*	*0.33*	*0.34*	*0.5671*
BC	*2.36*	*1*	*2.36*	*2.47*	*0.1382*
BD	*0.14*	*1*	*0.14*	*0.14*	*0.7098*
CD	*0.33*	*1*	*0.33*	*0.34*	*0.5677*
A^2	*1.52*	*1*	*1.52*	*1.59*	*0.2277*
B^2	*6.60*	*1*	*6.60*	*6.90*	*0.0199*
C^2	*9.06*	*1*	*9.06*	*9.47*	*0.0082*
D^2	*1.108E-004*	*1*	*1.108E-004*	*1.159E-004*	*0.9916*
Residual	13.39	14	0.96		
Lack of Fit	*12.23*	*10*	*1.22*	*4.24*	*0.0881*
Pure Error	*1.15*	*4*	*0.29*		

4.5.2 Graphical Residual Analysis

Figure 4-15 shows the predicted values versus actual values of fouling flux. It can be seen that majority of the actual experimental values were close to theoretical straight line, indicating developed model was useful in developing the correlation between input variables and corresponding flux.

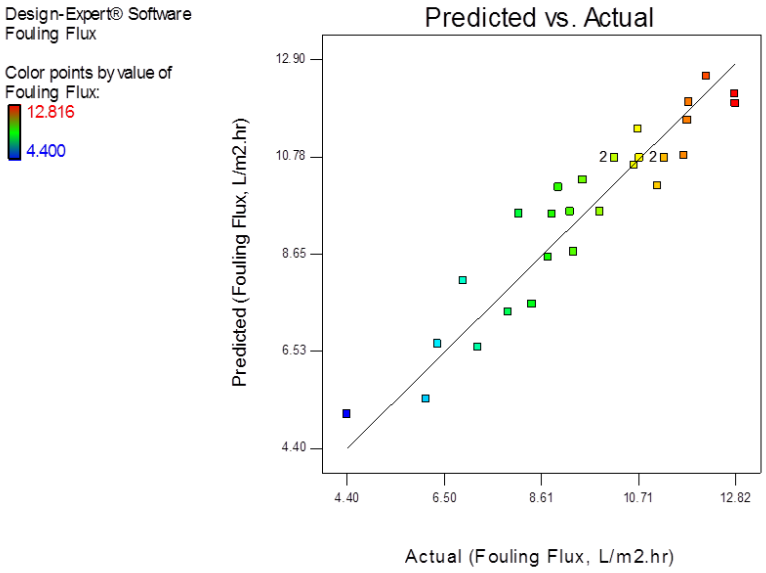

Figure 4-15: Predicted versus actual fouling flux

Figure 4-16 shows the normal plot of residuals for fouling flux. Since, all residuals lie on straight line except one point. It indicates that residuals follow normal distribution of errors with mean value of 1.5. The resulted residuals occurred due to noise.

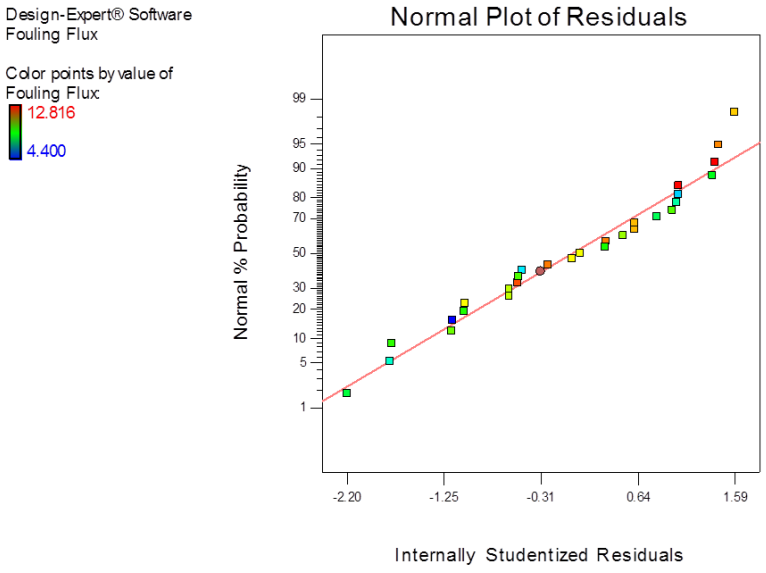

Figure 4-16: Normal plot of residuals

4.5.3 Three dimensional study for fouling flux

Figure 4-17 shows the combine effect of PEI concentration and number of layers on flux under fouling conditions (fouling flux). Flux decline after fouling decreased with increasing number of layers but PEI has dominant impact in achieving maximum fouling flux. Even, if the number of layers were kept constant, a rise in PEI concentration has remarked effect on boosting fouling flux. When the PEI concentration was 20 mg/L, it provided 6.926 L/m^2.hr of flux but it raised to 12.193 L/m^2.hr with 200 mg/L PEI concentration. This is a more than 43 % increase in flux. However, 58.6 % flux increase was achieved by increasing the PEI concentration from 20 to 200 mg/L with 50 bilayers. The flux rise can be explained as a result of more surface coverage which imparts hydrophilicity and reduced the surface roughness.

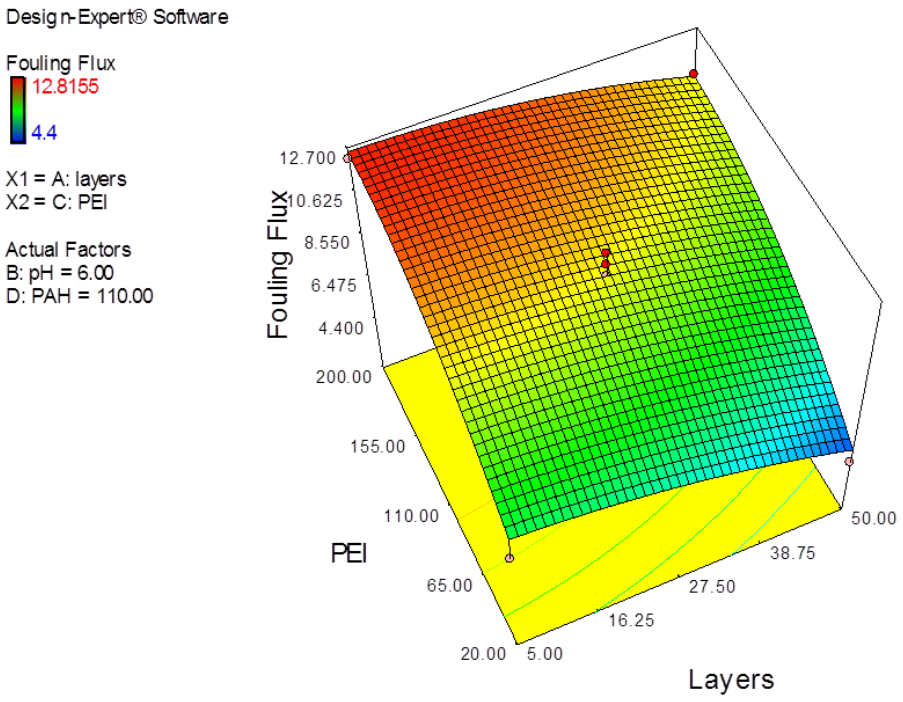

Figure 4-17: Response plot of fouling flux affected by number of layers and PEI concentration (PAH=110; pH=6)

Figure 4-18 shows the contour plot of fouling flux affected by pH and PEI concentration by keeping layers and PAH at constant levels. It is clear that higher pH is not in favor of getting greater flux. As, flux was 6.368 L/m^2.hr at 4.0 pH but decreased to 6.12 L/m_2.hr that is almost 3.9 % flux decline. However, pH and PEI both support each other at maximum experimental conditions to get higher flux. For example, flux rise of 46% was attained on shifting from lower to maximum operating conditions of pH and PEI.

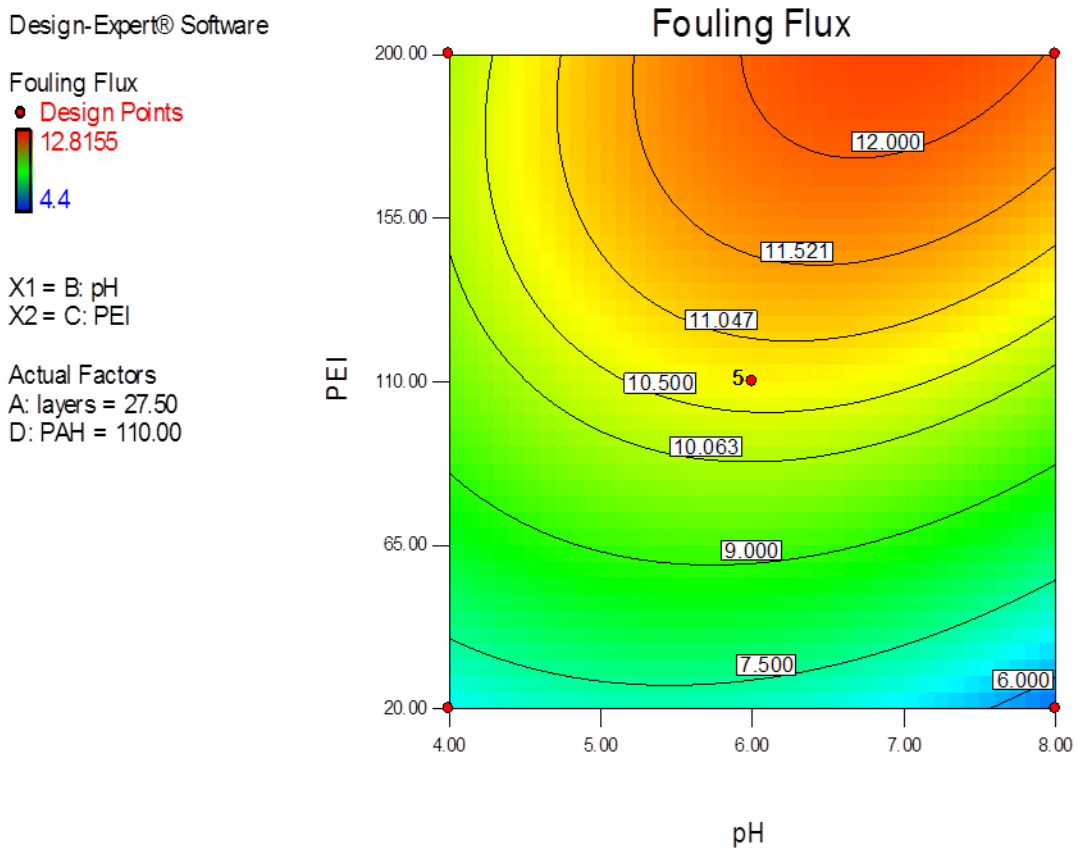

Figure 4-18: Contour plot of salt rejection affected by pH and PEI concentration (layers=27.5; PAH=110 mg/L

4.6 Flux Recovery after Membrane Cleaning

4.6.1 Analysis of Variance (ANOVA)

The coefficient of determination, R^2 for the model was 87.76%. The Model F-value of 7.17 confirms that model is significant. The smaller "Prob > F" (p value) shows the significant terms in the model. In the case of recovery flux, A, C, B^2 and C^2 are significant model terms. Signal to noise ratio of 9.844 indicates an adequate signal. So, this model can explain the experimental behaviour. The ANOVA summary is given in Table 4-7.

Final Equation in Terms of Actual Factors:

$$Recovery\ Flux\ \left(\frac{L}{m^2.hr}\right) = 2.43486 - 0.13773 * layers + 2.47207 * pH + 0.041411 * PEI + 9.13569E^{-3} * PAH + 0.01510 * layers * pH + 1.70753E^{-4} * layers * PEI + 1.77778\ E^{-4} * layers * PAH + 3.54028\ E^{-3} * pH * PEI + 5.55556\ E^{-5} * pH * PAH - 3.26852\ E^{-5} * PEI * PAH - 9.92609\ E^{-4} * layers^2 - 0.27044 * pH^2 - 1.68797\ E^{-4} * PEI^2 - 2.84871\ E^{-5} * PAH^2$$

By maintaining the significant model terms ,the improved expression is given below;

$$Recovery\ Flux\ \left(\frac{L}{m^2.hr}\right) = -0.13773 * layers + 0.041411 * PEI - 0.27044 * pH^2 - 1.68797 * 10^{-4} * PEI^2 + 2.43486$$

Table 4-7: ANOVA summary for recovery flux

Response 5	Recovery Flux				
ANOVA for Response Surface Quadratic Model					
Analysis of variance table [Partial sum of squares - Type III]					
Source	Sum of Squares	df	Mean Square	F Value	p-value Prob > F
Model	117.04	14	8.36	7.17	0.0004
A-layers	*24.40*	*1*	*24.40*	*20.94*	*0.0004*
B-pH	*0.068*	*1*	*0.068*	*0.058*	*0.8127*
C-PEI	*68.87*	*1*	*68.87*	*59.09*	*< 0.0001*
D-PAH	*1.96*	*1*	*1.96*	*1.69*	*0.2152*
AB	*1.85*	*1*	*1.85*	*1.58*	*0.2287*
AC	*0.48*	*1*	*0.48*	*0.41*	*0.5322*
AD	*0.52*	*1*	*0.52*	*0.44*	*0.5157*
BC	*1.62*	*1*	*1.62*	*1.39*	*0.2575*
BD	*4.000E-004*	*1*	*4.000E-004*	*3.432E-004*	*0.9855*
CD	*0.28*	*1*	*0.28*	*0.24*	*0.6314*
A^2	*1.64*	*1*	*1.64*	*1.41*	*0.2556*
B^2	*7.59*	*1*	*7.59*	*6.51*	*0.0230*
C^2	*12.13*	*1*	*12.13*	*10.40*	*0.0061*
D^2	*0.35*	*1*	*0.35*	*0.30*	*0.5948*
Residual	16.32	14	1.17		
Lack of Fit	*14.95*	*10*	*1.50*	*4.38*	*0.0838*
Pure Error	*1.37*	*4*	*0.34*		

4.6.2 Graphical Residual Analysis

Figure 4-19 shows the predicted versus actual recovery flux. It can be estimated that majority of the actual values were close to straight line. Also, there is almost equal scattering above and below the straight line. It indicates that proposed mathematical model is sufficient to explain the real behavior.

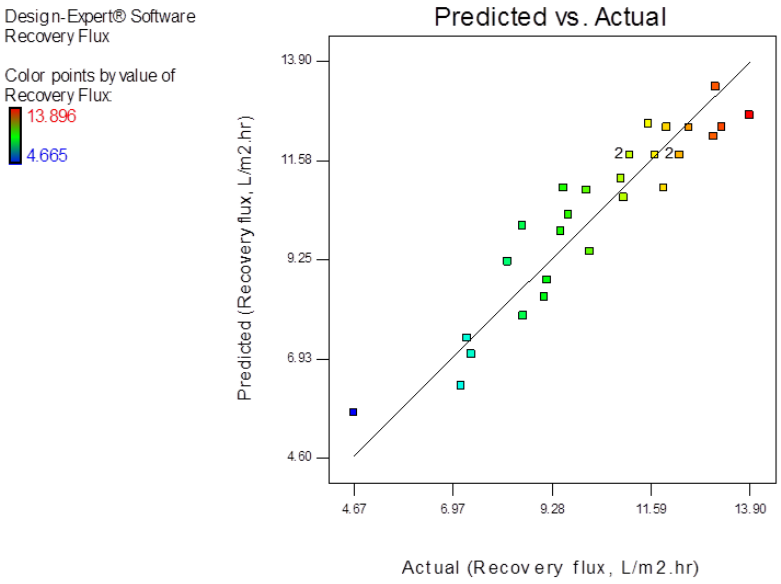

Figure 4-19: Predicted versus actual fouling flux

Figure 4-20 shows the normal plot of residuals for recovery flux. Majority of the residuals lie on straight line indicating normal distribution of errors with 1.9 mean values. It predicts the adequacy of the model to illustrate the experimental behavior.

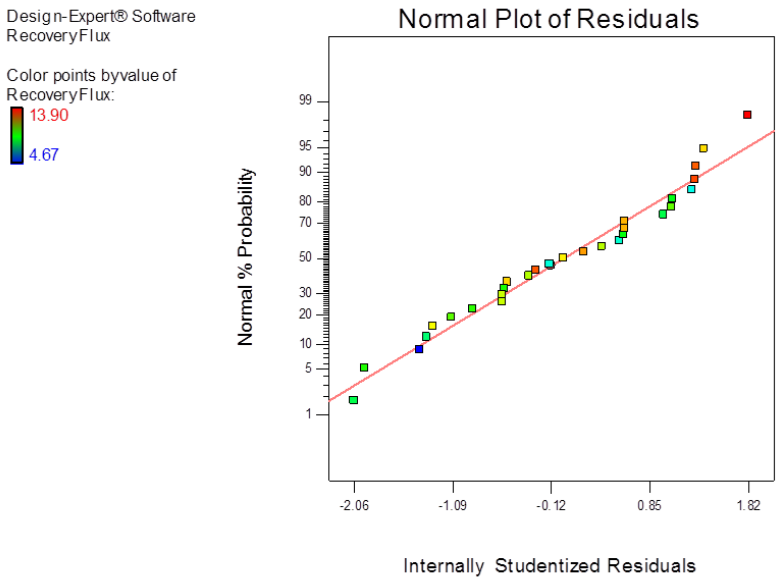

Figure 4-20: Normal plot of residuals

4.6.3 Three dimensional study for Recovery flux

Figure 4-21 shows the combine effect of pH and number of layers on recovery flux; which is flux after cleaning the fouled membrane. It is clear that flux increased substantially by decreasing the depositing layers and pH. Moving from maximum to mid-point, more than 20% flux enhancement was observed. However, flux was recorded maximum with lowest pH and lowest number of deposited layers. It is obvious that by increasing the layers, thickness of the deposited films will increase resulting in less flux.

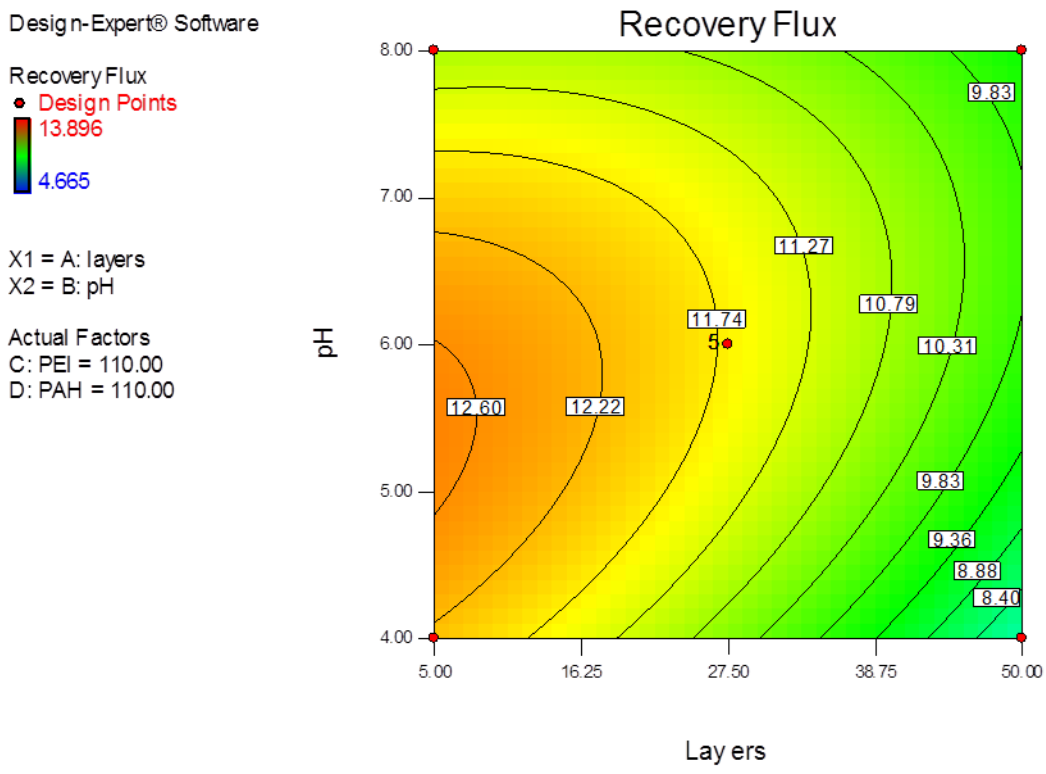

Figure 4-21: Contour plot of recovery flux collectively affected by number of layers and pH at 110 mg/L PEI/PAH

4.7 Contact Angle

4.7.1 Analysis of Variance (ANOVA)

The coefficient of determination, R^2 for the model was 90.66%. The Model F-value of 9.70 endorses the significance of mathematical model. Here, A, D, and C^2 were significant model terms due to less p values. Adequecy of mathematical model was shown by high value of signal to noise ratio. A ratio of 11.678 was present, which usually a value of 4.0 is required for model suitability. So, this model can describe the experimental behaviour. The ANOVA summary is given in Table 4-8.

Final Equation in Terms of Actual Factors:

$$
\begin{aligned}
Contact\ Angle \\
&= 60.07407 \ - 0.32469 * layers \ - \ 4.19681 * pH \ + 0.19460 \\
&* PEI \quad + 0.028333 \ * PAH \ + 1.72840E^{-4} * layers * PEI \\
&- 1.97531\ E^{-4} \ * layers * PAH - 4.72222\ E^{-3} * pH * PEI \\
&+ 4.86111\ E^{-3} * pH * PAH - 9.56790\ E^{-5} * PEI * PAH \\
&+ 2.96296\ E^{-3} \ * \ layers^2 + 0.37187 * \ pH^2 - 7.299938\ E^{-4} * \ PEI^2 \\
&- 1.26543\ E^{-4} * \ PAH^2
\end{aligned}
$$

After removing the insignificant model terms ,the improved expression is given below;

$$
\begin{aligned}
Contact\ Angle \\
&= -0.32469 * layers \ + 0.028333 \ * PAH \ - 7.299938\ E^{-4} * \ PEI^2 \\
&+ \ 60.07407
\end{aligned}
$$

Table 4-8: ANOVA summary for contact angle

Response 7	Contact Angle				
ANOVA for Response Surface Quadratic Model					
Analysis of variance table [Partial sum of squares - Type III]					
Source	Sum of Squares	df	Mean Square	F Value	p-value Prob > F
Model	504.46	14	36.03	9.70	< 0.0001
A-layers	*164.28*	*1*	*164.28*	*44.24*	*< 0.0001*
B-pH	*3.74*	*1*	*3.74*	*1.01*	*0.3325*
C-PEI	*8.333E-004*	*1*	*8.333E-004*	*2.244E-004*	*0.9883*
D-PAH	*18.25*	*1*	*18.25*	*4.92*	*0.0437*
AB	*0.000*	*1*	*0.000*	*0.000*	*1.0000*
AC	*0.49*	*1*	*0.49*	*0.13*	*0.7218*
AD	*0.64*	*1*	*0.64*	*0.17*	*0.6843*
BC	*2.89*	*1*	*2.89*	*0.78*	*0.3925*
BD	*3.06*	*1*	*3.06*	*0.82*	*0.3791*
CD	*2.40*	*1*	*2.40*	*0.65*	*0.4346*
A^2	*14.59*	*1*	*14.59*	*3.93*	*0.0674*
B^2	*14.35*	*1*	*14.35*	*3.87*	*0.0694*
C^2	*226.75*	*1*	*226.75*	*61.07*	*< 0.0001*
D^2	*6.81*	*1*	*6.81*	*1.84*	*0.1970*
Residual	51.98	14	3.71		
Lack of Fit	*51.94*	*10*	*5.19*	*519.42*	*< 0.0001*
Pure Error	*0.040*	*4*	*0.010*		

4.7.2 Graphical Residual Analysis

Residual analysis was used to check the fitting of mathematical model with experimental data. Figure 4-22 shows the predicted versus actual contact angle. It can be seen that actual values were close to straight line. There was little variability that was not being explained by model. It indicates that proposed model is satisfactory to explain the real behavior.

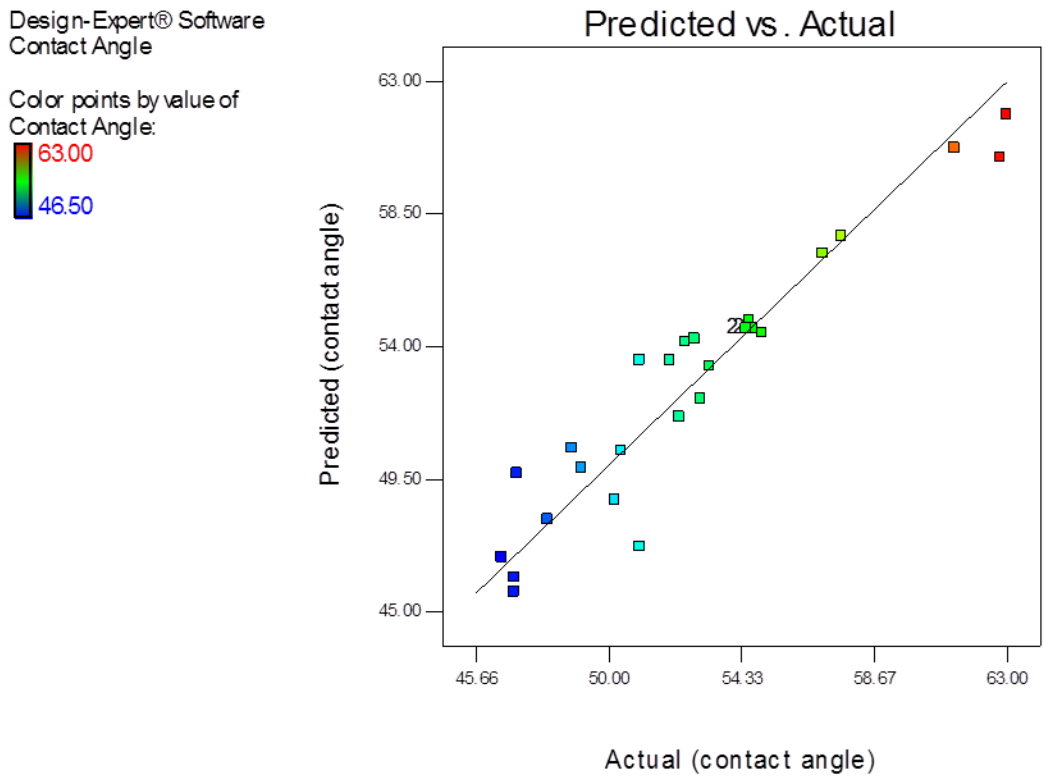

Figure 4-22: Predicted versus actual contact angle

Box Behnken design model was tested by calculating the residuals. Figure 4-23 shows the normal plot of residuals for contact angle. Maximum residuals lie on straight line around mean of one. It forecasts the suitability of model to determine the experimental behavior due to normal distribution of error.

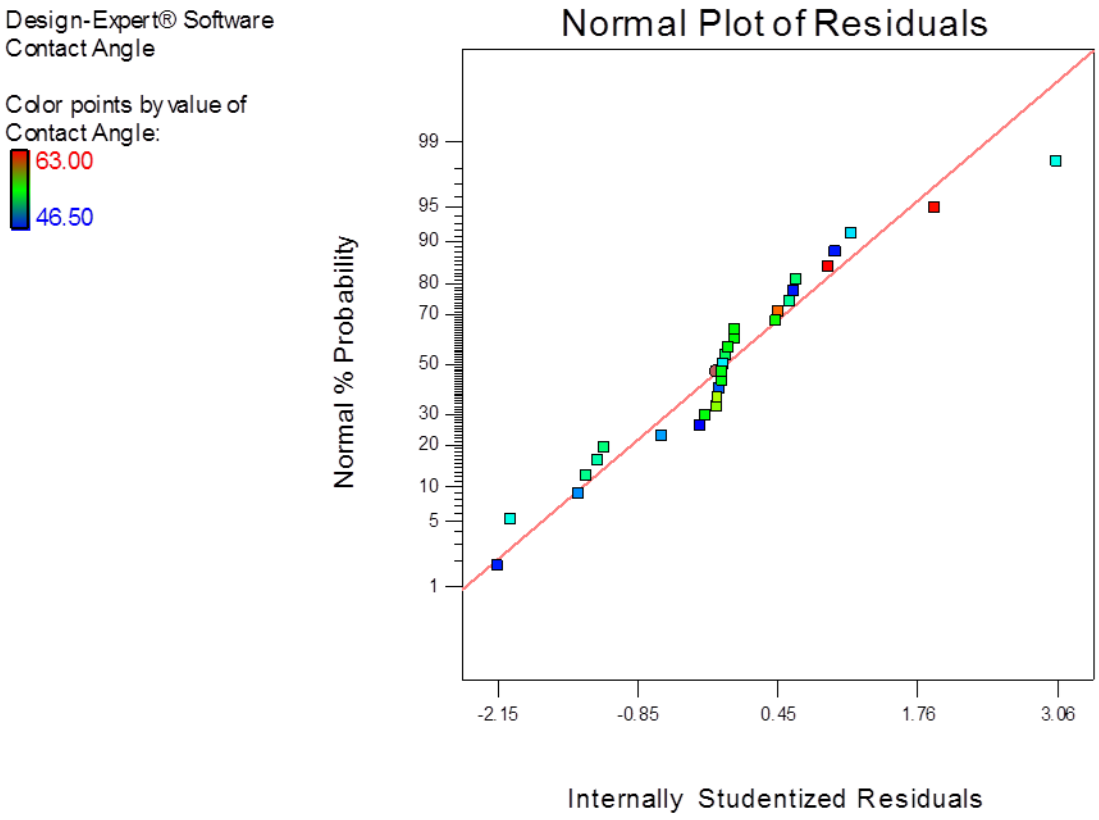

Figure 4-23: Normal plot of residuals

4.7.3 Three dimensional study for contact angle

Figure 4-24 shows the effect of concentration of both depositing polyelectrolytes on contact angle keeping constant pH and layers. The measurement of contact angle shows the smoothness of surface. A lower contact angle is an indication of smoother surface. It is evident that by increasing the concentration of both polyelectrolytes from 20 mg/L to 110 mg/L, contact angle increased from 46.9^{o} to 54.5^{o}. However, further increasing the concentration to 200 mg/L resulted in decline of contact angle to 48^{o}. Therefore, it can be easily stated that smooth surface was achieved at mid-point conditions. In addition, there was an interesting finding that although increasing the concentration of both

polyelectrolytes was enhancing smoothness, however, increase in PEI concentration has much greater effect than increasing PAH concentration.

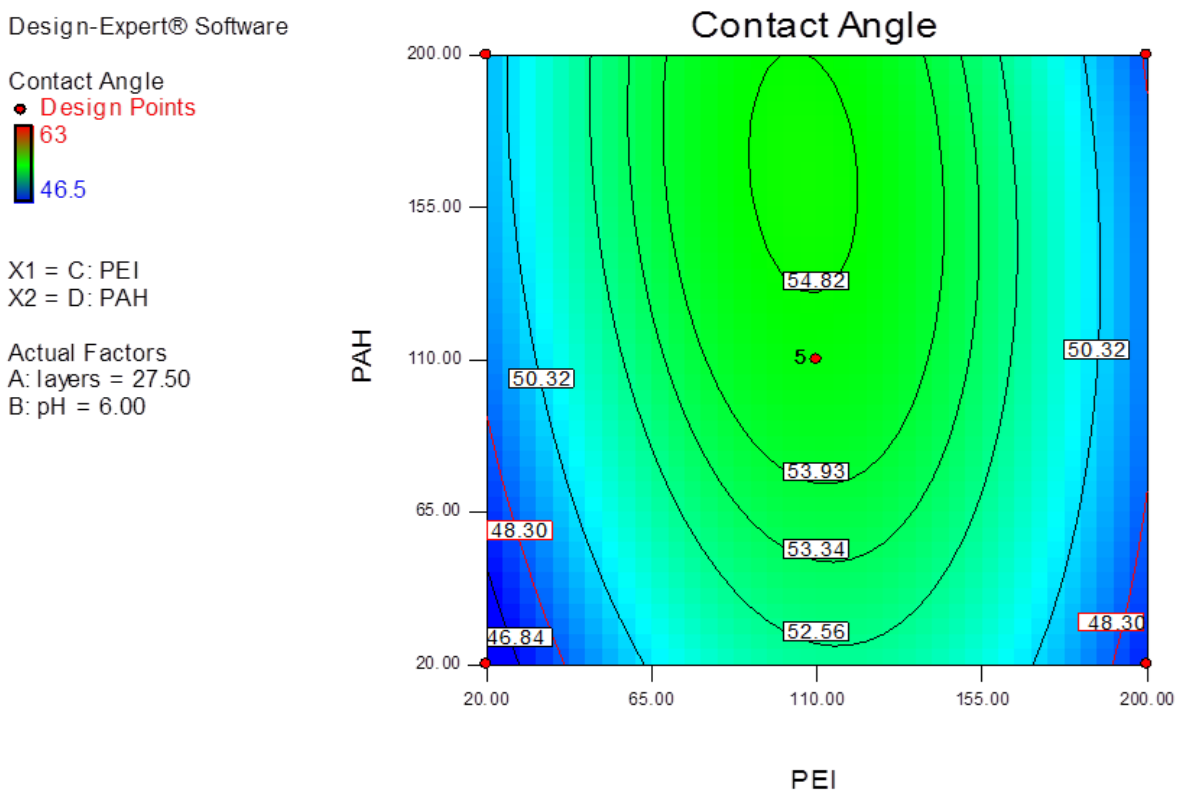

Figure 4-24: Contour plot of contact angle affected by concentration of PEI and PAH

Table 4-9: ANOVA summary for all responses

Response/Constraint	Co-efficient of determination R^2 %	Model F value	Adequate Precision	Significant Terms
Pure flux	85.23	5.77	9.386	A, C
Saline flux	86.30	6.30	9.417	A, C, B^2
Salt rejection	85.81	3.13	6.746	A, C^2, D^2
Fouling Flux	89.23	8.28	10.508	A, C, B, C^2
Recovery flux	87.76	7.17	9.844	A, C, B^2, C^2
Contact angle	90.66	9.70	11.678	A, D, C^2

4.8 Optimization

To optimize all the input parametrs and the measured responses, desired goals were set. All the input variables were taken in range while all the responses were set to maximize except the contact angle that was set to mimium value. Inputs were set at an significance of 3 which shows medium satisfactory level. All Responses were set at high importance of 5 except the recovery flux that was set at the satisfactory level. All these conditions are given in Table 4-10. Optimization was run for 30 cycles.

Table 4-10: Constraints level for optimization

Constraints				
Name	**Goal**	**Lower Limit**	**Upper Limit**	**Upper Importance**
Layers	in range	5	50	3
pH	in range	4	8	3
PEI	in range	20	200	3
PAH	in range	20	200	3
Pure Flux	maximize	7.842	15.813	5
Saline Flux	maximize	6.46	14.5	5
Salt Rejection	maximize	88	99.99	5
Fouling Flux	maximize	4.4	12.8155	5
Recovery Flux	maximize	4.665	13.896	3
Contact Angle	minimize	46.5	63	5

The overall desirability of the optimized solution was 0.865; a value close to one is considered as good. The histogram for satisfactory level of each response and input is also shown in Figure 4-25. The optimum conditions of inputs and the corresponding responses are summarized in Table 4-11.

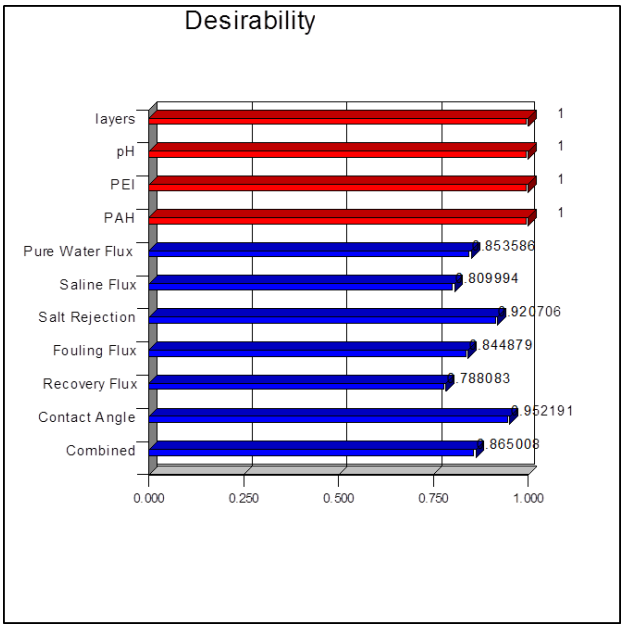

Figure 4-25: Desirability histogram for all constraints

It is manifested that both the polyelectrolytes must be used with their maximum input concentration with 7.6 pH to get the higher optimum flux and salt rejection. However, 48.5 bilayers are enough to modify the existing polyamide layer, in order to impart sufficent hydrophilic charteristics to get minimal flux drop.

Table 4-11: Optimum performance Parameters

Constraint	Unit	Optimum Level
Layers	No.	48.5
pH	---	7.6
Poly (ethylene imine)	mg/L	200
Poly (allyl amine hydrochloride)	mg/L	200
Pure water flux	$L/m^2.hr$	14.64
Saline flux	$L/m^2.hr$	12.95
Salt Rejection	%	99.2
Fouling flux	$L/m^2.hr$	11.48
Recovery Flux	$L/m^2.hr$	11.91
Contact Angle	Degree	47.35

CHAPTER 5

RESULTS AND DISCUSSION

5.1 Scanning Electron Microscopy

The unique structure of RO membrane is clearly visible in Figure 5-1 (a). The surface morphology is rough and has typical ridge and valley structure [142], [143] which is the distinctive behavior of interfacial polymerization. It happens due to fast and uncontrolled reaction at the interface during the process of polymerization [144]. The noddle like particles are scattered on the surface of the membrane showing the presence of active polyamide layer but in a non-uniform arrangement. However, with the deposition of polyelectrolyte solution, a noticeable variation in surface morphology is observed as in Figure 5-1 (b). With only 5 bilayers, the surface becomes fairly smooth as compare to un-modified RO membrane. The polyelectrolyte solution penetrated into the valley parts to fill the rough surface, resulting in the membrane smoothness. This feature is even more prominent in the case of 27 and 50 bilayers as shown in Figure 5-1 (c) and (d) respectively. By increasing the number of layers, increase in smoothness is observed. It is anticipated that, this increase in membrane smoothness can enhance the anti-fouling ability of the polyelectrolyte modified membrane [145].

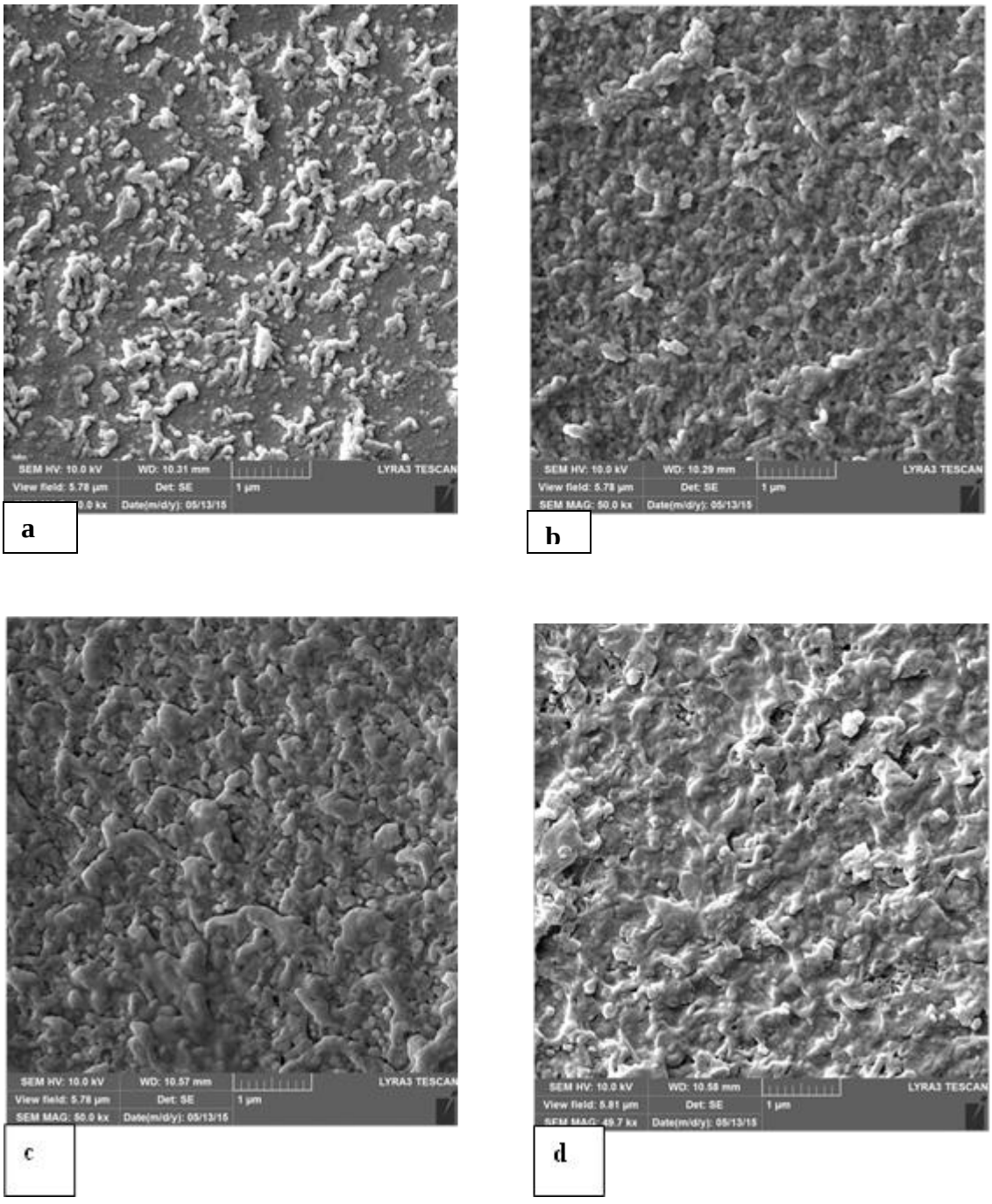

Figure 5-1: SEM images of (a) pristine polyamide (b) 5 bilayers (c) 27.5 bilayers (d) 50 bilayer

Another useful finding is the effect of increasing concentration of polyelectrolyte during deposition of layers as shown in Figure 5-2. By increasing the polyelectrolyte concentration, membrane surface is becoming smooth. It seems that particles has arranged themselves one above the other in the form of stacking; leaving behind no

empty region on the surface which has noticeable uniformity. Effect of concentration is prominent in case of 200 mg/L of polyelectrolyte as in Figure 5-2 (d). The surface is shiny and it seems that it has some brushing that has made the surface smooth. The increase in concentration is expected to enhance in water flux as was achieved by Sanchuan et al [146].

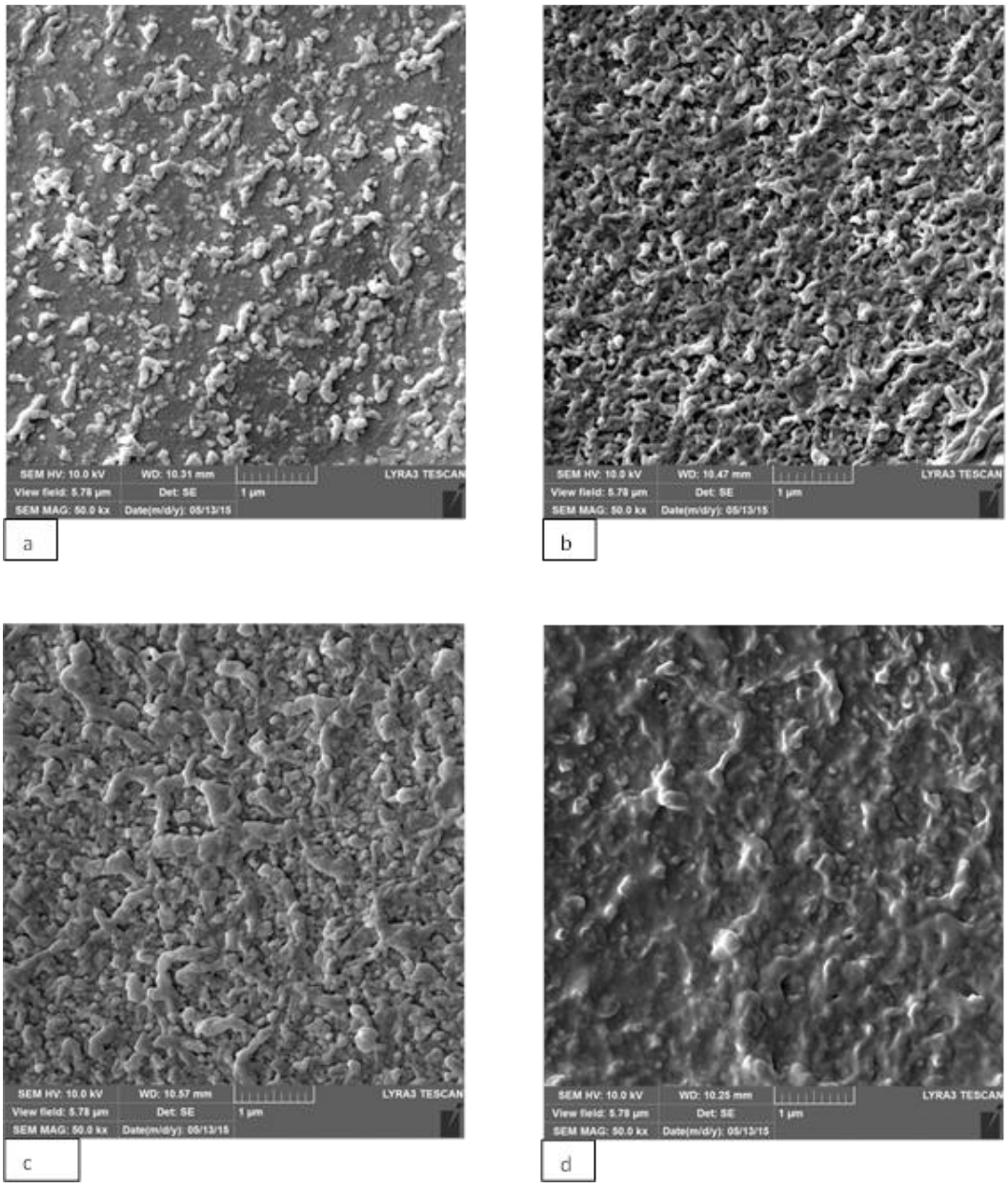

Figure 5-2: SEM images of (a) pristine polyamide (b) 20 mg/L PEI/PAH (c) 110 mg/L PEI/PAH (d) 200 mg/L PEI/PAH

The successful deposition of polyamide barrier layer is clearly visible in cross section image as shown in Figure 5-3 (a). The rough polyamide structure is in accordance with Jeong et al [37]. The estimated thickness of the active layer is found to be 264.5 nm, comparable with 255 nm as mentioned by Leckie et al [147]. The effect of bilayer deposition is demonstrated in Figure 5-3 (b)-(d). By increasing the number of layers, thickness of the barrier layer increased as shown in Table 5-1. It also resulted in the compactness of the polyamide active layer. The random looking barrier layer got aligned with the deposition of polyelectrolyte multilayers. This alignment can be linked with decrease in membrane roughness and increase in arrangement of noddle like particles. On the other hand, increase in thickness may contribute in enhancing resistance to water flow. So, it is expected that the rise in resistance with number of layers will decrease the water flux. Anyhow, thickness achieved was less as compared to reporting by Seo et al [117] using layer by layer assembly of PEO/PAA multilayers. Their average bilayer thickness was 21 nm per bilayer after depositing 50 multilayers. In this study, the average increment of polyelectrolyte bilayers was 6 nm after depositing 50 bilayers.

Table 5-1: Effect of bilayers on membrane thickness

Membrane	***Thickness (nm)**
Pristine Polyamide	264.5
5 bilayers membrane	282.1
27.5 bilayers membrane	393.2
50 bilayers membrane	567

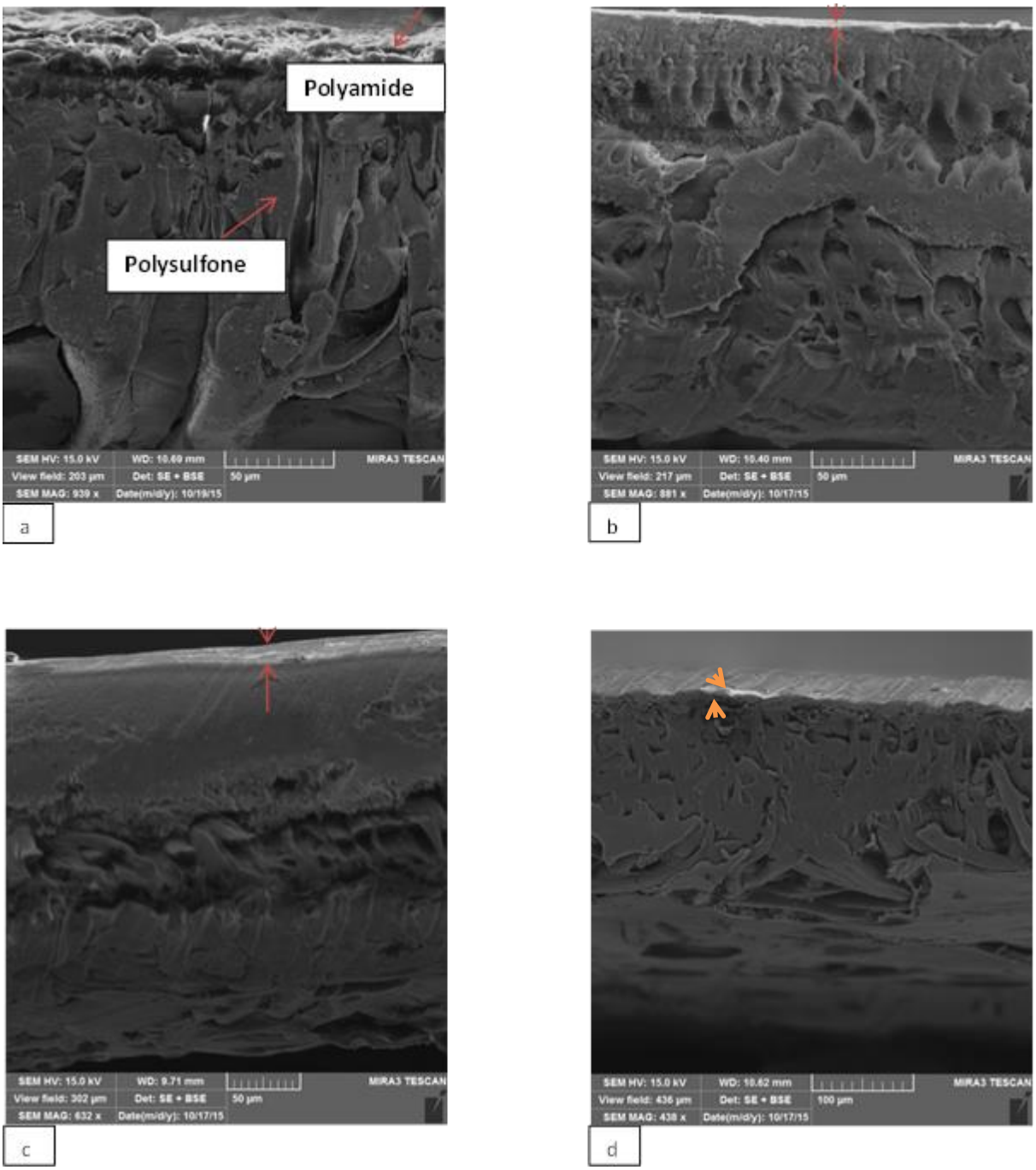

Figure 5-3: Cross section SEM images of (a) pristine polyamide (b) 5 bilayers PEI/PAH (c) 27 bilayers PEI/PAH (d) 50 bilayers PEI/PAH
Concentration of both polyelectrolytes = 110 mg/L

*bilayer thickness includes pristine polyamide of 264.5 nm.

5.2 Contact Angle

The investigation of membrane surface hydrophilicity was done by measuring the contact angle. The wettability of both the modified and un-modified RO membrane was analyzed. A lower value of contact angle is an indication of good wettability of the surface as well as its smoothness [148]. From SEM analysis, it was expected that polyelectrolyte coating will develop smooth and hydrophilic surface that will reduce the contact angle. Hydrophilic surfaces are less attacked by foulant materials and thereby enhance membrane life [26].

Table 5-2 shows the contact angle value for pristine and modified RO membranes. It can be seen that virgin membrane has higher contact angle, indicating its higher roughness as it was analyzed in SEM analysis. Increasing the number of coating layers resulted in decreasing contact angle indicating increased hydrophilicity of membrane surface. The pure polyamide prepared in this study has contact angle of 70^{o} which is way better than commercial Hydronautics SWC membrane which has contact angle of 96^{o}. However, after modification by depositing 50 bilayers of PEI/PAH, it was decreased to 53.3^{o}. Hence, polyelectrolyte modified membranes are fairly smooth and hydrophilic as compare to unmodified membrane. The relationship of increasing layer numbers and the corresponding less contact angle is in accordance with the observations of other researchers [119], [121], [149].

Table 5-2: Effect of layer number on contact angle

Membrane	Contact angle (^{o})
Pristine Polyamide	70
5 bilayers membrane	63
27.5 bilayers membrane	54.6
50 bilayers membrane	53.3
All modified membrane has 110 mg/L PEI/PAH	

5.3 Atomic Force Microscopy

AFM was used to study the surface roughness of the modified and un-modified RO membranes and the results are presented in Table 5-3. The membrane roughness is a valuable tool to study the fouling phenomena on membrane surface. However, the relationship between membrane roughness and fouling depends on various parameters as described by Johnson et al [150]. It can be seen from Table 5-3 that the average membrane surface roughness of pristine RO membrane is 119.4 nm. This much high surface roughness is in accordance with Hashaikeh et al [151] who described that reverse osmosis membranes are rougher than cellulose acetate membrane and is more attacked by

the foulant particles. Moreover, high root mean square roughness is attributed to ridge and valley structure of typical polyamide RO membrane that can be seen in Figure 5-4. The valleys in the structure will offer more surface area to the foulant particles to accumulate and will result in severe fouling and eventually flux decline [23].

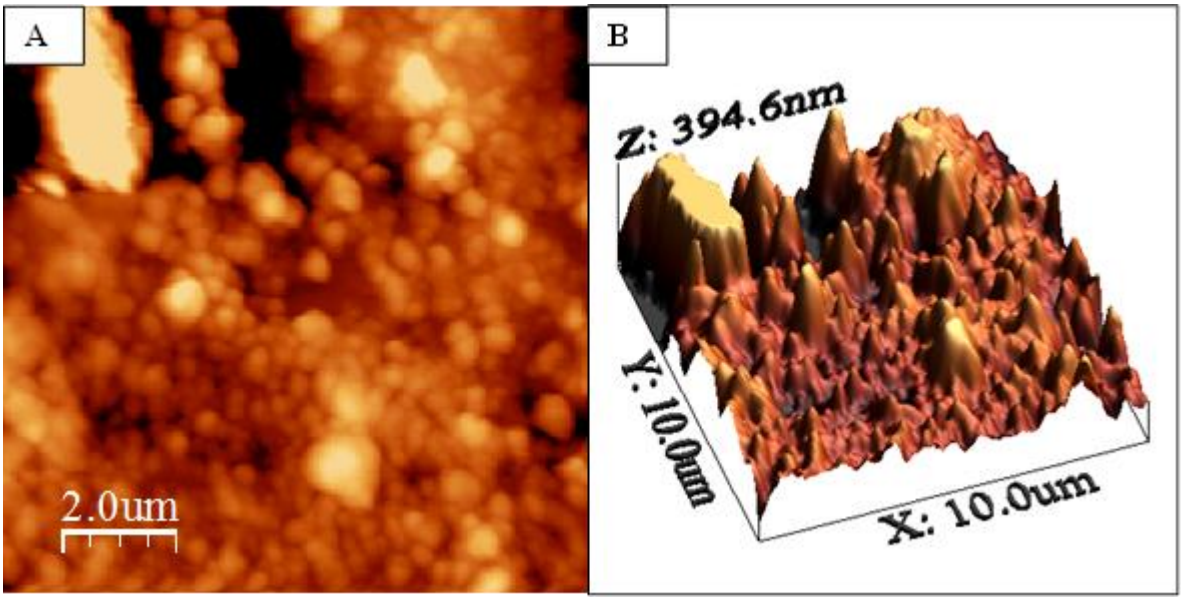

Figure 5-4: AFM images of pristine polyamide (A) top view (B) 3D view

On the other hand, coating of PEI/PAH polyelectrolyte multilayers has significantly reduced the membrane surface roughness. It was expected that deposition of polyelectrolyte solutions will decrease the available area to the foulants [152], thereby reducing the clogging of valley parts. This reduction in membrane roughness will significantly contribute in enhancement of flux due to rise in smoothness [153]. Figure 5-5 shows the top and three dimensional views of modified membranes. The increase in smoothness and vanishing of valley parts is clearly noticeable as multilayer deposition cycle increase from 5 to 50.

The increase in number of layers is found to be favorable in making the surface smooth. The reduced roughness is due to presence of hydrophilic hydroxyl and amine groups, as they impart smoothness to the surface. Therefore, increase in layer numbers resulted in increase in the density of these hydrophilic groups which contributes in enhancing smoothness as obvious from reduced roughness values of Table 5-3.

Table 5-3: Effect of layer number on membrane surface roughness

Membrane	**Average roughness nm**
Pristine Polyamide	119.4
5 bilayers membrane	85.79
27.5 bilayers membrane	63.64
50 bilayers membrane	42

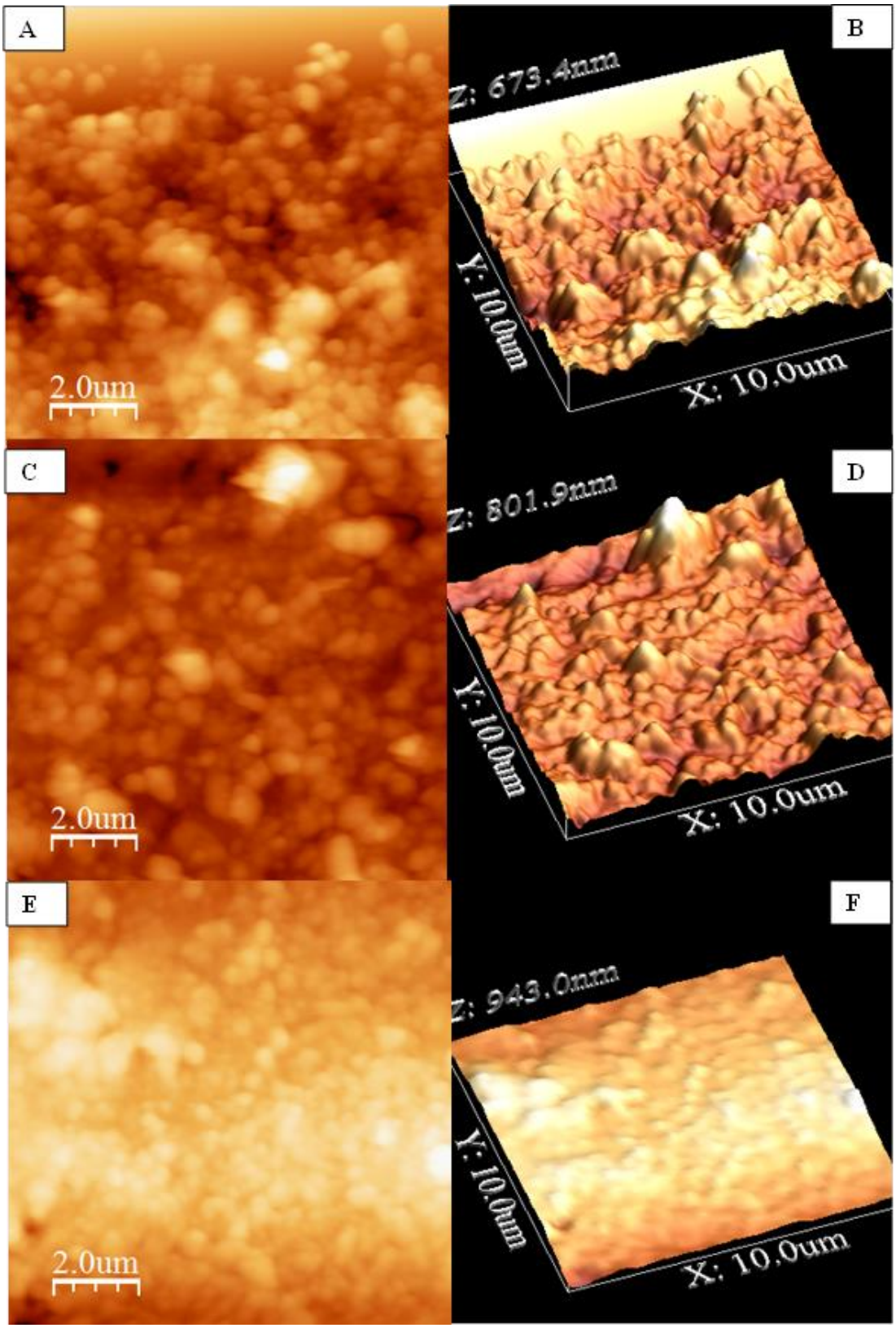

Figure 5-5: AFM images of modified membranes A&B (5 bilayers), C&D (27.5 bilayers), E&F (50 bilayers)

5.4 Thermal Gravimetric Analysis

Figure 5-6 shows the thermo gravimetric analysis of the modified and unmodified membranes in inert nitrogen environment at 1000 ^{o}C. In case of pure polyamide membrane, thermal degradation was started after 300^{o}C which is due to melting of polymer side chains and cyclic oligomers [154]. It is clear that 900^{o}C was enough for complete degradation of un-modified polyamide membrane with a residue of approximately 6 %.

However, after depositing PEI/PAH multilayers on the polyamide membrane, the starting degradation temperature shifted to 350 ^{o}C which is attributed to additional protective coating of the polyelectrolytes on the polyamide surface. This shift in temperature can be explained on the restricted movement of polyamide chains after depositing polyelectrolytes, even at greater temperature. Moreover, by increasing the number of layers, residue amount was also increased after complete degradation. With 5 bilayers, residue increased to 7 % which further grew to almost 9.6% with 27 bilayers of PEI/PAH.

In case of 50 bilayers PEI/PAH coating, degradation occurred in two steps: almost 10% weight loss occurred up to 40 ^{o}C and the second phase was the similar to 5 and 27 bilayers. The unusual first loss is referred to the loss in water that was absorbed during interfacial polymerization or during any of the washing steps [155]. In addition to this, residue was more than 13 % that is even higher than all other modified membranes.

Therefore, it was observed that thermal resistance of the base membrane was enhanced by coating the PEI/PAH polyelectrolyte multilayers.

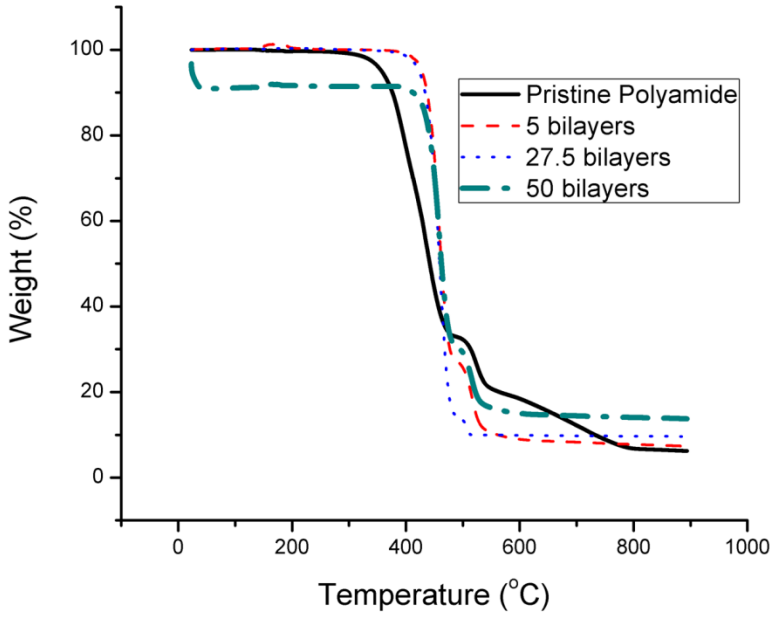

Figure 5-6: TGA curves for pristine and modified polyamide membranes

5.5 Fourier Transform Infra-Red Spectroscopy

FTIR spectrums of modified and unmodified membrane are shown in Figure 5-7. The peaks of both membranes are identical and there is no prominent difference between them. This indicates the lack of presence of any undesirable product. It also conforms the fact that after depositing 50 bilayers of PEI/PAH polyelectrolyte solutions, the parent polyamide structure remain unchanged. Both the spectrum contains characteristics polyamide peaks of aromatic ring stretching vibration and amide II band C-NH plane bending at 1609 cm^{-1} and 1543 cm^{-1} respectively [156], [157]. In addition to this, characteristics peak of polysulfone base membrane at 1243 cm^{-1} is also present in spectra. [158].

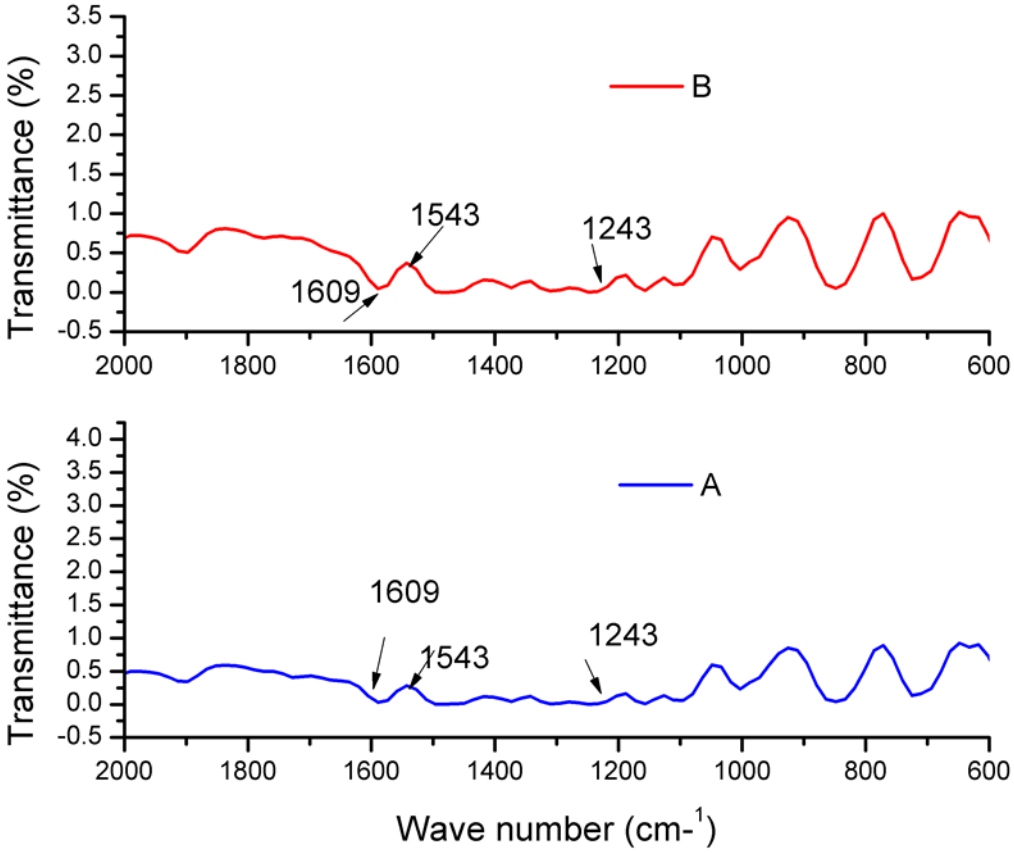

Figure 5-7: FTIR spectrums of (A) Pristine polyamide (B) 50 bilayer PEI/PAH

5.6 Permeation Results

5.6.1 Effect of Layer Number

Figure 5-8 shows the effect of number of layers on pure water flux of virgin and polyelectrolytes modified polyamide membranes. All the polyelectrolyte multilayers were synthesized at 110 mg/L solution concentrations. It is evident from Figure 5-8 that flux of pure polyamide is higher as compared to the modified membranes. In case of virgin membrane, flux achieved was 16.6 L/m^2.hr that is far better than reported by Lee et al [113] and Kwon et al [159] for a typical polyamide membrane with a value of 11.8 L/m^2.hr at similar operating conditions. This indicates an increase of approximately 28.9 % which is attributed to careful preparations of polyamide membrane including the MPD soaking time and rinsing with rubber roller. Also, heating the TFC PA membrane after preparation, at 60 ^oC contributes in the additional cross linking in the polymeric structure to get higher flux.

The flux decline after depositing polyelectrolyte multilayers is obvious as it is the outcome of additional thickness on the polyamide surface which is contributing more resistance to the flow of water across the membrane. As described earlier in the cross-section analysis, as the number of layers increased the thickness of the films increase. Therefore, flux decline take place with the layer number.

A very interesting observation is the flux decline behavior of modified and un-modified membranes. The flux decline in case of pristine polyamide is very sharp and with the passage but it is comparatively gradual drop after deposition of the polyelectrolytes multilayers, irrespective of the number of layers. It is due to preliminary compaction

gained by modified membranes after polyelectrolyte deposition. As it can be seen in Figure 5-9, for pure polyamide the flux decline after one hour is from 21 L/m^2.hr to 17 L/m^2.hr whereas in case of only 5 bilayers the flux decline for the same duration is from 16 L/m^2.hr to 14.5 L/m^2.hr. It seems that polyelectrolytes has successfully added protective layer over polyamide surface which was also mentioned during TGA analysis.

From Figure 5-8 it is noteworthy that initial flux of PEM films is quite different as it is due to the difference in number of layers on the polyamide surface. Final values after compaction of two hours are presented in Table 5-4. Flux decreased to 13.35 L/m^2.hr after 5 bilayers and reached to 11.2 L/m^2.hr after depositing 50 bilayers of PEI/PAH. So, overall 32.5 % flux decline occurred after depositing 50 bilayers, which is still better as compared to Farid et al [111]. Although flux per unit pressure was 0.75 L/m^2.hr.bar that is approximately similar to our case of 0.746 L/m^2.hr.bar, However they suffered with 50 % flux decline after polyelectrolytes deposition.

Table 5-4: Effect of layer number on pure water flux

Membrane	**Pure water flux, J (L/m^2.hr)**
Pristine Polyamide	16.6
5 bilayers membrane	13.35
27.5 bilayers membrane	12.64
50 bilayers membrane	11.20

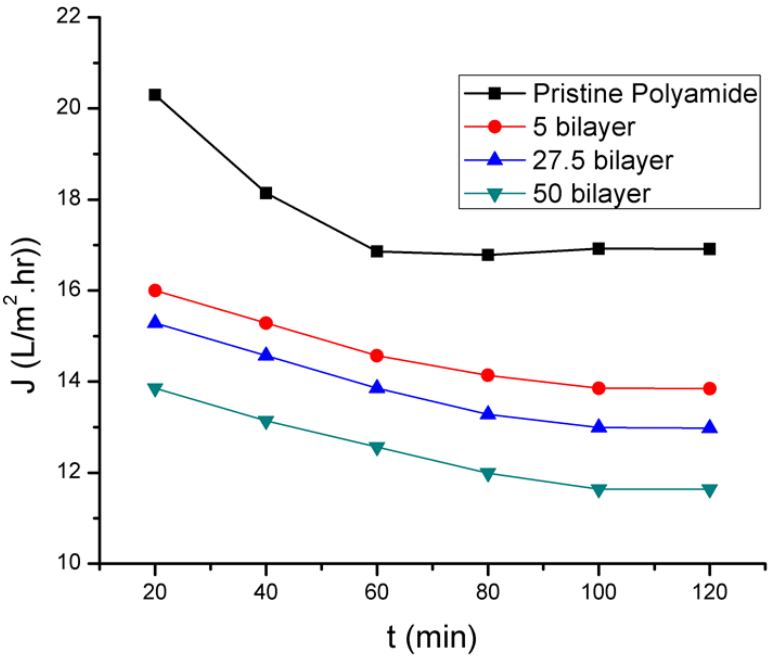

Figure 5-8: Pure water flux profile of unmodified and modifed membranes (modifed membranes have 110 mg/L PEI/PAH

Figure 5-9 shows the effect of number of layers on flux performance under BSA fouling conditions for three hours of continuous operation. It is noteworthy that pure polyamide has very sharp flux decline during fouling conditions indicating the higher flux loss and absence of protective coatings. However, the modified PEI/PAH films have less and gradual flux drop indicating the significance of polyelectrolyte coatings.

After 3 hours of fouling, more than 42 % flux loss was witnessed for pure polyamide membrane but when the PEI/PAH films were deposited, this huge flux loss reduced to only 12.6 % with only 5 bilayers. Moreover, flux loss further decreased to 11 % after coating of 50 PEI/PAH layers. This decrease in flux loss is in accordance with AFM

results that show by increasing the layer numbers, surface becomes smooth and less prone to fouling due to maximum surface coverage after multilayer deposition.

From Figure 5-9, flux decline for all the membranes is divided in 2 stages: (i) 0-120 minutes (ii) 120-180 minutes. In first two hours, initial and sharp decline occurs which can be explained with the early attachment of foulant layer on the surface of membrane. Maximum flux loss occurs during this initial period. However, in the second stage gradual and gentle flux drop took place after establishing equilibrium between the foulant layers and is represented by plateau [152], [160].

12.6 % flux loss with 5 PEI/PAH bilayers is much better than as reported by ishigami et al [109] with 12 bilayers of PSS/PAH on commercial polyamide membrane. They observed approximately 15 % flux loss in only 2 hours of BSA filtration.

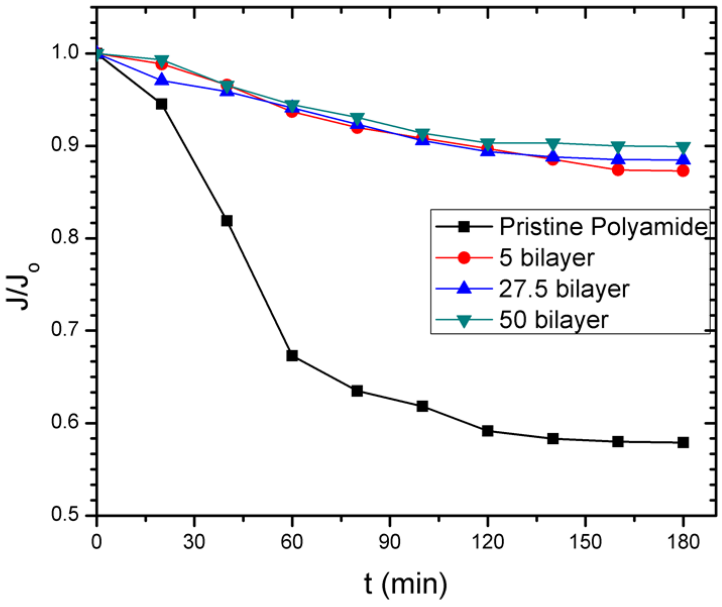

Figure 5-9: Effect of layer number on Flux after 180 minutes of BSA (100mg/L) filtration

Figure 5-10 shows the effect of layer number on salt rejection and permeability of polyelectrolytes modified polyamide membranes. It is visible that by increasing the layer numbers, salt rejection also increased but permeability decreased. The increase in salt rejection is due to the dense structure obtained by increasing the coating of PEI/PAH multilayers. The decrease in permeability is due to the increase in hydrodynamic resistance by adding more multilayers on the polyamide membrane. With 5 bilayers, only 91% salt rejection was obtained which escalated to 95% after depositing 50 PEI/PAH bilayers. The increase in rejection is solely attributed to enhancement in the dense structure.

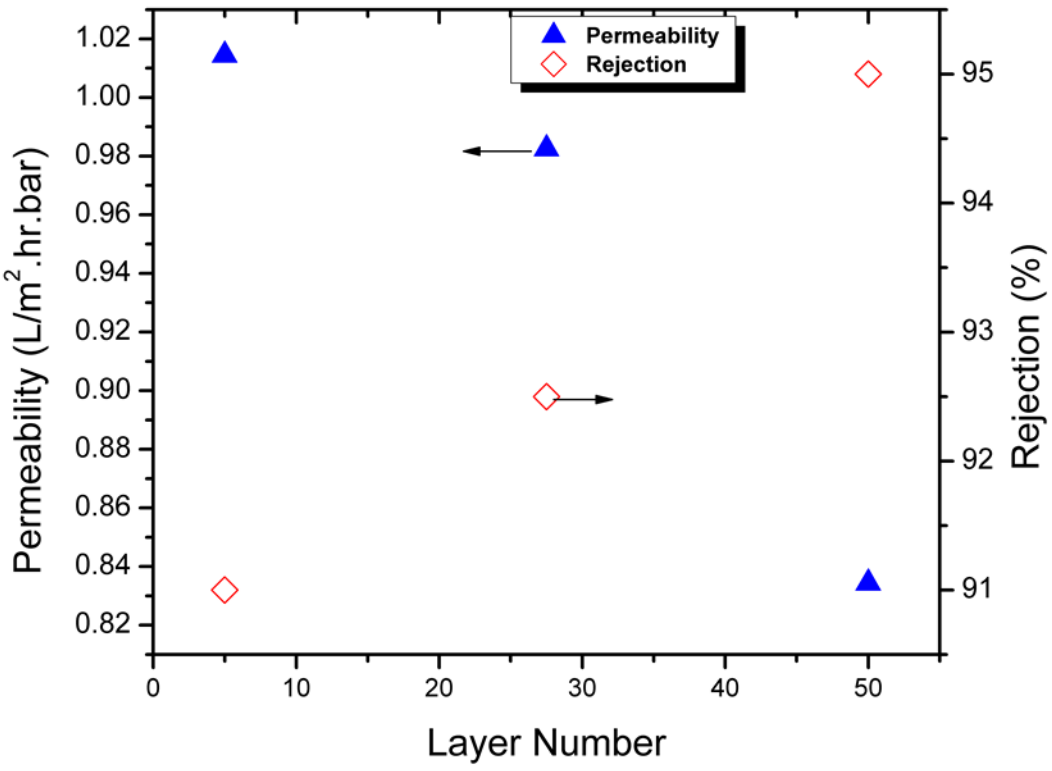

Figure 5-10: Effect of layer number on permeability and salt rejection

5.6.2 Effect of Concentration

Figure 5-11 shows the effect of concentration of PEI/PAH solutions on pure water flux. The number of bilayers was fixed to 27.5. It was found that pure water flux increased by increasing the concentration of PEI/PAH solutions. At low concentration of 20 mg/L, just 9.4 L/m^2.hr of pure water flux was achieved but it increased to 15.8 L/m^2.hr, when the concentration escalated to 200 mg/L. It means that flux was enhanced up to 40.5 %. Also, it should be noted that at higher concentration of polyelectrolytes, flux was very close to that of pristine polyamide (16.6 L/m^2.hr). The increase in flux by increasing the polyelectrolyte concentration is in accordance with the findings of Xu et al [161].

The improvement in flux is dedicated to complete surface coverage of the base membranes as it was shown in the SEM analysis. On the other hand, increasing solution concentration contributed in enriching hydrophilic functional groups. The hydrophilic enhancement on the membrane surface was confirmed by contact angle measurement. The contact angle of 20 mg/L modified membrane was 56.9^o that decreased to 48^o after deposition of 200 mg/L polyelectrolyte solutions. It shows that hydrophilicity of the membranes increased by increasing the concentration of depositing solutions that contributed in flux enhancement.

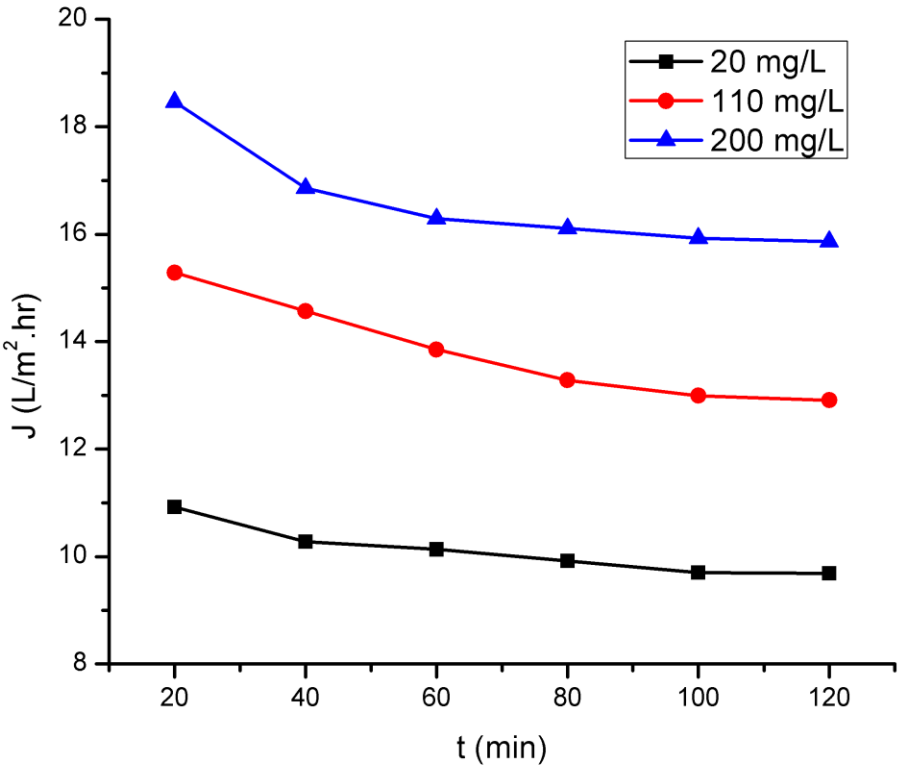

Figure 5-11: Effect of Concentration on pure water flux of 27.5 bilayers modified membranes

Figure 5-12 shows the effect of PEI/PAH solution concentrations on flux decline during BSA fouling conditions. The drop in flux is obvious with the changing concentration. It is clear that using the lower concentration yields higher flux loss. At 20 mg/L concentration, flux loss was observed approximately up to 12.8% of its initial value but with 110 mg/L, flux loss was reduced to 11.5 %. It shows that by increasing the concentration, membrane surface is getting more protection and resistance against foulant. Maximum antifouling ability was witnessed at solution concentration of 200 mg/L that retained more than 89 % flux of its initial value in fouling conditions. The decrease in flux loss is due to rise in hydrophilicity of the modified membranes as was confirmed by contact angle measurement.

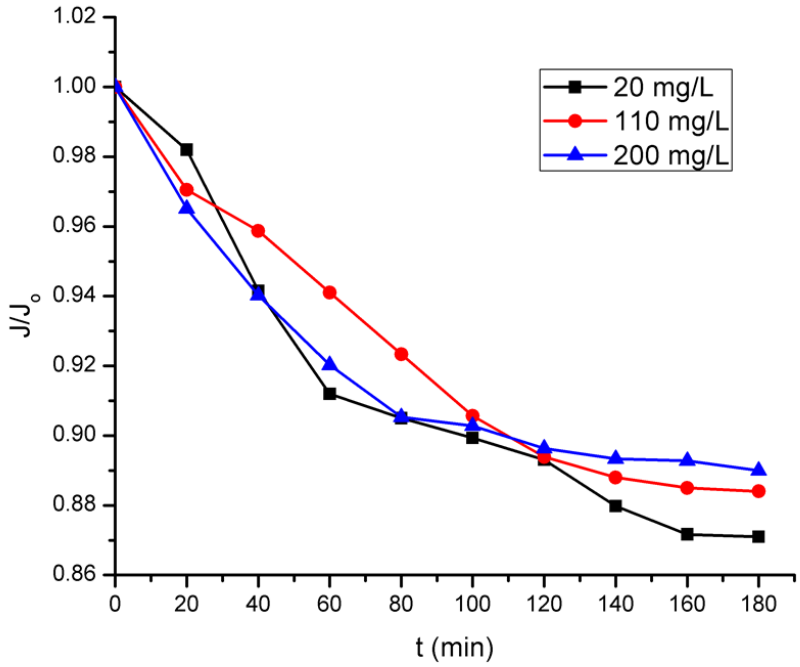

Figure 5-12: Effect of concentraion on flux decline of 27.5 bilayers PEI/PAH membranes in BSA (100 mg/L) fouling conditions

Figure 5-13 shows the effect of PEI/PAH concentration on salt rejection and permeability of 27.5 bilayers modified membranes. It is noticeable that increasing the concentration of the depositing solutions results in better performance of the modified membranes in terms of increased permeability and salt rejection. 95% NaCl rejection was achieved with 20 mg/L that increased further to 98 % after modification with 200 mg/L depositing solution. The rise in salt rejection is attributed to dense and compact multilayer structure that is favorable for salt rejection. On the other hand, increase in permeability is linked to increase in hydrophilicity of membrane surface by increasing the polyelectrolyte concentration.

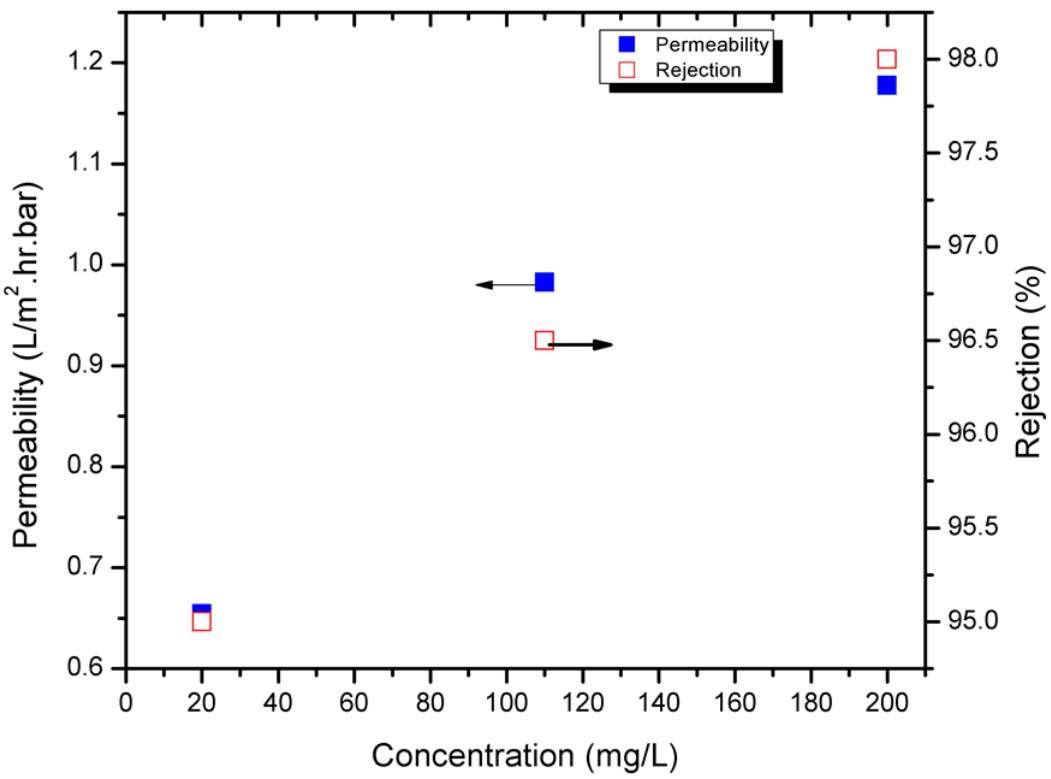

Figure 5-13: Effect of PEI/PAH concentration on permeation

5.6.3 Effect of Solution pH on Permeation Performance

Figure 5-14 shows the effect of pH of PEI/PAH solutions on the performance of 27.5 bilayers modified polyamide membrane. The multilayers were deposited at fixed concentration of 110 mg/L. It is evident that by increasing the pH, pure water flux increased. The degree of ionization of polar groups depends on the pH [162]. Depending upon the type of polyelectrolyte, increase in pH either produces thick or thin films since each polyelectrolyte has its specific charge density and distinct dependence of pH on ionization state [163], [164]. At, 4.0 pH pure water flux was 12.8 L/m^2.hr that increased to 15.28 L/m^2.hr at pH 6. Effect of pH on membrane performance is in accordance with study of Wang et al [165].

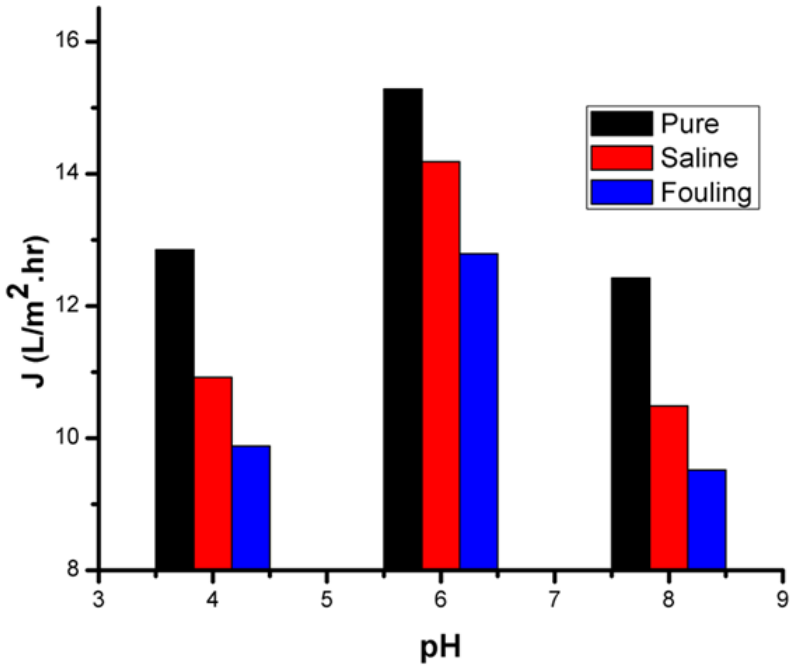

Figure 5-14: Effect of pH on performance of 27.5 PEI/PAH modified membranes

From Figure 5-14, it looks that increasing the pH of polyelectrolyte solution from 4 to 6 increased the surface charge density and degree of ionization of both polyelectrolytes so that a thin film was produced where lower resistance for mass transfer can be anticipated. Further increase of the pH to 8 may decreased the surface charge density and partially protonated the polyelectrolytes that caused more polyelectrolytes to be deposited. This will result in a thick film that will increase the resistance to mass transfer manifested as a decrease in flux. Effect of pH is summarized in Table 5-5.

Effect of pH on flux loss of modified membranes can be evaluated from Figure 5-15. At pH 4, modified membrane retained 91% of its initial flux which indicates 9% flux loss, however it was reduced to 8% at 6 pH; confirming the enhancement in antifouling resistance. As shown in Table 5-5, flux loss was increased to 10%, when the pH was

increased to 8. Results show that pH 6 is the optimum to get high flux and greater fouling resistance.

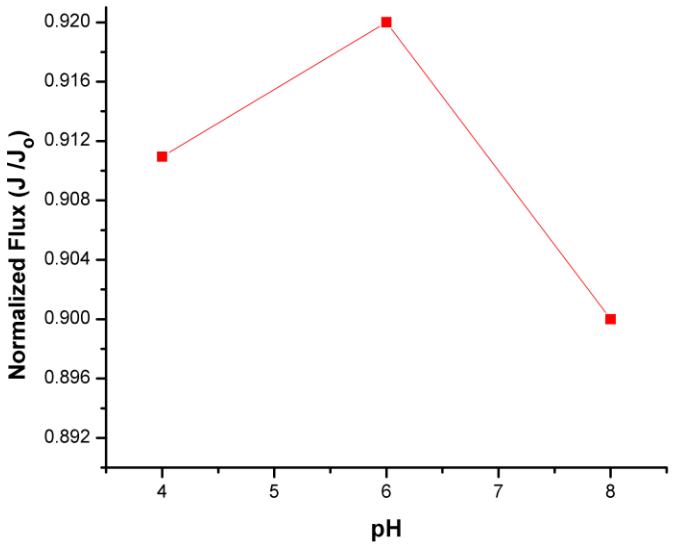

Figure 5-15: Effect of pH on permeation performance of 27.5 bilayers membranes

Table 5-5: Effect of pH on performance of 27.5 bilayer membrane at 110 mg/L concentration

pH	Pure water flux L/m^2.hr	Saline flux L/m^2.hr	Flux after fouling L/m^2.hr	Flux loss %
4	12.85	10.92	9.88	9
6	15.28	14.18	12.79	8
8	12.42	10.49	9.52	10

CHAPTER 6

CONCLUSION AND RECOMMENDATIONS

6.1 Conclusion

Polyamide membrane was successfully deposited over polysulfone support through dip coating. Polyelectrolytes were successfully deposited over polyamide membrane using spin assisted layer by layer technique. It was revealed that hydrophilicity was enhanced after deposition of polyelectrolytes and results were supported by contact angle measurement. AFM results showed that modified membranes possess smoother surface as compared to pristine polyamide. By increasing the layer number, hydrophilicity was increased and surface roughness was decreased. The synthesized membranes were tested in brackish water conditions. The antifouling study was performed using BSA as a model foulant and it was found that modified membranes have much better performance in terms of flux drop as compared to pristine polyamide. The decrease in flux decline with layer number is attributed to protective layers of polyelectrolytes. Modified membranes retain more than 85% flux after fouling as compared to 62% of pristine polyamide. Design expert was found to be an excellent tool to study the combine effect of layer numbers, pH and the polyelectrolytes concentration. Optimization was performed which revealed that all the input parameters must be used at higher levels to get the maximum optimum response. The optimum membrane with 48.5 bilayers, 7.6 pH and 200 mg/L

polyelectrolytes concentration, outperformed pristine polyamide in terms of fouling resistance.

The statistical analysis showed that;

- The significant factors to predict pure water flux were number of layers and concentration of poly (ethylene imine).
- Saline and flux after fouling was influenced by number of layers, pH of the solutions along with concentrations of poly (ethylene imine).
- The number of layers and maximum concentrations of both the polyelectrolytes were found to be favorable for salt rejection.

6.2 Recommendations

- To study the membrane performance after modification with other pair of polyelectrolytes.
- To analyze the membranes under sea water conditions.
- To perform stability test in order to investigate long term adhesion of the coating layers on the membrane surface.

REFERENCES

[1] W. H. Organization, “Progress on Drinking Water and Sanitation.”

[2] F. R. Rijsberman, “Water scarcity: Fact or fiction?,” *Agric. Water Manag.*, vol. 80, no. 1–3, pp. 5–22, Feb. 2006.

[3] Maggie A. Montgomery, “Water and Sanitation in Developing Countries: Including Health in the Equation,” *Environ. Sci. Technol.*, 2007.

[4] S. Pfister, A. Koehler, and S. Hellweg, “Assessing the Environmental Impacts of Freshwater Consumption in LCA,” vol. 43, no. 11, pp. 4098–4104, 2009.

[5] C. J. Vorosmarty, “Global Water Resources: Vulnerability from Climate Change and Population Growth,” *Science (80-.).*, vol. 289, no. 5477, pp. 284–288, Jul. 2000.

[6] K. P. Lee, T. C. Arnot, and D. Mattia, “A review of reverse osmosis membrane materials for desalination—Development to date and future potential,” *J. Memb. Sci.*, vol. 370, no. 1–2, pp. 1–22, Mar. 2011.

[7] M. a Shannon, P. W. Bohn, M. Elimelech, J. G. Georgiadis, B. J. Mariñas, and A. M. Mayes, “Science and technology for water purification in the coming decades.,” *Nature*, vol. 452, no. 7185, pp. 301–10, Mar. 2008.

[8] W. R. Engineering-lth, “Worldwide Oil Prize , Desalination and Population Growth Correlation Study,” pp. 37–46, 2009.

[9] L. Landau, *Desalination and Water Purification*. 1937.

[10] L. F. Greenlee, D. F. Lawler, B. D. Freeman, B. Marrot, and P. Moulin, “Reverse osmosis desalination: water sources, technology, and today’s challenges.,” *Water Res.*, vol. 43, no. 9, pp. 2317–48, May 2009.

[11] H. Cooley, P. H. Gleick, and G. Wolff, *DESALINATION , WITH A GRAIN OF SALT A California Perspective*, no. June. 2006.

[12] Sabine Lattemann, “Development of an Environmental Impact Assessment And Decision Support System For SeaWater Desalination Plants,” 2010.

[13] M. G. Buonomenna, “Nano-enhanced reverse osmosis membranes,” *Desalination*, vol. 314, pp. 73–88, Apr. 2013.

[14] U. Nations, *WATER DEVELOPMENT REPORT 3. ECONOMIC AND SOCIAL COMMISSION FOR WESTERN ASIA (ESCWA)*. 2009.

[15] R. Nel, "Thermal fluid analysis of combined power and desalination concepts for a high temperature reactor," no. 21891907, 2011.

[16] Joint water Reuse & Desalination Task Force, "Implemantation of The Desalination & Water Purification Technologies Roadmap," in *Water Innovation Symposium*, 2005.

[17] M. Sadrzadeh and T. Mohammadi, "Sea water desalination using electrodialysis," *Desalination*, vol. 221, no. 1–3, pp. 440–447, Mar. 2008.

[18] T. Mezher, H. Fath, Z. Abbas, and A. Khaled, "Techno-economic assessment and environmental impacts of desalination technologies," *Desalination*, vol. 266, no. 1–3, pp. 263–273, Jan. 2011.

[19] "RO membranes and components market is growing at 10.5% CAGR," *Membr. Technol.*, vol. 2015, no. 5, p. 4, 2015.

[20] S. A. Avlonitis, K. Kouroumbas, and N. Vlachakis, "Energy consumption and membrane replacement cost for seawater RO desalination plants," vol. 157, pp. 151–158, 2003.

[21] T. F. Speth, A. M. Gusses, and R. Scott Summers, "Evaluation of nanofiltration pretreatments for flux loss control," *Desalination*, vol. 130, pp. 31–44, 2000.

[22] H. . Shon, S. Vigneswaran, I. S. Kim, J. Cho, and H. . Ngo, "Effect of pretreatment on the fouling of membranes: application in biologically treated sewage effluent," *J. Memb. Sci.*, vol. 234, no. 1–2, pp. 111–120, May 2004.

[23] E. M. Vrijenhoek, S. Hong, and M. Elimelech, "Influence of membrane surface properties on initial rate of colloidal fouling of reverse osmosis and nanofiltration membranes," *J. Memb. Sci.*, vol. 188, pp. 115–128, 2001.

[24] A. Sarkar, P. I. Carver, T. Zhang, A. Merrington, K. J. Bruza, J. L. Rousseau, S. E. Keinath, and P. R. Dvornic, "Dendrimer-based coatings for surface modification of polyamide reverse osmosis membranes," *J. Memb. Sci.*, vol. 349, pp. 421–428, 2010.

[25] F. F. Stengaard, "Characteristics and performance of new types of ultrafiltration membranes with chemically modified surfaces," *Desalination*, vol. 70, pp. 207–224, 1988.

[26] J. Nikkola, X. Liu, Y. Li, M. Raulio, H. L. Alakomi, J. Wei, and C. Y. Tang, "Surface modification of thin film composite RO membrane for enhanced anti-biofouling performance," *J. Memb. Sci.*, vol. 444, pp. 192–200, 2013.

[27] S. Kaur, Z. Ma, R. Gopal, and G. Singh, "Plasma-Induced Graft Copolymerization of Poly (methacrylic acid) on Electrospun Poly (vinylidene fluoride) Nanofiber Membrane," no. 12, pp. 13085–13092, 2007.

[28] K. Kato, E. Uchida, E. T. Kang, Y. Uyama, and Y. Ikada, "Polymer surface with graft chains," *Prog. Polym. Sci.*, vol. 28, pp. 209–259, 2003.

[29] a. Bhattacharya and B. N. Misra, "Grafting: A versatile means to modify polymers: Techniques, factors and applications," *Prog. Polym. Sci.*, vol. 29, pp. 767–814, 2004.

[30] S. Belfer, Y. Purinson, and O. Kedem, "Surface modification of commercial polyamide reverse osmosis membranes by radical grafting: An ATR-FTIR study," *Acta Polym.*, vol. 49, pp. 574–582, 1998.

[31] C.-M. Chan, T.-M. Ko, and H. Hiraoka, "Polymer surface modification by plasmas and photons," *Surf. Sci. Rep.*, vol. 24, pp. 1–54, 1996.

[32] H. Chen and G. Belfort, "Surface modification of poly (ether sulfone) ultrafiltration membranes by low-temperature plasma-induced graft polymerization," *J. Appl. Polym. Sci.*, pp. 1699–1711, 1999.

[33] H. I. Kim and S. S. Kim, "Plasma treatment of polypropylene and polysulfone supports for thin film composite reverse osmosis membrane," *J. Memb. Sci.*, vol. 286, pp. 193–201, 2006.

[34] H. Susanto, "Fouling Study in Ultrafiltration : Mechanism and Control via Membrane Surface Modification (Untersuchung zum Fouling in der Ultrafiltration : Mechanismen und Kontrolle durch Oberflächenmodifizierung von by Heru Susanto Thesis submitted to the Department ," 2007.

[35] V. Kochkodan, D. J. Johnson, and N. Hilal, "Polymeric membranes: Surface modification for minimizing (bio)colloidal fouling," *Adv. Colloid Interface Sci.*, vol. 206, pp. 116–140, 2014.

[36] C. Kong, T. Shintani, and T. Tsuru, "'Pre-seeding'-assisted synthesis of a high performance polyamide-zeolite nanocomposite membrane for water purification," *New J. Chem.*, vol. 34, no. 10, p. 2101, 2010.

[37] B. H. Jeong, E. M. V Hoek, Y. Yan, A. Subramani, X. Huang, G. Hurwitz, A. K. Ghosh, and A. Jawor, "Interfacial polymerization of thin film nanocomposites: A

new concept for reverse osmosis membranes," *J. Memb. Sci.*, vol. 294, no. 1–2, pp. 1–7, 2007.

[38] N. Ma, J. Wei, R. Liao, and C. Y. Tang, "Zeolite-polyamide thin film nanocomposite membranes: Towards enhanced performance for forward osmosis," *J. Memb. Sci.*, vol. 405–406, pp. 149–157, 2012.

[39] G. Schmid and L. F. Chi, "Metal clusters and colloids," *Adv. Mater.*, vol. 10, pp. 515–526, 1998.

[40] Vinod K Gupta, "Water Treatment by Reverse Osmosis Method," in *Environmental Water*, Elsevier, 2013, pp. 117–134.

[41] D. E. Potts, R. C. Ahlert, and S. S. Wang, "A CRITICAL REVIEW OF FOULING OF REVERSE OSMOSIS MEMBRANES," vol. 36, pp. 235–264, 1981.

[42] S. Loeb, "The Loeb-Sourirajan Membrane: How It Came About," *Synth. Membr. Desalin.*, 1981.

[43] J. E. Cadotte, R. J. Petersen, R. E. Larson, and E. E. Erickson, "A NEW THIN-FILM COMPOSITE SEAWATER REVERSE OSMOSIS MEMBRANE," *Desalination*, no. 32, pp. 25–31, 1980.

[44] D. Rana and T. Matsuura, "Surface modifications for antifouling membranes.," *Chem. Rev.*, vol. 110, no. 4, pp. 2448–71, Apr. 2010.

[45] R. J. Petersen, "Composite reverse osmosis and nanofiltration membranes," vol. 83, pp. 81–150, 1993.

[46] G. Chai and W. B. Krantz, "Formation and characterization of polyamide membranes via interfacial polymerization," vol. 93, no. 94, 1994.

[47] D. E. Potts, R. C. Ahlert, and S. S. Wang, "A CRITICAL REVIEW OF FOULING OF REVERSE OSMOSIS MEMBRANES," *De*, vol. 36, pp. 235–264, 1981.

[48] G. Kang and Y. Cao, "Development of antifouling reverse osmosis membranes for water treatment: A review.," *Water Res.*, vol. 46, no. 3, pp. 584–600, Mar. 2012.

[49] A. Matin, Z. Khan, S. M. J. Zaidi, and M. C. Boyce, "Biofouling in reverse osmosis membranes for seawater desalination: Phenomena and prevention," *Desalination*, vol. 281, pp. 1–16, Oct. 2011.

[50] T. Tran, B. Bolto, S. Gray, M. Hoang, and E. Ostarcevic, "An autopsy study of a fouled reverse osmosis membrane element used in a brackish water treatment plant," *Water Res.*, vol. 41, pp. 3915–3923, 2007.

[51] M. Science, “Opus: University of Bath Online Publication Store http://opus.bath.ac.uk/,” vol. 370, pp. 1–22, 2011.

[52] Hans-Curt Flemming, “Reverse Osmosis Membrane Biofouling,” *Exp. Therm. Fluid Sci.*, vol. 1777, no. 14, pp. 382–391, 1997.

[53] M. C. Amiri and M. Samiei, “Enhancing permeate flux in a RO plant by controlling membrane fouling,” *Desalination*, vol. 207, pp. 361–369, 2007.

[54] A. L. Zydney and C. K. Colton, “a Concentration Polarization Model for the Filtrate Flux in Cross-Flow Microfiltration of Particulate Suspensions,” *Chem. Eng. Commun.*, vol. 47, no. December 2012, pp. 1–21, 1986.

[55] S. P. Chesters, “Innovations in the inhibition and cleaning of reverse osmosis membrane scaling and fouling,” *Desalination*, vol. 238, no. 1–3, pp. 22–29, 2009.

[56] P. Bacchin, D. Si-Hassen, V. Starov, M. J. Clifton, and P. Aimar, “A unifying model for concentration polarization, gel-layer formation and particle deposition in cross-flow membrane filtration of colloidal suspensions,” *Chem. Eng. Sci.*, vol. 57, pp. 77–91, 2002.

[57] B. Van Der Bruggen, C. Vandecasteele, T. Van Gestel, W. Doyenb, and R. Leysenb, “Review of Pressure-Driven Membrane Processes,” *Environ. Prog.*, vol. 22, no. 1, pp. 46–56, 2003.

[58] G. Ramon, Y. Agnon, and C. Dosoretz, “Dynamics of an osmotic backwash cycle,” *J. Memb. Sci.*, vol. 364, no. 1–2, pp. 157–166, 2010.

[59] A. Sagiv and R. Semiat, “Backwash of RO spiral wound membranes,” *Desalination*, vol. 179, no. November 2004, pp. 1–9, 2005.

[60] A. Sagiv, N. Avraham, C. G. Dosoretz, and R. Semiat, “Osmotic backwash mechanism of reverse osmosis membranes,” *J. Memb. Sci.*, vol. 322, pp. 225–233, 2008.

[61] N. Avraham, C. Dosoretz, and R. Semiat, “Osmotic backwash process in RO membranes,” *Desalination*, vol. 199, no. September, pp. 387–389, 2006.

[62] M. F. a. Goosen, S. S. Sablani, H. Al-Hinai, S. Al-Obeidani, R. Al-Belushi, and D. Jackson, “Fouling of Reverse Osmosis and Ultrafiltration Membranes: A Critical Review,” *Sep. Sci. Technol.*, vol. 39, no. September 2013, pp. 2261–2297, 2005.

[63] a Abdelrasoul, H. Doan, and a Lohi, “Fouling in Membrane Filtration and Remediation Methods,” 2013.

[64] W. S. Ang, N. Y. Yip, A. Tiraferri, and M. Elimelech, “Chemical cleaning of RO membranes fouled by wastewater effluent: Achieving higher efficiency with dual-step cleaning,” *J. Memb. Sci.*, vol. 382, no. 1–2, pp. 100–106, 2011.

[65] N. M. D’Souza and a J. Mawson, “Membrane cleaning in the dairy industry: a review.,” *Crit. Rev. Food Sci. Nutr.*, vol. 45, no. March 2015, pp. 125–134, 2005.

[66] S. Lee and M. Elimelech, “Salt cleaning of organic-fouled reverse osmosis membranes,” *Water Res.*, vol. 41, pp. 1134–1142, 2007.

[67] D. Der Naturwissenschaften, “Polyelectrolyte Complexes and Multilayers at Solid Surfaces via Polymer Brushes,” 2008.

[68] B. Kim, S. W. Park, and P. T. Hammond, “Surfaces,” vol. 2, no. 2, pp. 386–392.

[69] M. Andersson, P. J. Ra, C. Elvingson, and P. Hansson, “Single Microgel Particle Studies Demonstrate the Influence of Hydrophobic Interactions between Charged Micelles and Oppositely Charged Polyions,” no. 22, pp. 3773–3781, 2005.

[70] T. Industrial, “MULTILAYERS OF COLLOIDAL PARTICLES* R. K. Iler,” vol. 594, pp. 569–594, 1966.

[71] G. Decher and J. Schmitt, “Buildup of ultrathin multilayer films by a self-assembly process : III . Consecutively alternating adsorption of anionic and cationic polyelectrolytes on charged surfaces,” pp. 831–835, 1992.

[72] S. S. Shiratori and M. F. Rubner, “pH-Dependent Thickness Behavior of Sequentially Adsorbed Layers of Weak Polyelectrolytes,” pp. 4213–4219, 2000.

[73] L. Ouyang, R. Malaisamy, and M. L. Bruening, “Multilayer polyelectrolyte films as nanofiltration membranes for separating monovalent and divalent cations,” *J. Memb. Sci.*, vol. 310, pp. 76–84, 2008.

[74] R. Steitz, V. Leiner, and R. Siebrecht, “Influence of the ionic strength on the structure of polyelectrolyte films at the solid / liquid interface,” vol. 163, pp. 63–70, 2000.

[75] B. Schoeler, G. Kumaraswamy, and F. Caruso, “Investigation of the Influence of Polyelectrolyte Charge Density on the Growth of Multilayer Thin Films Prepared by the Layer-by-Layer Technique,” pp. 889–897, 2002.

[76] F. Hua and Y. M. Lvov, “Layer-by-layer assembly,” in *The New Frontiers of Organic and Composite Nanotechnology*, 2007.

[77] G. Decher, “Fuzzy Nanoassemblies: Toward Layered Polymeric Multicomposites,” *Science (80-.).*, vol. 277, no. 5330, pp. 1232–1237, Aug. 1997.

[78] H. Ai, S. A. Jones, and Y. M. Lvov, “Biomedical Applications of Electrostatic Layer-by-Layer Nano-Assembly of Polymers , Enzymes , and Nanoparticles,” vol. 39, 2003.

[79] S. Liu, D. Volkmer, and D. G. Kurth, “Functional Polyoxometalate Thin Films via Electrostatic Layer-by-Layer Self-Assembly *,” vol. 14, no. 3, pp. 405–419, 2003.

[80] L. Krasemann, A. Toutianoush, and B. Tieke, “Self-assembled polyelectrolyte multilayer membranes with highly improved pervaporation separation of ethanol / water mixtures,” vol. 181, pp. 221–228, 2001.

[81] L. Krasemann and B. Tieke, “Ultrathin self-assembled polyelectrolyte membranes for pervaporation,” vol. 150, pp. 23–30, 1998.

[82] C. Lu, I. Do, M. Nolte, and A. Fery, “Au Nanoparticle-based Multilayer Ultrathin Films with Covalently Linked Nanostructures : Spraying Layer-by-layer Assembly and Mechanical Property Characterization,” no. 14, pp. 6204–6210, 2006.

[83] B. S. L. Clark and P. T. Hammond, “Engineering the Microfabrication of Layer-by-Layer Thin Films,” no. 18, pp. 1515–1519, 1998.

[84] S. S. Shiratori and M. Yamada, “Nano-scale Control of Composite Polymer Films by Mass-controlled Layer- by-layer Sequential Adsorption of Polyelectrolytes,” vol. 814, no. November 1999, pp. 810–814, 2000.

[85] S. Srivastava and N. A. Kotov, “Composite Layer-by-Layer (LBL) Assembly with Inorganic Nanoparticles and Nanowires,” vol. 41, no. 12, pp. 1831–1841, 2008.

[86] W. Chen and T. J. Mccarthy, “Layer-by-Layer Deposition : A Tool for Polymer Surface Modification,” vol. 9297, no. 96, pp. 78–86, 1997.

[87] N. G. Hoogeveen, M. A. C. Stuart, G. J. Fleer, and M. R. Bo, “Formation and Stability of Multilayers of Polyelectrolytes,” vol. 7463, no. 12, pp. 3675–3681, 1996.

[88] A. J. Khopade and F. Caruso, “Investigation of the Factors Influencing the Formation of Dendrimer / Polyanion Multilayer Films,” no. 13, pp. 7669–7676, 2002.

[89] a. C. Fou, O. Onitsuka, M. Ferreira, M. F. Rubner, and B. R. Hsieh, “Fabrication and properties of light-emitting diodes based on self-assembled multilayers of poly(phenylene vinylene),” *J. Appl. Phys.*, vol. 79, no. 10, p. 7501, 1996.

[90] J. J. Ramsden, Y. M. Lvovb, and G. Decher, “Determination of optical constants of molecular films assembled via alternate polyion adsorption,” vol. 254, pp. 246–251, 1995.

[91] A. Toutianoush, T. Bemd, P. Chemie, D. Universitat, and D.- Koln, “azobenzene-containing ionene polycations and anionic pol y elec trol y tes,” vol. 595, no. 11, pp. 591–595, 1998.

[92] Y. Lvov, F. Essler, and C. Decher, “Combination of Polycation/Polyanion Self-Assembly and Langmuir-Blodgett Transfer for the Construction of Superlattice Films,” pp. 13773–13777, 1993.

[93] T. M. Cooper, A. L. Campbell, R. L. Crane, and W. A. F. Base, “Formation of Polypeptide-Dye Multilayers by an Electrostatic Self-Assembly Technique,” no. 23, pp. 2713–2718, 1995.

[94] S. T. Dubas, T. R. Farhat, J. B. Schlenoff, and R. V March, “Multiple Membranes from ‘ True ’ Polyelectrolyte Multilayers,” no. 20, pp. 5368–5369, 2001.

[95] J. B. Schlenoff, S. T. Dubas, and T. Farhat, “Sprayed Polyelectrolyte Multilayers,” pp. 9968–9969, 2000.

[96] A. Izquierdo, S. S. Ono, J. Voegel, P. Schaaf, and G. Decher, “Dipping versus Spraying : Exploring the Deposition Conditions for Speeding Up Layer-by-Layer Assembly,” vol. 16, no. 19, pp. 7558–7567, 2005.

[97] J. J. Harris, J. L. Stair, and M. L. Bruening, “Layered Polyelectrolyte Films as Selective , Ultrathin Barriers for Anion Transport,” no. 22, pp. 1941–1946, 2000.

[98] D.- Ko, “Selective Ion Transport across Self-Assembled Alternating Multilayers of Cationic and Anionic,” no. 15, pp. 287–290, 2000.

[99] S. S. Method, “Fabrication of Highly Ordered Multilayer Films,” no. 14, pp. 1076–1078, 2001.

[100] K. Ariga, J. P. Hill, and Q. Ji, “Layer-by-layer assembly as a versatile bottom-up nanofabrication technique for exploratory research and realistic application.,” *Phys. Chem. Chem. Phys.*, vol. 9, no. 19, pp. 2319–40, May 2007.

[101] P. A. Chiarelli, M. S. Johal, D. J. Holmes, J. L. Casson, J. M. Robinson, and H. Wang, “Polyelectrolyte Spin-Assembly,” no. 18, pp. 168–173, 2002.

[102] M. D. Miller and M. L. Bruening, “Controlling the Nanofiltration Properties of Multilayer Polyelectrolyte Membranes through Variation of Film Composition,” no. 18, pp. 11545–11551, 2004.

[103] A. Toutianoush, W. Jin, H. Deligöz, and B. Tieke, “Polyelectrolyte multilayer membranes for desalination of aqueous salt solutions and seawater under reverse osmosis conditions,” *Appl. Surf. Sci.*, vol. 246, no. 4, pp. 437–443, Jun. 2005.

[104] R. Malaisamy and M. L. Bruening, “High-Flux Nanofiltration Membranes Prepared by Adsorption of Multilayer Polyelectrolyte Membranes on,” no. 29, pp. 10587–10592, 2005.

[105] W. Ritcharoen, P. Supaphol, and P. Pavasant, “Development of polyelectrolyte multilayer-coated electrospun cellulose acetate fiber mat as composite membranes,” *Eur. Polym. J.*, vol. 44, no. 12, pp. 3963–3968, Dec. 2008.

[106] J. Wang, Y. Yao, Z. Yue, and J. Economy, “Preparation of polyelectrolyte multilayer films consisting of sulfonated poly (ether ether ketone) alternating with selected anionic layers,” *J. Memb. Sci.*, vol. 337, no. 1–2, pp. 200–207, Jul. 2009.

[107] J. Park, J. Park, S. H. Kim, J. Cho, and J. Bang, “Desalination membranes from pH-controlled and thermally-crosslinked layer-by-layer assembled multilayers,” *J. Mater. Chem.*, vol. 20, no. 207890, p. 2085, 2010.

[108] R. Malaisamy, A. Talla-Nwafo, and K. L. Jones, “Polyelectrolyte modification of nanofiltration membrane for selective removal of monovalent anions,” *Sep. Purif. Technol.*, vol. 77, no. 3, pp. 367–374, Mar. 2011.

[109] T. Ishigami, K. Amano, A. Fujii, Y. Ohmukai, E. Kamio, T. Maruyama, and H. Matsuyama, “Fouling reduction of reverse osmosis membrane by surface modification via layer-by-layer assembly,” *Sep. Purif. Technol.*, vol. 99, pp. 1–7, 2012.

[110] C. Wang, G. K. Such, A. Widjaya, H. Lomas, G. Stevens, F. Caruso, and S. E. Kentish, “Click poly(ethylene glycol) multilayers on RO membranes: Fouling reduction and membrane characterization,” *J. Memb. Sci.*, vol. 409–410, pp. 9–15, Aug. 2012.

[111] F. Fadhillah, S. M. J. Zaidi, Z. Khan, M. M. Khaled, F. Rahman, and P. T. Hammond, “Development of polyelectrolyte multilayer thin film composite membrane for water desalination application,” *Desalination*, vol. 318, pp. 19–24, Jun. 2013.

[112] F. Fadhillah, S. M. J. Zaidi, Z. Khan, M. Khaled, and P. Hammond, “Reverse Osmosis Desalination Membrane Formed From Weak Polyelectrolytes by Spin Assisted Layer By Layer Technique.”

[113] J.-E. Gu, S. Lee, C. M. Stafford, J. S. Lee, W. Choi, B.-Y. Kim, K.-Y. Baek, E. P. Chan, J. Y. Chung, J. Bang, and J.-H. Lee, “Molecular layer-by-layer assembled

thin-film composite membranes for water desalination.," *Adv. Mater.*, vol. 25, no. 34, pp. 4778–82, Sep. 2013.

[114] J. L. Stair, J. J. Harris, and M. L. Bruening, "Enhancement of the Ion-Transport Selectivity of Layered Polyelectrolyte Membranes through Cross-Linking and Hybridization," no. 20, pp. 2641–2648, 2001.

[115] R. Hadj, A. Ben, and E. Ferjani, "Change of the performance properties of nanofiltration cellulose acetate membranes by surface adsorption of polyelectrolyte multilayers," vol. 163, pp. 193–202, 2004.

[116] S. U. Hong, R. Malaisamy, and M. L. Bruening, "Separation of Fluoride from Other Monovalent Anions Using Multilayer Polyelectrolyte Nanofiltration Membranes," no. 22, pp. 1716–1722, 2007.

[117] J. Seo, J. L. Lutkenhaus, J. Kim, P. T. Hammond, and K. Char, "Effect of the layer-by-layer (LbL) deposition method on the surface morphology and wetting behavior of hydrophobically modified PEO and PAA LbL films.," *Langmuir*, vol. 24, no. 15, pp. 7995–8000, Aug. 2008.

[118] C. Y. Tang, Y.-N. Kwon, and J. O. Leckie, "Effect of membrane chemistry and coating layer on physiochemical properties of thin film composite polyamide RO and NF membranes," *Desalination*, vol. 242, no. 1–3, pp. 168–182, Jun. 2009.

[119] R. Malaisamy, A. Talla-Nwafo, and K. L. Jones, "Polyelectrolyte modification of nanofiltration membrane for selective removal of monovalent anions," *Sep. Purif. Technol.*, vol. 77, no. 3, pp. 367–374, 2011.

[120] J. Seo, J. L. Lutkenhaus, J. Kim, and P. T. Hammond, "Effect of the Layer-by-Layer (LbL) Deposition Method on the Surface Morphology and Wetting Behavior of Hydrophobically Modified PEO and PAA LbL Films," no. 16, pp. 7995–8000, 2008.

[121] J. Kochan, T. Wintgens, J. E. Wong, and T. Melin, "Properties of polyethersulfone ultrafiltration membranes modified by polyelectrolytes," *Desalination*, vol. 250, no. 3, pp. 1008–1010, Jan. 2010.

[122] C. Wang, G. K. Such, A. Widjaya, H. Lomas, G. Stevens, F. Caruso, and S. E. Kentish, "Click poly(ethylene glycol) multilayers on RO membranes: Fouling reduction and membrane characterization," *J. Memb. Sci.*, vol. 409–410, pp. 9–15, Aug. 2012.

[123] H. Deng, Y. Xu, B. Zhu, X. Wei, F. Liu, and Z. Cui, "Polyelectrolyte membranes prepared by dynamic self-assembly of poly (4-styrenesulfonic acid-co-maleic acid) sodium salt (PSSMA) for nanofiltration (I)," *J. Memb. Sci.*, vol. 323, no. 1, pp. 125–133, Oct. 2008.

[124] S. U. Hong, R. Malaisamy, and M. L. Bruening, “Optimization of flux and selectivity in Cl−/SO42− separations with multilayer polyelectrolyte membranes,” *J. Memb. Sci.*, vol. 283, no. 1–2, pp. 366–372, Oct. 2006.

[125] K. Hoffmann and B. Tieke, “Layer-by-layer assembled membranes containing hexacyclen-hexaacetic acid and polyethyleneimine N-acetic acid and their ion selective permeation behaviour,” *J. Memb. Sci.*, vol. 341, no. 1–2, pp. 261–267, Sep. 2009.

[126] S. U. Hong, L. Ouyang, and M. L. Bruening, “Recovery of phosphate using multilayer polyelectrolyte nanofiltration membranes,” *J. Memb. Sci.*, vol. 327, no. 1–2, pp. 2–5, Feb. 2009.

[127] T. J. Su, R. K. Thomas, Z. F. Cui, and J. Penfold, “The Conformational Structure of Bovine Serum Albumin Layers Adsorbed at the Silica−Water Interface,” *J. Phys. Chem. B*, vol. 102, no. 98, pp. 8100–8108, 1998.

[128] A. G. Fane, C. Y. Tang, and R. Wang, “4 . 11 Membrane Technology for Water : Microfiltration , Ultrafiltration , Nanofiltration , and Reverse Osmosis,” 2011.

[129] W. Jin, A. Toutianoush, and B. Tieke, “Use of Polyelectrolyte Layer-by-Layer Assemblies as Nanofiltration and Reverse Osmosis Membranes,” vol. 24, no. 16, pp. 2550–2553, 2003.

[130] U. K. Aravind, J. Mathew, and C. T. Aravindakumar, “Transport studies of BSA, lysozyme and ovalbumin through chitosan/polystyrene sulfonate multilayer membrane,” *J. Memb. Sci.*, vol. 299, no. 1–2, pp. 146–155, Aug. 2007.

[131] K. Majewska-Nowak, “Synthesis and properties of polysulfone membranes,” *Desalination*, vol. 71, pp. 83–95, 1989.

[132] T. D. Sheet, “Dimethylacetamide,” pp. 3–6, 2008.

[133] “1 CMR means carcinogenic, mutagenic or toxic for reproduction,” pp. 1–9.

[134] H. Yun, H. Hong, J. Lee, and C. Choi, “Chemical and Structural Properties of Polyethyleneimine Film Coated on a SiO 2 Substrate in Different Concentrations,” vol. 55, no. 5, pp. 2–6, 2014.

[135] S. Janhom, “Polyethyleneimine/sodium dodecyl sulphate adsorbed silica particles and their adsorption properties,” *Colloids Surfaces A Physicochem. Eng. Asp.*, vol. 369, no. 1–3, pp. 186–190, 2010.

[136] V. Kaiser, C. Stropnik, V. Musil, and M. Brumen, “Morphology of solidified polysulfone structures obtained by wet phase separation,” *Eur. Polym. J.*, vol. 43, no. 6, pp. 2515–2524, 2007.

[137] J. Y. Kim, H. K. Lee, and S. C. Kim, "Liquid-liquid phase separation during polysulfone membrane preparation," *Korean J. Chem. Eng.*, vol. 17, no. 5, pp. 564–569, 2000.

[138] L. Yu. Yu, H. M. Shen, and Z. L. Xu, "PVDF–TiO2 Composite Hollow Fiber Ultrafiltration Membranes Prepared by TiO2 Sol–Gel Method and Blending Method," *J. Appl. Phys.*, vol. 113, pp. 1763–1772, 2009.

[139] I. J. Roh, A. R. Greenberg, and V. P. Khare, "Synthesis and characterization of interfacially polymerized polyamide thin films," *Desalination*, vol. 191, no. 1–3, pp. 279–290, 2006.

[140] W. Xie, G. M. Geise, B. D. Freeman, H. S. Lee, G. Byun, and J. E. McGrath, "Polyamide interfacial composite membranes prepared from m-phenylene diamine, trimesoyl chloride and a new disulfonated diamine," *J. Memb. Sci.*, vol. 403–404, pp. 152–161, 2012.

[141] A. Idris, F. Kormin, and M. Y. Noordin, "Application of response surface methodology in describing the performance of thin film composite membrane," vol. 49, pp. 271–280, 2006.

[142] J. Duan, Y. Pan, F. Pacheco, E. Litwiller, Z. Lai, and I. Pinnau, "High-performance polyamide thin-film-nanocomposite reverse osmosis membranes containing hydrophobic zeolitic imidazolate framework-8," *J. Memb. Sci.*, vol. 476, pp. 303–310, 2015.

[143] Y. N. Kwon, S. Hong, H. Choi, and T. Tak, "Surface modification of a polyamide reverse osmosis membrane for chlorine resistance improvement," *J. Memb. Sci.*, vol. 415–416, pp. 192–198, 2012.

[144] J.-E. Gu, S. Lee, C. M. Stafford, J. S. Lee, W. Choi, B.-Y. Kim, K.-Y. Baek, E. P. Chan, J. Y. Chung, J. Bang, and J.-H. Lee, "Molecular Layer-by-Layer Assembled Thin-Film Composite Membranes for Water Desalination," *Adv. Mater.*, vol. 25, no. 34, pp. 4778–4782, 2013.

[145] T. Ishigami, K. Amano, A. Fujii, Y. Ohmukai, E. Kamio, T. Maruyama, and H. Matsuyama, "Fouling reduction of reverse osmosis membrane by surface modification via layer-by-layer assembly," *Sep. Purif. Technol.*, vol. 99, pp. 1–7, 2012.

[146] S. Yu, X. Liu, J. Liu, D. Wu, M. Liu, and C. Gao, "Surface modification of thin-film composite polyamide reverse osmosis membranes with thermo-responsive polymer (TRP) for improved fouling resistance and cleaning efficiency," *Sep. Purif. Technol.*, vol. 76, no. 3, pp. 283–291, 2011.

[147] F. a. Pacheco, I. Pinnau, M. Reinhard, and J. O. Leckie, "Characterization of isolated polyamide thin films of RO and NF membranes using novel TEM techniques," *J. Memb. Sci.*, vol. 358, no. 1–2, pp. 51–59, 2010.

[148] P. Xu, J. E. Drewes, T.-U. Kim, C. Bellona, and G. Amy, "Effect of membrane fouling on transport of organic contaminants in NF/RO membrane applications," *J. Memb. Sci.*, vol. 279, no. 1–2, pp. 165–175, 2006.

[149] H. Jang, S. Kim, and K. Char, "Self-Assembly in Microfluidic Channels," vol. 13, no. 12, pp. 3094–3097, 2003.

[150] P. Kaner, D. J. Johnson, E. Seker, N. Hilal, and S. A. Altinkaya, "Layer-by-layer surface modification of polyethersulfone membranes using polyelectrolytes and AgCl/TiO2 xerogels," *J. Memb. Sci.*, vol. 493, pp. 807–819, 2015.

[151] B. S. Lalia, V. Kochkodan, R. Hashaikeh, and N. Hilal, "A review on membrane fabrication: Structure, properties and performance relationship," *Desalination*, vol. 326, pp. 77–95, 2013.

[152] V. Kochkodan and N. Hilal, "A comprehensive review on surface modified polymer membranes for biofouling mitigation," *Desalination*, vol. 356, pp. 187–207, 2015.

[153] K. Boussu, a. Belpaire, a. Volodin, C. Van Haesendonck, P. Van der Meeren, C. Vandecasteele, and B. Van der Bruggen, "Influence of membrane and colloid characteristics on fouling of nanofiltration membranes," *J. Memb. Sci.*, vol. 289, no. 1–2, pp. 220–230, 2007.

[154] K. Apaydin, a Laachachi, T. Fouquet, M. Jimenez, S. Bourbigot, and D. Ruch, "Mechanistic investigation of a flame retardant coating made by layer-by-layer assembly," *RSC Adv.*, vol. 4, no. 82, pp. 43326–43334, 2014.

[155] M. Fathizadeh, A. Aroujalian, and A. Raisi, "Effect of added NaX nano-zeolite into polyamide as a top thin layer of membrane on water flux and salt rejection in a reverse osmosis process," *J. Memb. Sci.*, vol. 375, no. 1–2, pp. 88–95, 2011.

[156] L. Li, S. Zhang, X. Zhang, and G. Zheng, "Polyamide thin film composite membranes prepared from 3,4′,5-biphenyl triacyl chloride, 3,3′,5,5′-biphenyl tetraacyl chloride and m-phenylenediamine," *J. Memb. Sci.*, vol. 289, no. 1–2, pp. 258–267, 2007.

[157] G. N. B. Baroña, J. Lim, M. Choi, and B. Jung, "Interfacial polymerization of polyamide-aluminosilicate SWNT nanocomposite membranes for reverse osmosis," *Desalination*, vol. 325, pp. 138–147, 2013.

[158] A. Matin, H. Z. Shafi, Z. Khan, M. Khaled, R. Yang, K. Gleason, and F. Rehman, "Surface modification of seawater desalination reverse osmosis membranes: Characterization studies & performance evaluation," *Desalination*, vol. 343, pp. 128–139, 2014.

[159] J.-E. Gu, J. S. Lee, S.-H. Park, I. T. Kim, E. P. Chan, Y.-N. Kwon, and J.-H. Lee, "Tailoring interlayer structure of molecular layer-by-layer assembled polyamide membranes for high separation performance," *Appl. Surf. Sci.*, vol. 356, pp. 659–667, 2015.

[160] H. Karkhanechi, R. Takagi, and H. Matsuyama, "Biofouling resistance of reverse osmosis membrane modified with polydopamine," *Desalination*, vol. 336, pp. 87–96, 2014.

[161] J. Xu, L. Xu, H. Xu, F. Sun, X. Gao, and C. Gao, "Stability and permeation behavior of a porous membrane modified by polyelectrolyte networks enabled by electro-deposition and cross-linking for water purification," *J. Memb. Sci.*, vol. 496, pp. 21–30, 2015.

[162] L. De Arcangelis, E. Del Gado, a Coniglio, and S. Fisiche, "P Hysical J Ournal E," vol. 282, pp. 277–282, 2002.

[163] J. Choi and M. F. Rubner, "Influence of the Degree of Ionization on Weak Polyelectrolyte Multilayer Assembly," pp. 116–124, 2005.

[164] C. Magnenet, F. E. Jurin, S. Lakard, C. C. Buron, and B. Lakard, "Polyelectrolyte modification of ultrafiltration membrane for removal of copper ions," *Colloids Surfaces A Physicochem. Eng. Asp.*, vol. 435, pp. 170–177, 2013.

[165] S. Rajabzadeh, C. Liu, L. Shi, and R. Wang, "Preparation of low-pressure water softening hollow fiber membranes by polyelectrolyte deposition with two bilayers," *Desalination*, vol. 344, pp. 64–70, 2014.

Curriculum Vitae

SAQIB JAVED (CHEMICAL ENGINEER)

Nationality: Pakistani *Passport No: CL8671741*

Date of Birth: 14th June 1989 *+966-53-6572891 +92-321-4800043*

saqibjaved31@yahoo.com *g201206500@kfupm.edu.sa*

Education

Degree Name	Field of Study	Grade	Institute
MS	Chemical Engineering	3.219/4	KFUPM, Saudi Arabia
B.Sc.	Chemical Engineering	3.72/4	University of the Punjab, Lahore, Pakistan

Research Publications

- **Saqib Javed**, Isam H. Aljundi, "Membrane fouling and modification using surface treatment and layer by layer assembly of polyelectrolytes: state-of-the art review", Journal of water process Engineering (under review, 29 Aug 2015).

- **Saqib Javed**, Isam H. Aljundi, "Fouling mitigation of TFC reverse osmosis membrane using spin-assisted layer by layer assembly of PEI/PAH polyelectrolytes", Journal of membrane science (submitted, 28 Nov 2015).

Conference Presentation

- Isam H. Aljundi, **Saqib Javed**, "Preparation and Characterization of Functional Polyamide RO Membrane via Spin Assisted Layer-by-Layer Assembly", 10th European congress of chemical engineering, 27, September 01- October 2015, France.

Academic Research Project

- **MS Thesis,** "Fouling Mitigation of Sea Water Reverse Osmosis Membrane using layer by layer deposition of Polyelectrolytes"

Box-Behnken design of experiment was used to study the effect of number of layers, concentration of polyelectrolyte solution, and pH on fouling mitigation. Polyamide membrane was synthesized over polysulfone support and then functionalized by a pair of polyelectrolyte. SEM, AFM, and contact angle was done for surface analysis of the modified membranes. Cross flow filtration experiments were carried out to investigate the performance of polyelectrolyte membranes in brackish water conditions. Optimum conditions were found to minimize flux loss.

- **BS Thesis,** on "Production of 10000 bbl. /day of Green Gasoline from Methanol via Mobil MTG Process"

Plant design study was carried out in synthesis of green gasoline in one step using a shape selective catalyst. It covers the design of heat exchanger, distillation column, separators and pumps. Cost estimation analysis was performed considering capital, operational, startup and utility cost. Hazop study was done to ensure smooth and safe operation of the plant.

Professional Experience

Internee Engineer

4 weeks internship in Presson Descon on Separator Designing (2010)

4 weeks internship in Ittehad Chemicals Limited on Brine Purification (2009)

Trainee Engineer (Production)

Worked as Trainee Shift Engineer on air separation unit (ASU) at Ghani Global Gases, Pakistan from Apr 2012 to Dec 2012-Responsibilities include handling of distributive control system (DCS), production calculations, manage smooth and safe daily production, plant startup and shut down.

Teaching (Lab Instructor)

Worked as an instructor in mass transfer lab at department of chemical engineering, KFUPM from Jan 2015 to Dec 2015-Used to guide and give individual attention to undergraduate students in demonstration of experiments.

Seminar Presentations

- Graduate seminar on polymeric membranes for natural gas separation.
- Isomerization of n-Heptane using ZSM-22 as a catalyst.
- Wet air oxidation for treatment of sulfidic spent caustic.

Academic Achievements

- Merit scholarship throughout my academic career.
- Got sponsorship from Nishat Group on excellent educational performance.
- Awarded KFUPM scholarship for MS Chemical Engineering.

Key Skills

- MATLAB , MATHEMATICA (Beginner Level)
- MS Office, Design Expert
- Hands-on practice on TGA, FTIR, BET and contact angle equipment.

Extra-curricular Activities

- Participated as an organizer for "3rd Symposium on Engineering Sciences, Lahore".
- Sports Coordinator for annual department and hostel sports.
- Basic Life Support Training from RESCUE 1122, on cardiopulmonary resuscitation (CPR).
- English Language Conversation course from BETS Lahore.

Activities/Hobbies

- Sports (Cricket, Soccer)
- Reading Books